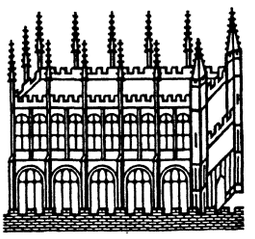

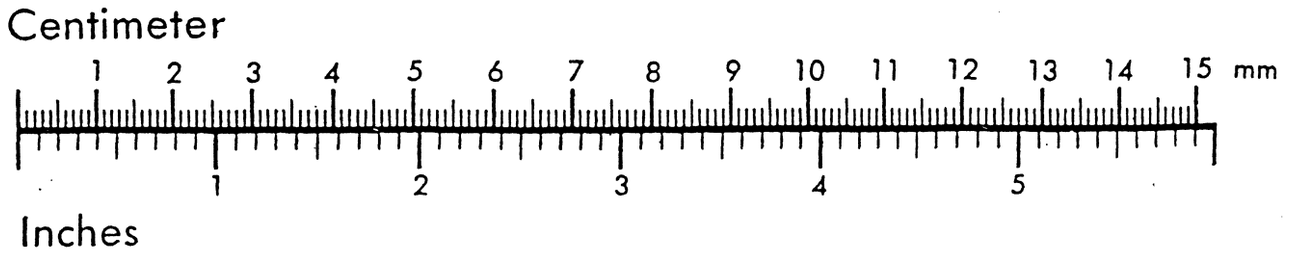

Tectonic Evolution of the Malay and Penyu Basins, Offshore Peninsular Malaysia

by

MAZLAN B. HJ. MADON

Thesis submitted for the degree of Doctor of Philosophy
to the University of Oxford

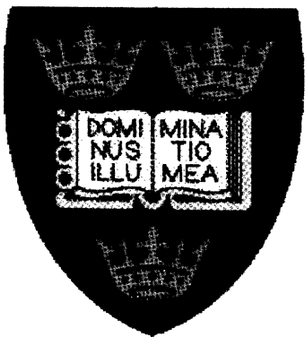

St. Peter's College &
Department of Earth Sciences

Michaelmas Term
December 1995

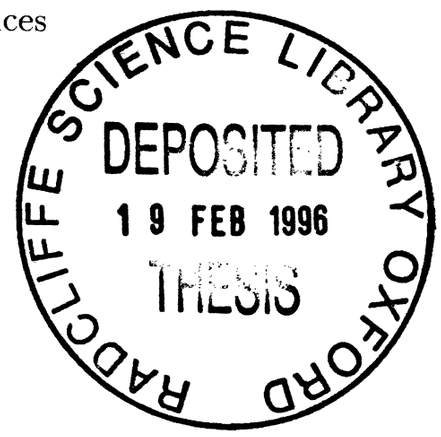

For Flora and Nadhila ...

Tectonic Evolution of the Malay and Penyu Basins, Offshore Peninsular Malaysia

MAZLAN B. HJ. MADON
St Peter's College & Department of Earth Sciences
Thesis submitted for the degree of Doctor of Philosophy to the University of Oxford
Michaelmas Term, 1995

Abstract: The Malay and Penyu Basins, offshore Peninsular Malaysia, were formed during the early Oligocene as a result of regional dextral shear deformation caused by the indentation of India into Eurasia in the early Tertiary. Pre-existing basement inhomogeneities exerted a strong control on basin development. The Penyu Basin developed, initially, as isolated grabens and half-grabens at basement fault intersections, in response to roughly N–S extension. The major structures, which include low-angle listric normal faults, pull-apart rhomb grabens and flower structures, suggest that "thin-skinned" crustal extension and strike-slip tectonics have played an important role in basin evolution.

Basement faults in the Malay Basin are oblique (E-W trending) to the basin trend (NW-trending). The Basin developed by transtension of a NW-trending sinistral shear zone, in which fault-bounded blocks rotate in response to the shear deformation, producing a series of E-trending half-graben depocentres. The Basins were subjected to transpressive inversion during the middle–late Miocene, as a result of rotation of the regional stress field, caused by progressive indentation of India into Eurasia.

Subsidence analysis suggests that lithospheric stretching was the dominant process of basin formation. The high heat flows (85–100 mW m^{-2}) are consistent with stretching factors, β, of 1.2 to 4.3. In the Malay Basin, uplift of the basin flanks preceeded subsidence during the rifting phase as a result of non-uniform stretching and lateral heat flow from the centre of the Basin. Both basins are undercompensated isostatically and characterised by low negative free-air gravity anomaly in the order of -20 mGal. Undercompensation suggests that the basins were formed, partly, by "thin-skinned" crustal extension which did not involve stretching of the subcrustal lithosphere.

Tectonic Evolution of the Malay and Penyu Basins, Offshore Peninsular Malaysia

MAZLAN B. HJ. MADON

St Peter's College & Department of Earth Sciences

Thesis submitted for the degree of Doctor of Philosophy to the University of Oxford

Michaelmas Term, 1995

Extended Abstract: The Malay and Penyu Basins are continental extensional basins located offshore east of Peninsular Malaysia, between the Gulf of Thailand and South China Sea. This thesis is a study of the tectonic evolution of the Basins, based on an integrated analysis of regional geology, structure, gravity anomaly, tectonic subsidence, and thermal history. The structural styles and kinematic histories of the Basins were studied based on seismic reflection and well data. Gravity and sediment isopach data were used to investigate the state of isostasy and its implications for the compensation mechanism in the Basins. The subsidence and thermal histories of the Basins were analysed using backstripping and basin modelling techniques, which utilize biostratigraphic data, bore-hole temperatures and vitrinite maturation data.

Geologically, the Malay and Penyu Basins are located at the centre of Sundaland — the Late Mesozoic continental core of Southeast Asia. This region underwent a phase of crustal/lithospheric thickening during the Indosinian Orogeny, following the closure of the Paleo-Tethys in the Late Triassic. The post-orogenic phase, spanning the Jurassic and Cretaceous, was a time of crustal extension, strike-slip tectonics, and widespread crustal heating, accompanied by sporadic

basaltic magmatism. This period of tectonism appears to have exerted a major influence on the Tertiary tectonics of the region. Although this regime of extension appears to have dominated the region since the Jurassic, it was not until the early Tertiary (Paleocene–Oligocene) that extensional basins began to form. In terms of age, the extensional basins of Sundaland fall into two groups: those located at the periphery seem to have formed slightly earlier (Paleocene) than those at the centre, including the Malay and Penyu Basins, which were formed during latest Eocene to Oligocene times (about 40–35 Ma B.P.). The peripheral basins are usually regarded as back-arc basins, although strike-slip faulting may have been a major control on their development. For the interior basins, however, back-arc extension could not have been the cause of basin formation because they are situated more than 1000 km away from subduction zones. The Malay and Penyu Basins, along with the Thai and West Natuna Basins, appear to have formed within a major zone of crustal extension associated with distributed shear deformation caused by the indentation of India into Eurasia in the mid-Eocene.

The structure and stratigraphy of the Penyu Basin were interpreted from seismic reflection data to investigate its structural history. A total of about 3500 line-km of industry-processed regional seismic data were used to map the major faults, subbasins, and key stratigraphic horizons. The Penyu Basin is a relatively small basin and is, basically, the westward continuation of the West Natuna Basin of Indonesia. It is about 150 km wide and has a maximum sediment thickness of about 8 km. Basin development was controlled by two main sets of parallel faults —ENE- and NW-trending faults. The rectilinear fault pattern suggests a strong influence of pre-existing basement faults on basin development. The NW-trending faults are parallel and, thus, may be related to major Late Cretaceous strike-slip faults on land. The Basin developed, initially, as isolated grabens and half-grabens at fault intersections, in response to N–S tension, as indicated by the overall fault trend and hangingwall-dip data. The different subbasins show markedly different structural styles, depending on the orientation of their bounding faults relative to the extension direction. E-trending half-grabens exhibit structures that are char-

acteristic of orthogonal extension involving normal dip-slip faults. They show the typical asymmetrical half-graben geometry, with a high-angle (40–50°) bounding fault and numerous, mainly synthetic, hangingwall faults. NW-trending grabens, on the other hand, show structures that are indicative of strike-slip tectonics, such as pull-apart rhomb grabens, negative flower structures, and listric low-angle bounding faults; the latter, in particular, is indicative of upper-crustal detachment faulting. The low-angle (30–35°) faults in the Rumbia Graben have arcuate map traces and show alternating polarity along the strike of the Graben. The major NW-trending bounding faults have dips exceeding 60° and also exhibit features indicative of strike-slip displacement.

The structural/sedimentation history of the Penyu Basin consists of four main phases: Synrift I, Synrift II, Postrift I and Postrift II. These tectono-sedimentary phases are punctuated by significant, but localised, breaks in sedimentation, which are represented by unconformities, recognised in seismic sections as surfaces of reflection termination, seismic facies changes and, in places, erosion or non-deposition. A Mid-Oligocene unconformity, separating Synrift I and Synrift II sequences, is the result of mild inversion tectonics that affected the Basin during the early stages of development. A more widespread inversion phase in the early–middle Miocene resulted in the Mid-Miocene Unconformity between Postrift I and Postrift II sequences, which is probably equivalent to the regional unconformity recognised in the neighbouring basins.

The Malay Basin is a very large basin, filled with at least 14 km of sediment. It has a NW trend, almost perpendicular to the strike of the Penyu–West Natuna Basin system. Its basement fault pattern, however, is dominated by E-trending faults, which are oblique to the basin trend. These faults are the bounding faults to major half-grabens which, subsequently, were inverted during the middle-late Miocene. The lack of through-going, basin-margin strike-slip faults suggests that a simple pull-apart origin, as proposed by previous workers, is highly unlikely. An alternative kinematic model is proposed whereby the Basin developed by distributed shear (transtension) of a NW-trending zone of deformation containing

pre-existing E-trending faults. These faults, and the crustal blocks they bound, rotated anticlockwise in response to sinistral shear during the early Oligocene, as a result of reactivation by the India–Eurasia collision. The block rotation caused transtensive oblique extension along the E-trending faults and resulted in half-grabens that are oblique to the basin trend.

Like most other Southeast Asian Tertiary basins, the Malay and Penyu Basins experienced a major phase of inversion in the middle–late Miocene. Inversion resulted in the reactivation of originally extensional faults and the formation of structures representing varying degrees of inversion, ranging from minor fault-propagation folds in the Penyu Basin to major anticlines and wrench-related flower structures in the southern Malay Basin. Basin inversion is the result of a change in the stress regime, caused by rotation of the regional stress field induced by progressive indentation of India into Eurasia since the collision in the mid-Eocene. In the Malay Basin, the change in the stress regime has resulted in the reversal of the sense of shear, from sinistral to dextral, which caused transpressional shortening of the half-grabens to form major *en echelon* anticlines. The intensity of the inversion in the Malay Basin increases southeastwards towards the West Natuna Basin, where southeast-verging reverse and thrust faults are common. The inversion has resulted, also, in a major zone of crustal shortening in the southern Malay and West Natuna Basins as a result of the buttressing effect of the Natuna Ridge, which resisted the dextral motion of the Malay shear zone. This is believed to be the cause of the major basement uplift observed in the southern Malay Basin and in the West Natuna Basin.

Both the Malay and Penyu Basins originated as nonmarine basins, dominated by lacustrine sedimentation during the early part of their history. The first signs of marine influence occurred during earliest Miocene, when active extension has ceased. The sedimentation pattern, subsidence history, and overall geometry suggest that the Basins were formed by a combination of lithospheric stretching and strike-slip faulting.

The great thickness of sediment in the Malay Basin implies a large amount

of crustal thinning. However, this is not reflected in the free-air gravity anomaly which, at most, is in the order of −20 mGal. Two-dimensional, flexural backstripping and gravity modelling techniques were used to investigate the role of lithospheric flexure during basin development and to estimate the effective elastic thickness of the lithosphere, T_e. The total tectonic subsidence in the Basin was determined by flexurally unloading the sediment column, which is assumed to have an exponentially- decreasing density resulting from compaction. The results suggest that the Basins are underlain by relatively thinned crust and, thus, indicate that some form of crustal stretching was involved in the basins' development. The tectonic subsidence obtained by flexural backstripping was used to calculate the depth of the Moho and, hence, the amount of crustal thinning. In both basins, the Moho depth that best explains the free-air gravity field is deeper than the isostatic Moho by about 25%. This implies that the Basins are undercompensated isostatically.

Two alternative explanations for the undercompensated nature of the Basins were considered. One hypothesis was that the crust may have been thickened after stretching as a result of magmatic underplating. The evidence suggests that underplating is unlikely because (1) no major regional uplift of the Basins has been observed, which would have occurred if the Basins had been underplated. (2) the extent of crustal thinning (β <2.5) is insufficient to have generated enough melt that can explain the apparent increase in crustal thickness.

A more plausible explanation for the undercompensation of the Basins is that part of the tectonic subsidence may have been caused by crustal extension that did not involve stretching of the mantle lithosphere. This implies that a process of "thin-skinned" detachment faulting, perhaps related to strike-slip tectonics, may have caused a large amount of additional subsidence unrelated to whole-lithosphere stretching. The Malay Basin is probably a "hybrid basin" formed by a combination of processes: whole-lithosphere stretching and thin-skinned crustal extension. This probably explains the low-amplitude free-air gravity anomaly over the Basins.

Flexural backstripping results suggest that the effective elastic thickness, T_e, of the lithosphere in the study area is low. Estimates of T_e based on the gravity data are less than about 12 km. For the Malay Basin, which is a very wide basin (~300 km), the flexural rigidity of the lithosphere appears to be negligible (T_e = 0), whereas for the Penyu Basin (~150 km wide), T_e=12 km, suggesting that the lithosphere behaves rigidly for this relatively narrow basin.

The Malay and Penyu Basins have a very high heat flow, with an estimated average heat flow of 85–100 mW m^{-2}. One-dimensional backstripping and maturity modelling techniques were used to investigate the subsidence and thermal histories of the Basins, using stratigraphic data from about 70 wells. Seismic and stratigraphic data suggest that extension began at about 35 Ma ago and lasted for at least 10 Ma. Application of the finite-rifting lithospheric stretching model suggests stretching factors, β, ranging from 1.2 on the flanks to 4.3 at the centre of the Malay Basin. The highest β value in the Penyu Basin is only about 2.4. In the Malay Basin, subsidence of the flanks was delayed by as much as 10 Ma after rifting began, probably, because of uplift during the rifting stage as a result of non-uniform stretching and lateral heat flow from the centre to the flanks of the Basin. Heat flow and thermal histories predicted using the stretching factors show decreasing heat flow with time, reflecting the decay of the thermal anomaly, and agree well with the results obtained by modelling vitrinite maturation data from a number of wells in the Malay Basin. Because the Basins are only about 35 Ma old, they may still be undergoing thermal subsidence. Hence, the thermal anomaly caused by lithospheric stretching has not dissipated completely, which explains the abnormally-high present-day heat flow.

Acknowledgements

This project was funded by PETRONAS, the national oil company of Malaysia, through a postgraduate scholarship. The company is thanked also for providing the data used in the study. I thank Dr. Khalid Ngah (General Manager, PETRONAS Research & Scientific Services, Kuala Lumpur) for his encouragement and support for the project.

I would like to thank Prof. John F. Dewey for his supervision and encouragement throughout the course of this study. Various people in the Department of Earth Sciences have helped me in one way or another. Special thanks to Jenny Collier, Moses Gachari, Nathan Hayward, Robin Owens, Jonathan Stewart, and Steve Usher. Discussions with Prof. Tony Watts on various aspects of basin analysis have greatly improved my understanding of basins. The line-integral gravity program used in Chapter 5 was written by Jon Stewart.

Thanks to various people at PETRONAS Research & Scientific Services for maintaining contact during the past three years. Special thanks to Abdul Rahim Md Arshad, Liew Kit Kong, and Mohammad Jamaal Hoesni for "digging up" some of the data for me. Thanks to Dr. Douglas W. Waples (Denver, Colorado) for pointing out the problem of vitrinite suppression in the Malay Basin, and to Dr. Steven Harder (University of Texas at El Paso) for sending a copy of the DMA gravity data.

My family and I would like to convey our deepest gratitude to Prof. Neville and Maureen Haile (Oxford) for their hospitality during our stay in Oxford. We have enjoyed their company, especially, during the countless outings to the countryside. Prof. Haile's personal library collection was an important resource for Southeast Asian literature.

Last but not least, I would like to thank Flora and Nadhila for their understanding and support. This work is dedicated to them. *Alhamdulillah.*

Mazlan Madon

Oxford

December 1995

Contents

List of Figures

List of Tables

Chapter 1

Introduction

1.1 Extensional Basins in Southeast Asia

The northern Sunda Shelf area between Peninsular Malaysia, Indochina and the Natuna Islands is underlain by a number of Tertiary extensional sedimentary basins: Malay, Penyu, and West Natuna Basins (Fig. 1.1). Numerous, but smaller, fault-bounded basins, also of Tertiary age, occur in the Gulf of Thailand and onshore Thailand to the north of this area. Understanding the geological evolution of these basins is important, not only because of their vast petroleum potential, but also because they represent a major zone of intracontinental extension within a complex region of overall plate convergence.

The continental part of Southeast Asia, known as "Sundaland", represents the eastern end of a Late Triassic orogen, the "Cimmerides" (Şengör and Hsü, 1984) or "Indosinian" (Hutchison, 1989b), which was the result of closure of the Paleo-Tethys Ocean. The Tertiary extensional basins occur in a broad zone of deformation that extends from northern Thailand, through the centre of Sundaland, to the Natuna Sea. Some authors (Tapponnier *et al.*, 1982; Daines, 1985) have suggested that this zone of continental extension represents a major strike-slip fault or shear zone.

The formation of the extensional basins is explained, commonly, in terms of the extrusion model (Tapponnier *et al.*, 1982), in which it was proposed that the India-Eurasia collision resulted in eastward and southward extrusion, and

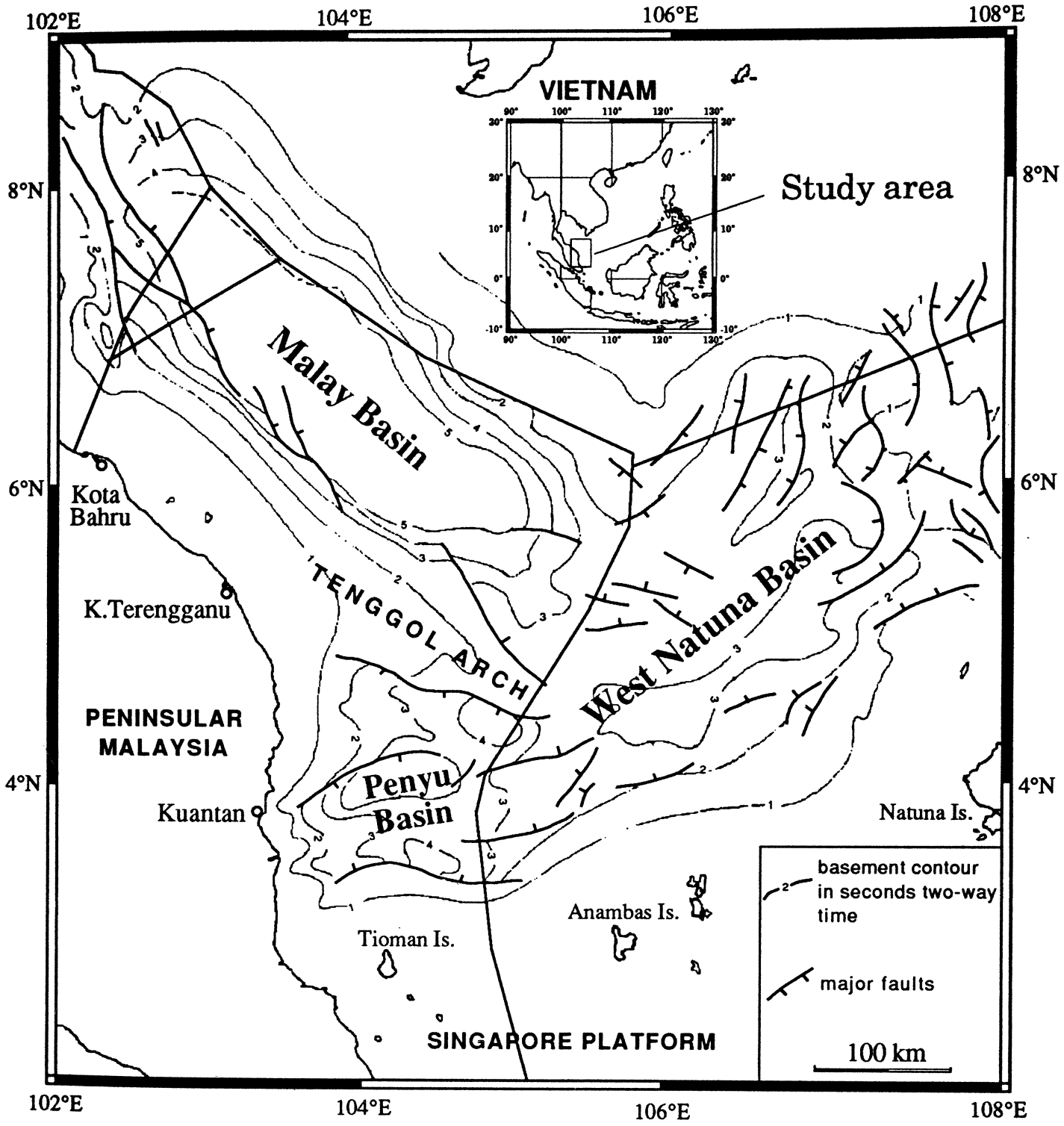

Figure 1.1. The three major Tertiary basins in the offshore region east of Peninsular Malaysia between the Gulf of Thailand and the Natuna islands (modified after ASCOPE, 1981).

clockwise rotation of large crustal blocks relative to the collision zone (Fig. 1.2). According to the model, major strike-slip faults that bound the crustal blocks — the Wang Chao, Three Pagodas, and Red River Faults — may be the sites of crustal extension and the formation of pull-apart basins. It is essential, therefore, to study the structural/tectonic evolution of the basins that occur within the zone and determine if the structural data are consistent with the predictions of the model. A major problem in the past has been the lack of detailed structural information from the basins themselves, mainly because the data are rarely published. A number of regional tectonic reconstructions of the Southeast Asian region have invoked the extrusion model to explain the development of the Tertiary basins (*e.g.* Wood, 1985; Daly *et al.* 1987, 1991; Packham, 1993). Until more detailed study is carried out, these regional models remain highly speculative.

Some studies have been carried out in the Thai and West Natuna Basins. The structural development of Tertiary basins in onshore and offshore Thailand have been studied by Polachan and Sattayarak (1989) and Polachan *et al.* (1991). These authors proposed a kinematic model in which the basins were formed at pull-aparts along NW-trending dextral strike-slip faults. They showed the northern part of the Malay Basin as being bounded by NW-trending strike-slip faults (Fig. 1.3). Recently, Ismail *et al.* (1994) has affirmed, however, that no through-going strike-slip faults have been observed anywhere in the Malay Basin.

The structure of the West and East Natuna Basins is relatively well-documented, compared to the Malay or Penyu Basins. Most authors have advocated a strike-slip origin for the basins, based also on the extrusion model of Tapponnier *et al.* (1982). Daines (1985) showed NW-trending faults in the West Natuna Basin, transverse to the general rift trend, and interpreted them as strike-slip or wrench faults (Fig. 1.4). Although these faults may have had strike-slip history during the early–late Miocene inversion phase, their role during basin formation was never convincingly demonstrated.

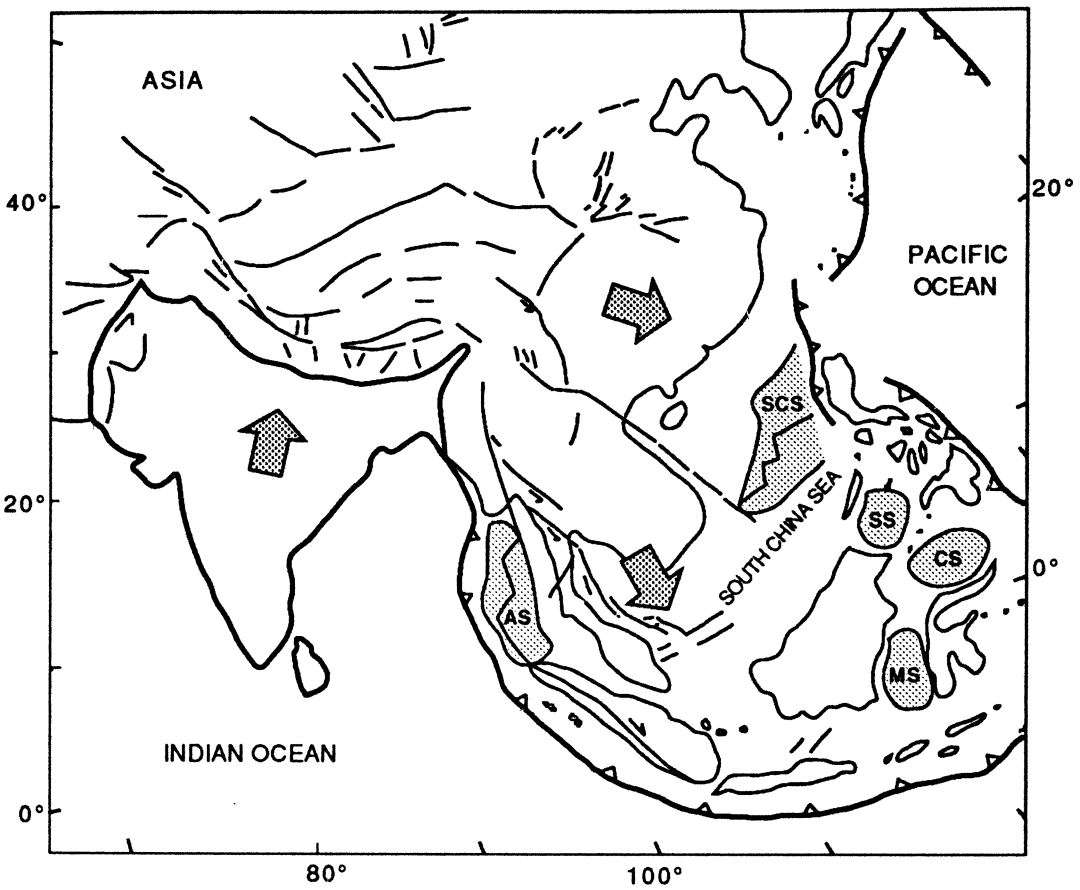

Figure 1.2. Extrusion tectonics model proposed by Tapponnier *et al.* (1982). The collision of India with Eurasia is thought to have caused the lateral expulsion of continental blocks (arrows) along major strike-slip faults and resulted in the development of pull-apart basins in the Gulf of Thailand, and also the formation of spreading centres in the Andaman and South China Sea (stippled areas) (see also Peltzer and Tapponnier, 1988). Note also the implied clockwise rotation of Southeast Asia with respect to India. Stippled areas in Southeast Asia represent young marginal seas/oceanic basins: SS– Sulu Sea, AS– Andaman Sea, CS– Celebes Sea, MS– Makassar Strait, SCS– South China Sea Basin.

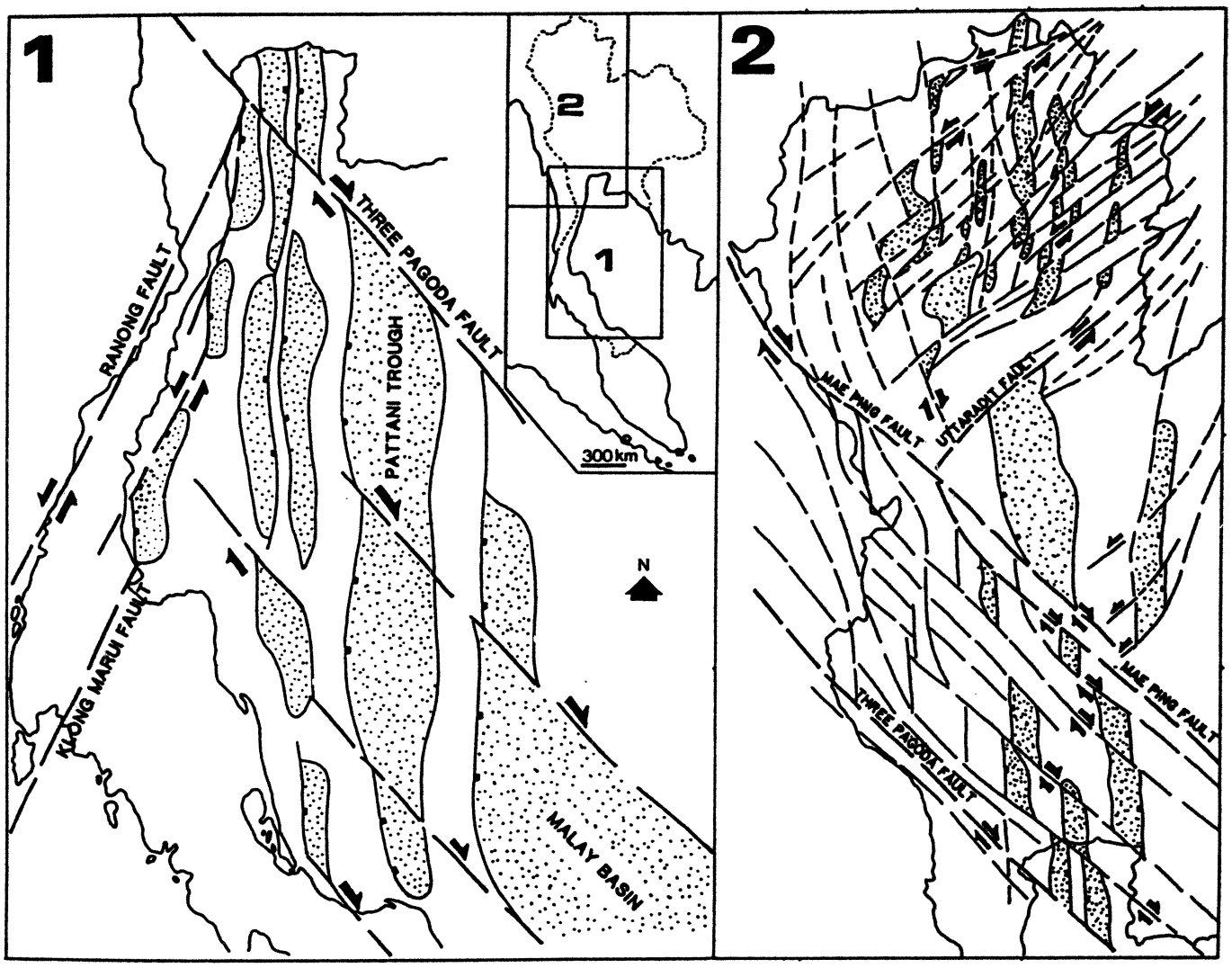

Figure 1.3. Model of pull-apart basins in Thailand by Polachan and Sattarayak (1989). Conjugate fault patterns in the Thai onshore and Gulf of Thailand were interpreted by Polachan and Sattayarak (1989) as indicating extension by dextral shear (map 2). The Malay Basin is depicted by the authors as a pull-apart basin between dextral strike-slip master faults (map 1).

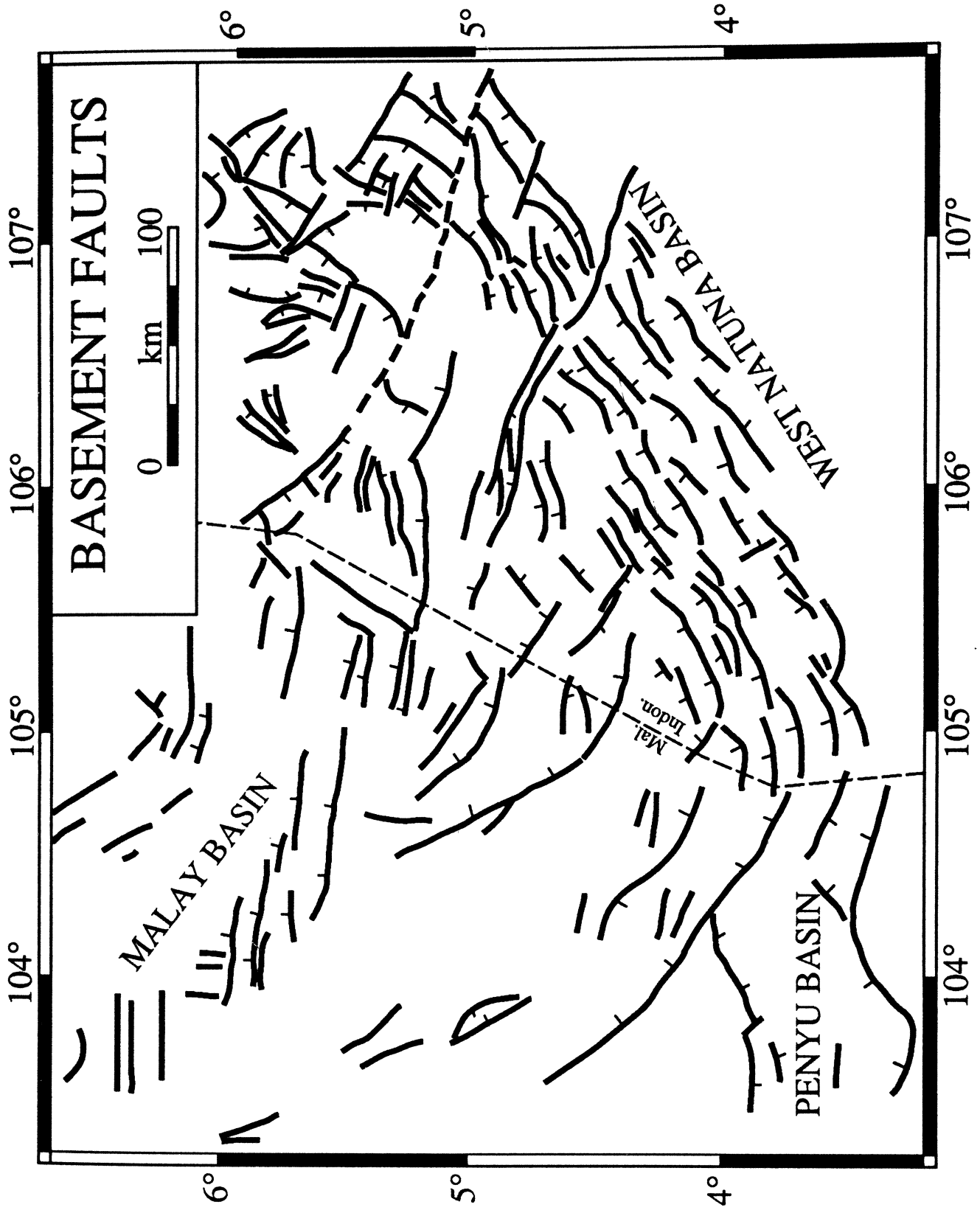

Figure 1.4. Semi-detailed basement fault map of Malay-Penyu-West Natuna Basins. Malay Basin data from unpublished PETRONAS map. Faults in the West Natuna Basin, compiled from Ginger *et al.* (1993). Structures in the Penyu Basin (western part of the map area) are based on this study. Note the general E–W trends in the basin, including the Malay Basin. Transverse NW–SE faults in the West Natuna Basin were interpreted as basin-controlling strike-slip faults by Ginger *et al.* (1993).

1.1.1 The Malay and Penyu Basins

The Malay and Penyu Basins are probably the least understood of all the basins in central Sundaland, largely because of poor documentation of the geology and structure by the industry. Proper study of the structure and stratigraphy of the basins are needed to test the various tectonic models that have been proposed.

During the early years of exploration, the Thai, Malay, Penyu and West Natuna Basins were considered as a large basin called the "Gulf of Thailand Basin". Later, it became clear that this great basin is made up of a number fault-bounded grabens and half-grabens. The "Thai Basin" itself consists of several smaller grabens (ASCOPE, 1981; Chinbunchorn *et al.*, 1989), the largest of which is the Pattani Basin.

The Malay Basin appears to be a large NW-trending trough parallel to the trend of Peninsular Malaysia (Fig. 1.1). Although a vast amount of geological and geophysical data have been acquired by oil companies exploring in the area during the last 25 years or so, very little has been published. To date, only two publications describe the Malay Basin in some detail (Hamilton, 1979; ASCOPE, 1981). Hamilton (1979) noted from unpublished industry sources the occurrence of E-trending, apparently, *en echelon* anticlines in the Basin, and suggested that the basin may have formed by right-lateral wrenching.

The gross structural history of the Malay Basin has been described as follows (*e.g.* Murphy, 1989).

1. Basin initiation in the early Oligocene by block-faulting of the Mesozoic basement and the formation of graben and half-graben. The time of initiation was inferred from the age of the oldest sediment penetrated in the southeastern parts of the Basin (ASCOPE, 1981; Ramli, 1988). Generally, sedimentation was accompanied by extensional faulting.

2. Cessation of extensional faulting. Subsidence and sedimentation accom-

panied by possible wrench fault movements, resulting in major uplift and erosion in the southeastern part of the Basin. Extensional faults were re-activated. In the southeastern part of the Basin, the uplift resulted in a regional erosional unconformity over the crests of compressional anticlines. It has been estimated that some 1200 m of sediment has been eroded off the crests of some anticlines (Murphy, 1989).

3. Continued subsidence and deposition during relative tectonic quiescence in late Miocene to the present day.

Ramli (1986) noted that the three-stage basin evolution resembles that of strike-slip basins (Reading, 1980). Indeed, within the local petroleum industry, the basin is thought of as a "wrench-related" basin, following the view of Hamilton (1979).

The Penyu Basin is smaller than the Malay Basin, and is separated from the latter by the Tenggol Arch (Fig. 1.1) The basin appears to structurally contiguous with the West Natuna Basin which, curiously, has a structural grain that is almost perpendicular to the Malay Basin.

Most authors agree that basin formation involved some mechanism of crustal or lithospheric extension. For example, White and Wing (1978) suggested that the "Gulf of Thailand Basin" (which includes the Malay Basin) and West Natuna basins were formed by *collapse of a regionally thinned continental crust*, based on the high geothermal gradients. Hutchison (1984) regarded the Malay Basin as a "Pannonian-type" extensional basin, characterized by attenuated continental crust in back-arc regions. As yet, no attempt has been made to study the tectonic processes during extension of the Malay or Penyu Basins, as was done in the Thai basins (Hellinger and Sclater, 1983; Pigott and Sattarayak, 1993). Although important advances have been made in the understanding of rift/extensional basins worldwide (Morley, 1995), many of the new ideas have rarely been applied or tested in this area.

The aim of this thesis project, therefore, is to achieve a better understanding of the evolution of the Malay and Penyu Basins, based on a detailed analysis of the structure, gravity anomaly, tectonic subsidence, and thermal history of the Basins and to integrate the results with regional geology. Structural interpretation of seismic data from the Basins are presented to show the geometry and style of extension, which are important to our understanding of their kinematic evolution. The subsidence mechanism and thermal history of the Basins are analysed using well-established backstripping and basin modelling techniques that utilize litho- and bio-stratigraphy, bore-hole temperatures, and vitrinite maturation data.

In this introductory chapter (Section 1.2), a brief review of the main theoretical aspects of extensional basins is given. The descriptions of scope of work, the data and methodology used, and the general outline of the thesis are given later in the chapter.

1.2 Brief Review of Extensional Basins

Relevant to our understanding of the evolution of extensional basins are (1) the origin of lithospheric tension and (2) the tectonic and thermal consequences of extension. The former relates to the gravitational and far-field causes of horizontal tension in the lithosphere reponsible for the development of extensional basins, while the latter is concerned with the vertical motions associated with lithospheric extension and the thermal history of the resulting basin. This brief review aims to highlight some key advances on these topics.

1.2.1 Origin of Lithospheric Tension

Forces that drive subsidence in some types of sedimentary basin can be explained by lithosphere-scale processes operating at plate boundaries. For example, it is widely accepted that passive margins subside as a result of lithospheric exten-

sion and thinning (McKenzie, 1978), which may be initiated at continental rift zones, either by active mantle plumes or by passive rifting (Şengör and Burke, 1978) induced by plate-driven forces. Foreland basins, on the other hand, are the flexural consequences of fold-thrust front loading in collision zones at convergent plate boundaries (Beaumont, 1981). Lithospheric tension in back-arc regions is primarily the result of slab pull on the overriding plate above subduction zones (Bott, 1982).

Continental extension may be caused also by gravitional forces within thickened lithosphere in orogenic belts. Extensional collapse of orogenic belts (Dewey, 1988) is an important mechanism of continental extension and the formation of some intermontane basins (*e.g.* Gabel *et al.* 1993). Extensional basins can also form in intraplate settings particularly along strike-slip or shear zones. Continental-scale strike-slip faults and shear zones in Central Asia may be the result of horizontal plane-strain deformation arising from the northwards indentation of India into Eurasia (Tapponnier and Molnar, 1976). These shear zones were activated by *indentation tectonics* and are thought to be the sites of extensional basin development, perhaps, as pull-apart basins (Tapponnier *et al.*, 1982). Pull-apart basins may be regarded as a special class of extensional basins, which form by localized extension at releasing bends of strike-slip faults (Crowell, 1974). Extension may also occur along weak zones by the reactivation of older contractional faults, as suggested by studies of deep seismic reflection profiles. Keen et al. (1991), for example, showed evidence that faults bounding Mesozoic half-grabens on the Nova Scotia continental margin are reactivated Palaeozoic features.

1.2.2 Structural Expression of Continental Extension

Regardless of the causes of lithospheric tension responsible for extensional basin formation, the lithosphere deforms, generally, by brittle faulting in the upper crust and plastic/ductile flow in the lower crust and mantle. Extensional, or "rift", basins are characterised by basin-margin normal faults as a result of upper crustal

extension during their formation. Field observations and physical modelling of extensional basins (*e.g.* McKenzie, 1978) suggest that they undergo two stages of structural development: (1) a fault-controlled subsidence or rifting phase, followed by (2) a thermal subsidence phase due to conductive cooling of the asthenosphere beneath the region of thinned crust. Rifting is manifested in brittle faulting in the upper lithosphere, which accommodates the extension by slip along listric or planar normal faults, whereas the thermal subsidence phase produces a sag basin as deposition takes place over an increasingly wider region. The resulting basin has the so-called "steer's head" geometry, which are typical of basins formed by lithospheric stretching (Dewey, 1982; Watts *et al.*, 1982; White and McKenzie, 1988) (Fig. 1.7).

Much of our understanding of upper lithosphere faulting has been gained from neotectonic studies of actively extending regions such as the Aegean (Jackson and McKenzie, 1983; Jackson, 1987; Jackson and White, 1989), and other areas of continental extension such as the Basin and Range Province of western U.S.A. (Wernicke, 1985) and the East African Rift Systems (Rosendahl, 1987). Studies in the Aegean, for example, have shown that seismogenic normal faults are generally planar down to a depth of about 15–20 km, corresponding to the depth of the seismogenic upper crust *i.e.* the brittle-ductile transition (Jackson, 1987). Large earthquake normal faults are high-angle faults with dips in the range of 30°–60°. Faults with shallower dips (<30°) occur near the base of the seismogenic layer and tend to be aseismic. During earthquake faulting, slip on normal faults results in footwall uplift and hangingwall subsidence. The magnitude of footwall uplift is about a tenth of that of hangingwall subsidence (Jackson and McKenzie, 1983). This suggests that the footwalls to normal faults are rarely rigid during extension, unlike as required by some fault-balancing models, *e.g.* White *et al.* (1986). Such geometric models may be applicable only to gravity-driven fault in the sedimentary cover rather than basement-involved crustal faults (Roberts and Yielding, 1994).

Normal faults are rarely continuous along strike, *i.e.* they are segmented, with individual fault segments having lengths generally in the order of 20 km. This length scale is apparently controlled by the thickness of the seismogenic layer. The area between fault segments are characterised by intense diffuse deformation rather than by discrete "transfer faults" (Roberts and Jackson, 1991). In recent years, observations in actively extending regions have shown that transfer faults, linking fault segments in rift basins, are less common than previously thought (Gibbs, 1984; Rosendahl, 1987; Cartwright, 1987), and could be the exception rather than the rule.

Sudies of fault displacement populations (Walsh and Watterson, 1988; Roberts *et al.*, 1993) indicate systematic variation in the displacement along strike, suggesting that faults grow by tip-line propagation and segment linkage. Footwall uplift and hangingwall subsidence are greatest at the centre of a fault and decrease towards the tips either side. This observation has important implications also for the tectono-sedimentary evolution of rift basins. Recent studies have demonstrated the importance of fault geometries and surface morphology of rifts in controlling the drainage patterns and sediment dispersal mechanisms (Leeder and Gawthorpe, 1987; Morley, 1989; Gawthorpe and Hurst, 1993) (Fig. 1.5). Along-strike variation in subsidence and uplift rates in normal fault systems affect the rate of creation of accommodation space, which can result in complex depositional sequence stacking patterns in half-graben basins (Gawthorpe *et al.*, 1994).

1.2.3 Thermo-Mechanical Models of Extensional Basins

Sedimentary basins form as the result of vertical motions (subsidence/uplift) of the lithosphere as it tries to maintain isostatic equilibrium in response to a tectonic driving force. Hence, fundamental to the understanding of sedimentary basin evolution is to try to explain the mechanism of subsidence. It is generally agreed that the three principal driving mechanisms of subsidence are lithospheric

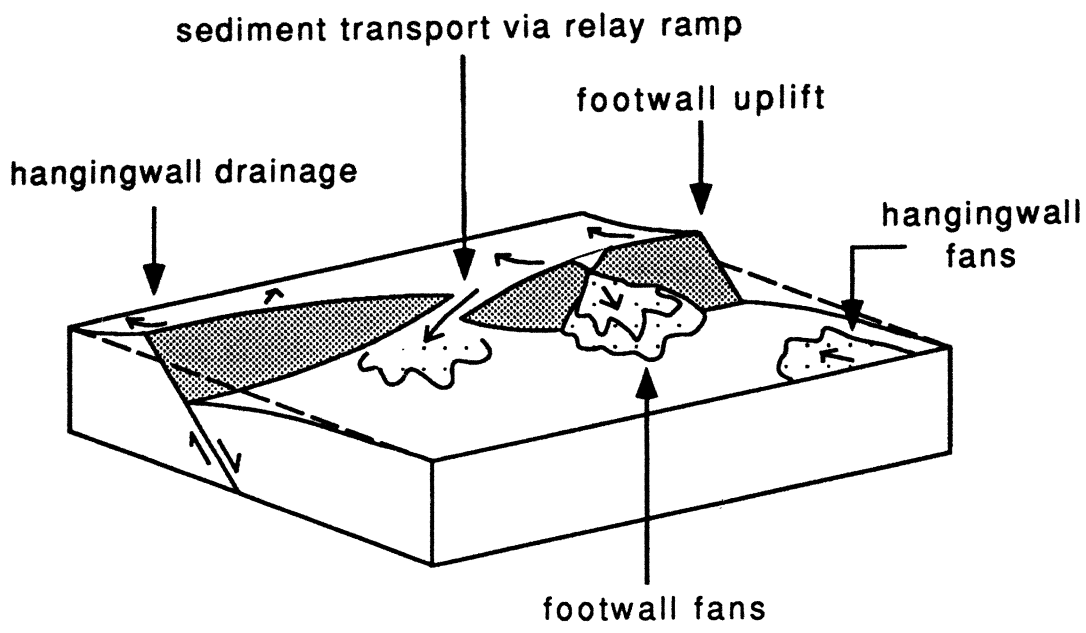

Figure 1.5. Idealized model of sedimentation in normal fault systems based on studies in active rift basins (*e.g.* Gawthorpe *et al.* 1994).

thinning, cooling of asthenosphere, and sediment loading. When the lithosphere thins, isostatic adjustment results in subsidence. Depending on the initial crustal and lithospheric thicknesses, thinning of the lithosphere raises the isotherms and causes temporary uplift which, eventually, subsides as the lithosphere cools to its original temperature structure. Subsidence resulting from crustal thinning and, later, from cooling of the lithosphere produces accommodation space for sediments to accumulate. The addition of sediment into the basin causes further subsidence. The depth of the basin at any time is thus determined by the extent of lithospheric thinning (or the stretching factor β) and the interplay between the thermally induced uplift and the subsidence due to sediment loading. Although sediment loading alone could not produce a sedimentary basin, studies in rift basins and passive margins (Watts, 1988, 1992) have shown that sediment loading can result in the accumulation of large thicknesses of sediment in basins.

One of the most important advances in understanding sedimentary basin evolution has been to explain the thermal/mechanical consequences of extension by means of simple physical models. Existing models, inspired by the uniform lithospheric stretching model of McKenzie (1978) (Fig. 1.6), assume either pure or

simple shear extension or a combination of both. The various models have discussed by many authors such as Burrus (1989), Keen and Beaumont (1990), Allen and Allen (1990), and only a brief account is given here. Pure shear models involve either uniform extension (McKenzie, 1978) or depth-dependent extension (Royden and Keen, 1980). Models incorporating simple shear have involve a variety of deformation styles, such as whole lithospheric simple shear (Wernicke, 1985) or a ramp/flat or domino faulting above a lower lithosphere that deforms in pure shear (Gibbs, 1989). In some models, such as the flexural-cantilever model of lithospheric extension (Kusznir and Ziegler, 1992), the brittle upper crust deforms by simple shear along planar normal faults while the lower crust and mantle lithosphere deform more by pure shear.

The uniform stretching model has been successful, generally, in predicting the gross geometry of extensional basins (Fig. 1.7). The two essential features of basins formed by lithospheric stretching: fault-controlled subsidence during the stretching phase, followed by a thermal subsidence phase. The stretching phase may be accompanied by uplift of the rift flanks, which may be due to various mechanisms: thermal (Cochran, 1983) or mechanical (Weissel and Karner, 1989; White and McKenzie, 1988). The uplifted flanks may be eroded and, later, covered by postrift sediments during thermal subsidence, which is enhanced by sediment loading. The postrift basin is supported over a larger and larger area, as the lithosphere gains rigidity through cooling of the lithosphere (Watts *et al.*, 1982), resulting in stratigraphic onlap at the basin margins (Fig. 1.7).

In McKenzie's uniform stretching model, instantaneous stretching induces fault-controlled subsidence and passive rise of hot asthenosphere. As the asthenosphere cools, a thermal subsidence ("sag") basin is produced. The stretching model can be used to predict the amount of subsidence and heat flow variation with time, which are determined, essentially by the amount of stretching, β. Subsidence is computed assuming that local Pratt-type compensation is maintained throughout the evolution of the basin. The most important parameter controlling

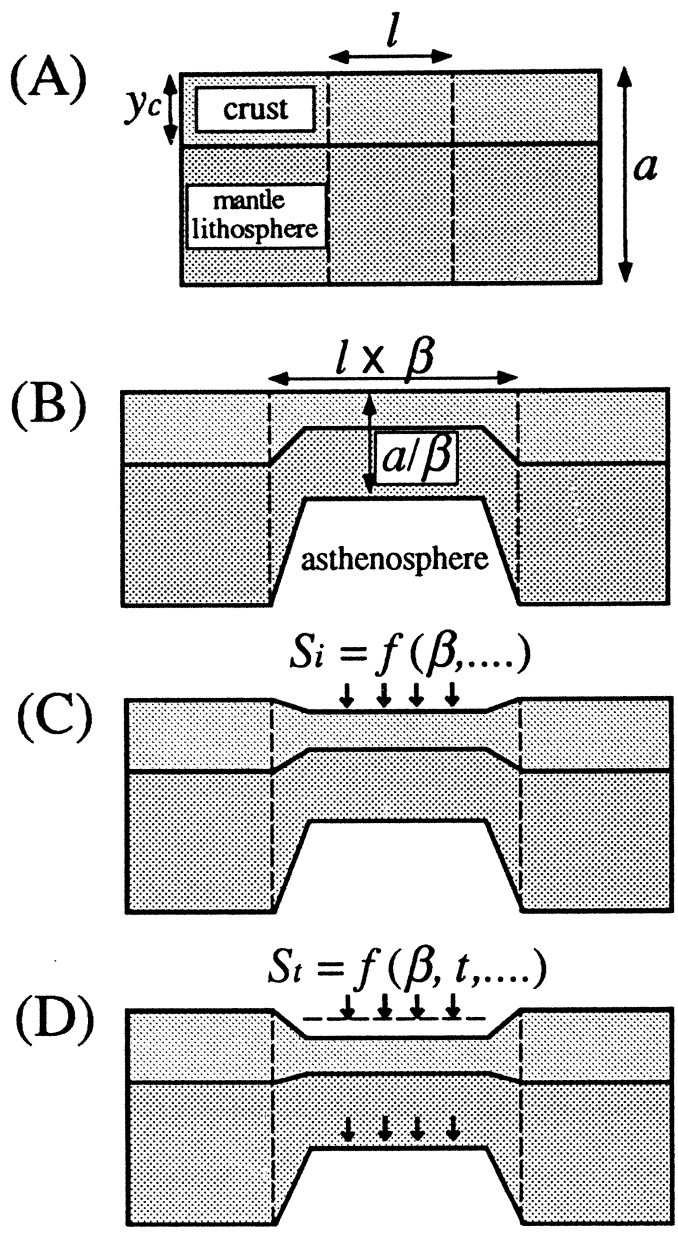

Figure 1.6. Illustration of McKenzie's (1978) uniform stretching model. (A) Initial condition with crustal thickness y_c and lithosphere thickness a. (B) A region of length l is *instantaneously* stretched by a factor β, resulting in thinning of the lithosphere to a/β. Thinning causes passive rise of the asthenosphere and perturbation of the initial temperature structure. (C) Isostatic adjustment of the thinned lithosphere results in an initial subsidence S_i, which is governed, essentially, by the stretching factor β. (D) Additional subsidence $S_t(t)$ follows as the lithosphere equilibrates to its original pre-stretching temperature structure.

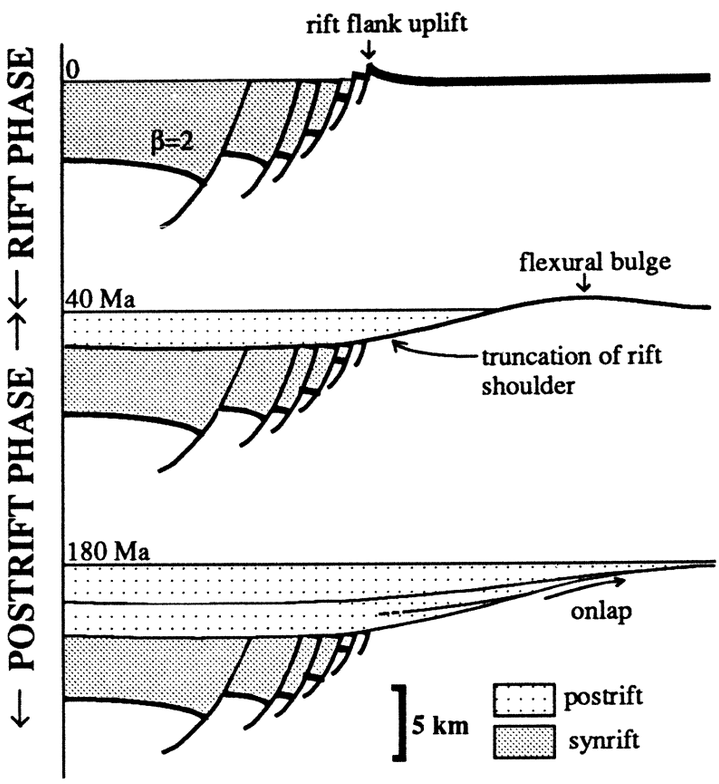

Figure 1.7. The "steer's head" geometry of basins formed by lithospheric stretching. Redrawn from Dewey (1982).

subsidence and heat flow is the lithospheric and crustal thicknesses (Dewey, 1982). For a "normal" thermal thickness of the lithosphere of 125 km, subsidence will occur if the pre-stretching thickness of the crust is greater than about 18 km.

McKenzie's (1978) model assumes that the crust and lithosphere are stretched by the same amount (hence the term "uniform stretching") and, because stretching is considered instantaneous, the magnitude of the thermal subsidence is a direct measure of the amount of extension, β. In reality, the processes leading to basin formation are more complex. This has led to numerous *ad hoc* modifications of the stretching models. The uniform stretching model has been modified by many workers to investigate the effects of, for example, (1) non-uniform stretching (Royden and Keen, 1980; Hellinger and Sclater, 1983; Rowley and Sahagian,

1986; White and McKenzie, 1988); (2) lateral heat flow during stretching (Watts *et al.*, 1982; Jarvis, 1984; Pitman and Andrews, 1985), (3) stretching over a finite duration (Jarvis and McKenzie, 1980; Beaumont *et al.*, 1982; Cochran, 1983), and (4) spatial and temporal changes in the mechanical properties, such as flexural rigidity and rheology, of the crust/lithosphere (Beaumont *et al.*, 1982; Braun and Beaumont, 1989; Weissel and Karner, 1989; Kooi *et al.*, 1992; Bassi *et al.*, 1993; Liu, 1994; van der Beek, 1995).

The finite-duration stretching model (*e.g.* Jarvis and McKenzie, 1980; Cochran, 1983) assumes that the lithosphere is stretched over a certain period of time rather than instantaneously. As a result, asthenopheric heat is conductively removed from the lithosphere more rapidly during the stretching phase, thereby accentuating the syn-rift subsidence while diminishing the magnitude of the postrift subsidence. Jarvis and McKenzie (1980) showed that the simple instantaneous stretching model gives a good approximation of subsidence and heat flow provided the duration of stretching is less than about 20 Ma.

Two-dimensional stretching models take into account horizontal as well as vertical heat conduction when predicting subsidence and heat flow variation with time (Watts *et al.*, 1982). Lateral heat flow increases the subsidence rate during stretching, but at the same time causes temporary uplift of the rift shoulder as heat is removed from the heated region. Jarvis (1984), for example, showed that narrow grabens subside much faster than wide grabens, and suggested that for a 1-D stretching model (McKenzie, 1978) to be reasonably accurate, the basin width should be greater or equal to the lithosphere thickness. The effect of lateral heat flow in the model is significant particularly for narrow "thick-skinned" pull-apart basins. Accelerated synrift subsidence can result in sediment-starved basin (Pitman and Andrews, 1985), which has important implications for source rock deposition.

Other workers have found that heat flow through the surface of an evolving basin may be reduced by the blanketing effect of sediments (Hutchinson, 1985;

Keen *et al.*, 1981; Stephenson *et al.*, 1989). Bond and Kominz (1984) showed that the predicted surface heat flow can be reduced by as much as 50% due to sedimentation. Lucazeau and Le Douaran (1985) found that in the Gulf of Lion where the sedimentation rate is high (620 m/Ma) the sediments absorb 30% of the surface heat flow whereas in the Viking Graben where the average sedimentation rate is much less (37 m/Ma) the insulating effect is only 10%. Karner (1991) investigated the effects of sediment blanketing on subsidence of passive margins and found that, although it had little effect on flexural rigidity, sediment blanketing reduces the cooling rate and, hence, the subsidence rates.

In recent years, research has focussed on magmatism associated with continental extension (McKenzie and Bickle, 1988; Latin and Waters, 1992) and its role in magmatic underplating and basin inversion (Brodie and White, 1994).

1.3 Aims and Scope of Work

The principal aim of the study is to gain a better understanding of the tectonic origin and evolution of the Malay and Penyu Basins. The study was designed to cover three main aspects of basin evolution

1. kinematics of basin formation
2. gravity anomalies and isotatic compensation
3. subsidence and thermal histories

The first part of the study involves the structural interpretation of the seismic data, mainly from the Penyu Basin, for the purposes of mapping the major extensional faults and examining the gross tectono-stratigraphic evolution. This part of the study attempts to answer some questions regarding the origin of the basins *i.e.* whether the basins are pure rift basins or was there significant strike-slip

component? The study focusses on structure as interpreted from seismic reflection data.

The second aspect of study is concerned with the tectonic subsidence and isostatic compensation mechanism, which tell us something about the process of basin formation. In this part of the work, commonly-used techniques for basin analysis, such as backstripping, gravity modelling, and subsidence/thermal modelling, were used. Model predictions were compared with the available data, which include thermal maturity of sediment and present-day temperatures and heat flow.

1.4 Data

The data for the study were supplied by PETRONAS, the Malaysian national petroleum corporation. For the Penyu Basin study, the main data source is a set of regional seismic reflection data acquired between 1968 and 1991, with a total line coverage of about 3500 km. The database consists of a grid of about 5–10 km line spacing. The seismic data had already been processed and migrated in time, and were supplied in the form of paper sections with a vertical scale of 5 cm per seconds. Unpublished geological, well-completion, and drilling reports from the 6 exploration wells were also provided. Relevant geological information were compiled from wireline logs, well-site lithological descriptions, biostratigraphic analyses, and check-shot velocity surveys (Appendix A.3).

The Malay Basin data are mostly in the form of well stratigraphic data and selected regional seismic lines. Its study was limited to compiling unpublished maps and re-interpreting its structural/tectonic development. Data from about 70 wells, including wireline logs, lithological information, biostratigraphy, and velocity check-shot surveys, were also provided. Temperature, heat flow, and sediment maturation data were compiled from published reports and unpublished well records.

1.5 Outline of Thesis

- Chapter 1: Introduction to Southeast Asian Tertiary basins, including a brief review of extensional basins.

- Chapter 2 is a review of the regional tectonics of the northern Sunda Shelf region and summarizes the main Paleozoic and Mesozoic tectonic history leading to the Indosinian Orogeny, while documenting the important tectonic and igneous events.

- Chapter 3 is a detailed analysis of the structural evolution of the Penyu Basin, based on interpretation of reflection seismic and well data. The main aspects covered are the geometries of half-grabens and faults in relation to the kinematic evolution of the Basin.

- Chapter 4 is a study of the kinematic evolution of the Malay Basin based on seismic data and maps compiled from previously unpublished sources. A re-interpretation of the tectonic development of the Basin is made.

- Chapter 5: Analysis of gravity anomalies, tectonic subsidence, and isostatic compensation in the Malay and Penyu Basins, using 2D flexural backstripping and gravity modelling techniques.

- Chapter 6 Analysis of the subsidence histories of the Penyu and Malay Basins based on backstripping analysis of stratigraphic data. The heat flow and thermal histories of the Malay and Penyu Basins were investigated using vitrinite reflectance modelling techniques and the lithospheric stretching model.

- Chapter 7 concludes thesis by summarizing the main findings, and discussing the tectonic evolution of the Penyu and Malay Basins in its regional context.

Chapter 2

Regional Tectonic Framework

2.1 Present-Day Tectonic Setting

Southeast Asia is a tectonically complex region where three lithospheric plates converge — the Pacific, the Indo-Australian, and the Eurasian plates. The region consists of a continental core of Late Mesozoic age, known as "Sundaland", that extends from Burma to southern Borneo and forms, effectively, a southeastern protrusion of the Eurasian continent. The boundary of this continental terrane corresponds, approximately, with the present-day shelf edge which is marked by the 200 m isobath. Sundaland is surrounded by younger micro-continental fragments, accreted during the late Cretaceous and Tertiary, and by numerous Cenozoic island arcs and marginal seas. Its borders are delineated (Hutchison, 1989a) in the north by the Saigang Fault in eastern Burma and the Red River Fault Zone in northern Vietnam, extending further southwards between the Sumatra Fault Zone and the Lupar Line in West Borneo. Its southeastern margin is poorly defined but is taken generally as a line extending from western Java across the Java Sea towards the Meratus Mountains in southern Borneo (Hamilton, 1979; Hutchison, 1989a).

2.2 Pre-Tertiary History

To understand the Tertiary evolution of the region, we need to understand, first, its pre-Tertiary history. This section is a review of the pre-Tertiary tectonic history of the region based on published work, emphasising the main tectonic events, particularly in Peninsular Malaysia where the basement of the offshore Tertiary basins crop out. Several publications on the geology of the region are worth mentioning. The book by Gobbett and Hutchison (1973) on the geology of the Malay Peninsula is still the only comprehensive account of the geology of the peninsula, even though our knowledge has improved much since then. Hamilton's (1979) landmark publication entitled *Tectonics of the Indonesian Region* was the first interpretation of the wider Southeast Asian region in terms of plate tectonics. A recent book by Hutchison (1989a) on *Geological Evolution of Southeast Asia* gives a more updated review of Southeast Asian geology and includes a substantial chapter on the Tertiary sedimentary basins.

The pre-Tertiary history of the region may be thought of comprising three main phases (Figs. 2.1, 2.2):

1. **Rift-drift phase** during the Paleozoic to early Mesozoic. This phase is dominated by the continental rifting and drifting of fragments off Gondwanaland and their subsequent accretion onto the southern margin of Eurasia.

2. **Collisional phase** during the Late Triassic–Early Jurassic. The amalgamation of Gondwanaland terranes in Southeast Asia ended with the collisional Late Triassic Indosinian Orogeny.

3. **Post-orogenic phase** during post-Early Jurassic to Cenozoic. The Jurassic–Cretaceous is characterized post-orogenic tectonics dominated by uplift, crustal extension, strike-slip faulting, and intermontane basin formation.

Figure 2.1 summarizes the three tectonic phases in the evolution of the Southeast Asia: before, during, and after the Indosinian Orogeny. The main features of

these tectonic phases are discussed below.

2.2.1 Palaeozoic–Mesozoic Events and the Indosinian Orogeny

The tectonic events during Permo-Triassic times leading to the formation of Sundaland involved subduction, continental accretion and, finally, collision in late Triassic times (Fig. 2.2). It is now generally accepted that Sundaland represents the eastern end of the Late Triassic Cimmeride or Indosinian Orogen (Şengör, 1979; Şengör and Hsü, 1984; Hutchison, 1989a). The Indosinian orogeny resulted in the amalgamation of continental fragments that rifted off Gondawanaland and accreted onto the southern margin of Laurasia in the Late Triassic (Gatinsky, 1986; Şengör and Hsü, 1984; Şengör, 1987; Metcalfe, 1988). The orogeny marked the closure of the Palaeo-Tethys Ocean, the remnants of which are represented by a belt of ophiolites, melange, and flysch extending from central Thailand and northern Laos (Nan-Uttarradit and Luang Prabang–Dien Ben Phu Lines) to central Peninsular Malaysia (Bentong–Raub Line). Stratigraphical, palaeobiological and palaeomagnetic evidence (Metcalfe 1988, 1991) suggest that the Sundaland craton comprises two main continental terranes separated by the Paleo-Tethyan suture along the Dien-Bien Phu and Bentong–Raub ophiolite lines. On the eastern side of this line, are continental fragments comprising Thailand, Indochina, eastern Malaya, and western Borneo, which were already attached to Eurasia before the Late Permian, whereas on the western side are Gondwanian blocks, which include the Shan states of Burma, northwestern Thailand, Malaya, and Sumatra, which collided with southern Eurasia during the Late Triassic Indosinian Orogeny (Fig. 2.3).

The Indosinian Orogeny was accompanied by widespread emplacement of Late Triassic to Early Jurassic granites which characterise the Southeast Asian tin belt stretching from northern Thailand through Peninsular Malaysia to the Indonesian

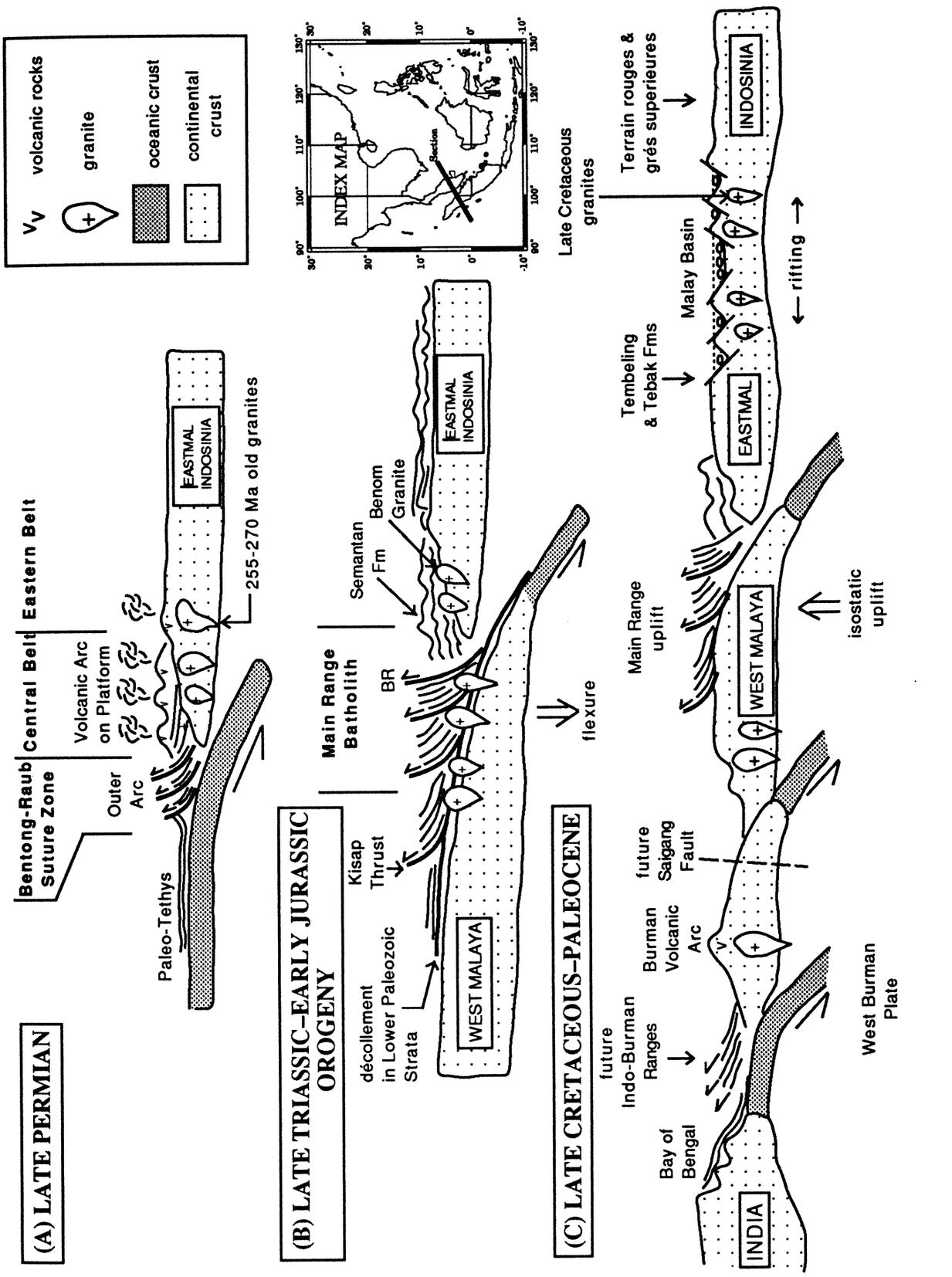

Figure 2.1. Summary of the tectonic evolution of Southeast Asia, from Late Permian to early Tertiary, based on the geology across the profile shown in index map. (A) Late Permian phase of convergent margin tectonics at the northern margin of the Paleo-Tethys. (B) Late Triassic–Early Jurassic collision phase (Indosinian Orogeny). Suturing of Western Malaya Block with EastMal, leading to formation of Main Range Batholith. (C) Late Cretaceous–Paleocene phase of post-orogenic tectonics in Sundaland, characterised by continental rifting. (Redrawn and simplified from Hutchison, 1989a).

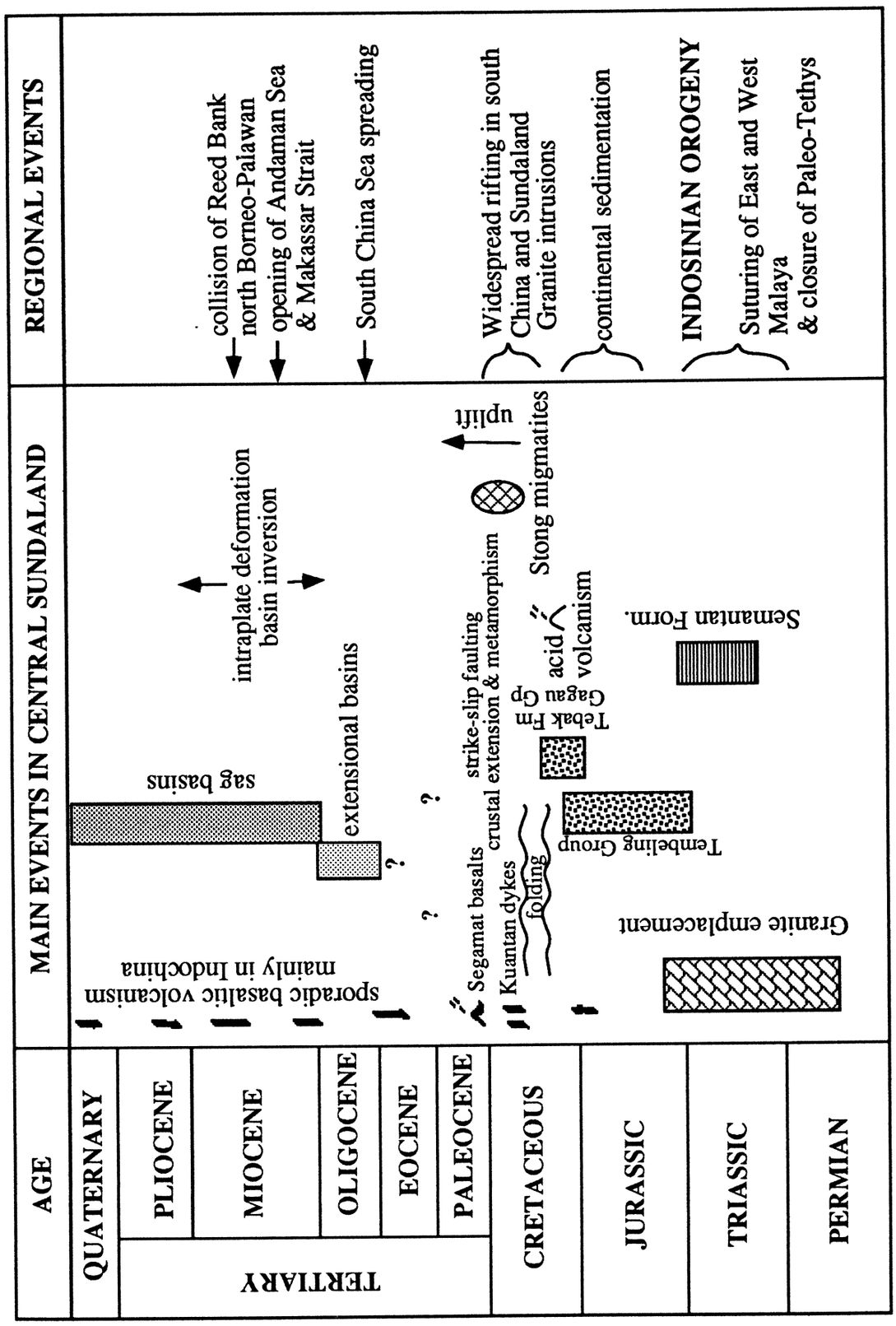

Figure 2.2. Summary of the major tectonic events in Southeast Asia.

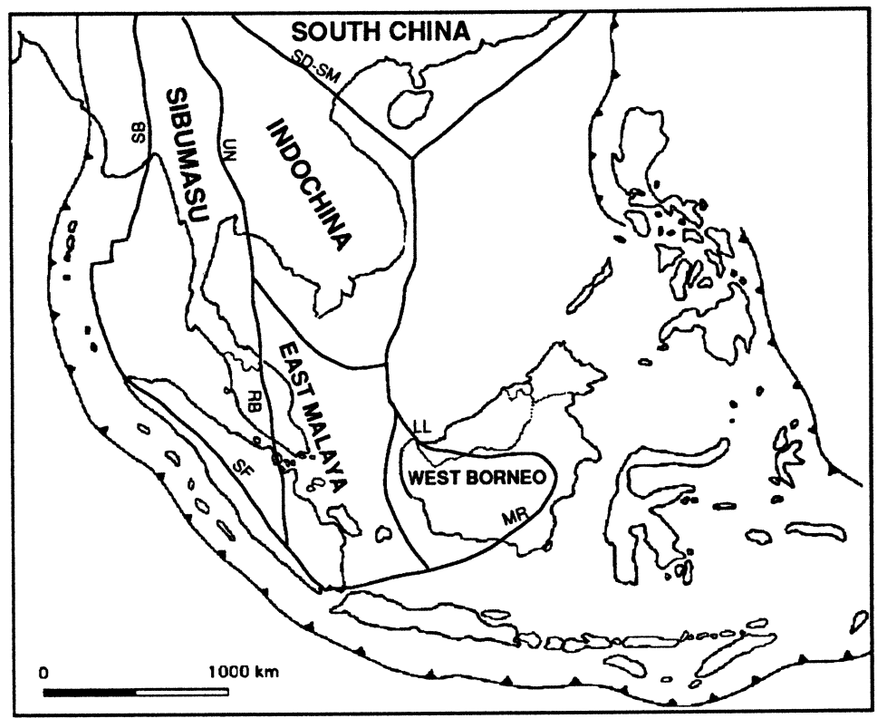

Figure 2.3. Pre-Tertiary tectono-stratigraphic terranes in Southeast Asia (Modified after Metcalfe, 1988). Major Pre-Tertiary suture zones: UN– Uttaradit-Nan, SD-SM– Song Da-Song Ma, SB– Shan Boundary, RB– Raub Bentong, SF– Sumatra Fault Zone, LL– Lupar Line, MR– Meratus Ophiolite.

"tin islands" off Sumatra. Structures formed during the orogeny have a predominantly N–S to NNW–SSE structural grain, as shown by the linear belts of granites on Peninsular Malaysia and Thailand, roughly parallel to the Paleo-Tethyan suture. Sundaland has remained emergent since the Indosinian collision and no marine sediments younger than the Triassic are known to exist (Hutchison, 1989a). The subsequent period, from Late Triassic through to Early Cretaceous, is usually thought of as one of relative tectonic quiescence. Sedimentation was largely continental, as indicated by the nonmarine intermontane basins in the Khorat Plateau, Thailand, and the Tembeling-Gagau formations in Peninsular Malaysia. Some Triassic extensional basins in northern Thailand may have formed as a result of late-orogenic extensional tectonics (Gabel *et al.*, 1993). Sedimentation in the Central Belt of Peninsular Malaysia also seems to have taken place in an

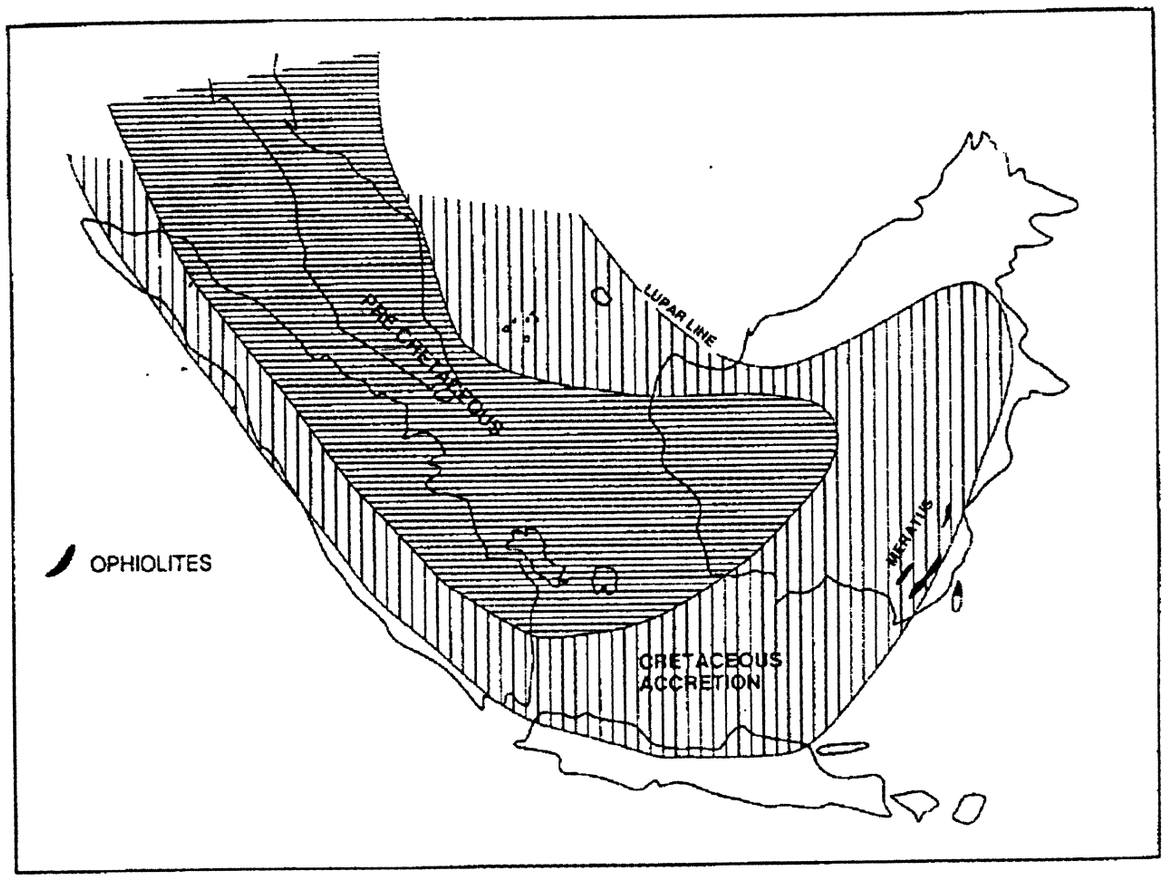

Figure 2.4. Schematic map of Sundaland which consists of a continental core, mantled by a belt of Jurassic to earliest Tertiary subduction and acrretionary complexes (after Clure, 1991).

extensional graben setting (Metcalfe, 1989).

2.2.2 Late Mesozoic Post-Orogenic Tectonics

From the Late Mesozoic to the early Tertiary, the western, southern, and eastern margins of Sundaland were the sites of active subduction and continental accretion. The end result is a wide zone of Jurassic to earliest Tertiary subduction-related complexes around the Indosinian core (Fig. 2.4). Ophiolitic suture zones, which mark the former sites of subduction, may be traced from eastern Burma along the Saigang Fault Zone to west Sumatra and into south Borneo (Hutchison, 1975). They represent an important phase of continental accretion onto the southern margin of Eurasia during the Jurassic to Late Cretaceous, probably associated

with the closure of Neo-Tethys Ocean (Şengör and Hsü, 1984). In Sumatra, this suture is recognised by ophiolite and melange of the Woyla Group, which was accreted during the early to middle Cretaceous (Wajzer *et al.*, 1991). Eastwards, in southern Borneo, the Meratus Ophiolite has been dated as Cenomanian to Turonian (Hamilton, 1979) and marks the southern limit of Sundaland.

The eastern margin of Sundaland was also a subduction margin (Daly *et al.*, 1991), for late Cretaceous granites are widespread in South China (Hutchison, 1989a). During Paleocene times, the south China margin evolved through an extensional regime, forming rift basins such as the Pearl River Mouth basin (Su *et al.*, 1989) and a new ocean basin, the South China Sea basin (Taylor and Hayes, 1980; Ru and Pigott, 1987). To the south, an ocean basin (the proto-South China Sea) was being subducted under the northern margin of Borneo, producing the melange and flysch belt along the Lupar line (Williams *et al.* 1986, 1988), which continues east- and northeastwards as the massive Rajang Group accretionary complex (Hutchison, 1989a). The northward continuation of this Late Cretaceous to Oligocene subduction complex is rather obscure but, probably, lies along the steep continental margin east of Vietnam, which is, probably, a major dextral transform fault (Hamilton, 1979) or shear zone (Roques *et al.*, 1995). Late Mesozoic–Early Tertiary tectonism in the area culminated in the uplift and erosion of the pre-Tertiary surface prior to renewed extension and subsidence in the early Tertiary which led to the formation of Tertiary extensional basins. Subduction along the northern margin of the West Borneo Basement (marked by the Lupar Line Ophiolite and the Rajang Group flysch belt) also falls within a similar time frame but may have continued into the early Miocene (Williams *et al.*, 1988; Tan and Lamy, 1991).

In Figure 2.2, we can see the contrasting tectonic styles between the events before, during, and after the Indosinian Orogeny. The rift-drift phase is characterised by subduction and continental accretion and, finally, collision in late Triassic times. The tectonic style during the rift-drift phase is basically contrac-

tional, dominated by subduction and continental accretion, and is characterised by acidic to intermediate magmatism (Mitchell, 1981). Crustal thickening, uplift, and granite magmatism dominates the collisional phase, and were followed with syn- or late-orogenic crustal extension, which may have resulted in the formation of intermontane basins, in which sedimentation is known to have taken place until at least the early Cretaceous (Burton, 1973). Burton (1973) described the Gagau Group (?upper Jurassic to lower Cretaceous) as consisting of continental sediments and extrusive rocks in a wedge-shaped basin, bounded to the west by the east-dipping NNW-trending Lebir Fault. This suggests, therefore, that some of the major NW-trending strike-slip faults, including the Lebir Fault, may have been active since late Jurassic times. The faults were generally thought to be Late Cretaceous-Tertiary features (Tjia, 1972).

In contrast, the post-orogenic phase is dominated by extensional and strike-slip tectonics, with sporadic but widespread occurrences of intraplate basaltic magmatism — an element that is particularly absent during the pre-collisional phase (Fig. 2.2). Hutchison (1989a, p. 181) interpreted this change in tectonic style as being due to post-orogenic rift tectonics. Orogenic belts with thickened crust and high elevation are likely to undergo extensional collapse (Dewey, 1988). The main implication is that the Sundaland craton has been under tension since at least Jurassic times, although widespread rift basin formation did not take place until probably late Eocene–Oligocene times.

Because of the lack of basaltic magmatism during much of the Jurassic, it is probable that the Jurassic-Cretaceous Tembeling Group and Terrain Rouge continental facies (*cf.* Hutchison, 1989a) represent deposition in intermontane basins formed by "thin-skinned" upper crustal extension without mantle involvement. Only in mid–late Cretaceous times did whole lithospheric stretching began to take place, accompanied by basaltic magmatism and, in places, resulted in the formation of rift basins. The mid-Cretaceous folding event which affected the Tembeling Group rocks (Harbury *et al.*, 1990) appears to coincide with this

major change in tectonic climate. The earliest record of basaltic volcanism in Peninsular Malaysia is in the Upper Jurassic-Cretaceous Gagau Group (Hutchison 1973a, p.209) and marks the beginning of rift-related intraplate volcanism in Sundaland. Other well-known occurrences include the 110 Ma (Albian) basaltic dykes at Kuantan (Haile *et al.*, 1983) and the 62 Ma basaltic lavas in Segamat (Bignell and Snelling, 1977).

Apart from basaltic volcanism and dyke intrusion, Late Cretaceous tectonism is also indicated by widespread granite magmatism and uplift of high-grade metamorphic rocks along the central belt of Peninsular Malaysia. Burton and Bignell (1969) found abnormally young ages of granites in western Thailand and speculated that a major event of crustal heating occurred in the late Cretaceous. Hutchison (1989a) has reviewed the occurrences of Late Cretaceous granites in central Thailand, in Peninsular Malaysia, in Sumatra, and in the adjacent offshore on the Sunda Shelf beneath the Malay and West Natuna basins. Hutchison (1989a, p. 180) correlated these granites with the "Yenshanian phase" in southern China and attributed them to a regional thermal and rifting event. He argued that this event was also reponsible for Cretaceous granites in the Central Belt and as well as the extension in the Gulf of Thailand. Along the Central Belt of Peninsular Malaysia, there is a linear zone of Cretaceous migmatitic granites and high-grade metamorphic rocks *e.g.* the Stong and Benta migmatite complexes (Hutchison, 1973; Singh *et al.*, 1984), which are probably correlatable with the I-type granites of the same age in central-north Thailand (Cobbing *et al.*, 1986). Recently, MacDonald *et al.* (1993) described a possible late Cretaceous metamorphic core complex in NW Thailand. A similar origin for the Stong and other high-grade metamorphic bodies along the Central belt of Peninsular Malaysia is likely. The faulted and sheared margins of these central belt complexes (Hutchison, 1973, p.267), bringing amphibolite facies rocks in juxtaposition with greenschist cover sequence suggest that the uplift of these rocks may have been due to extreme crustal extension, rather like in the metamorphic core complexes in the Basin and Range province, USA (Coney and Harms, 1984). Gravity studies of Ryall (1982)

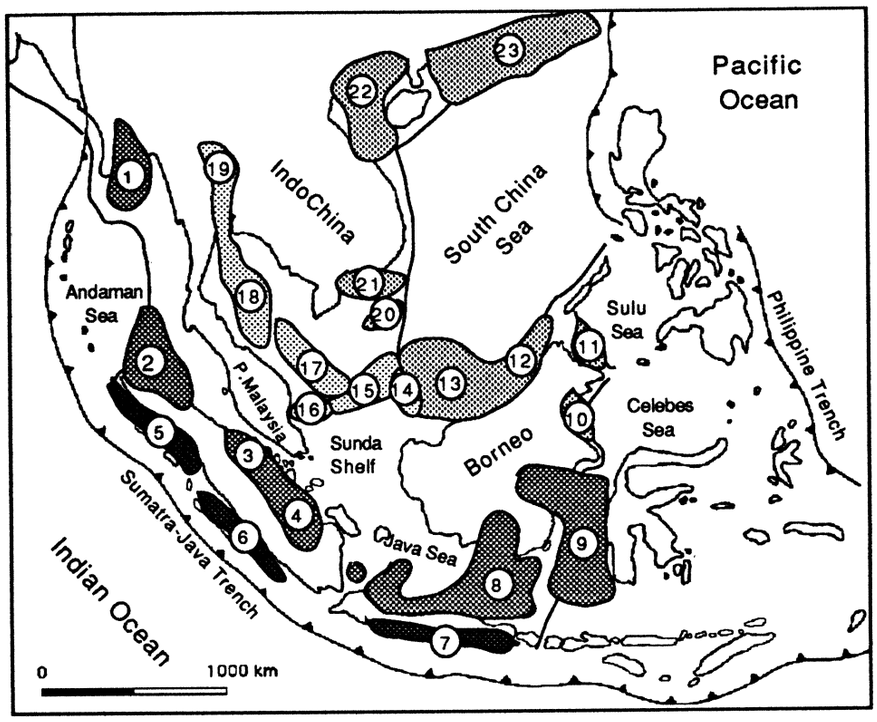

Figure 2.5. Map showing the location of major Tertiary basins in Southeast Asia. The Penyu and Malay Basins are numbered 16 and 17, respectively. Dark stipple represents fore-arc basins, medium stipple — back-arc basins, light stipple — interior extensional basins.

and Loke *et al.* (1983) have shown that the Central Belt is underlain by a relatively thin crust, which also suggests that an extensional event had affected the area.

2.3 Tertiary Basins

The early Tertiary saw widepread extensional tectonism and basin formation across Sundaland. The tectonic setting and hydrocarbon potential of the Tertiary basins have been discussed by several workers (Murphy, 1975; Seoparjadi *et al.*, 1975; Beddoes, 1980; Hutchison, 1984; Hutchison, 1989a). Murphy (1975) classified the Tertiary basins in Southeast Asia according to their geographical positions: shelfal, continental margin, archipelagic, and marginal sea basins. The

Thai, Malay, and Penyu Basins were regarded as "shelfal" basins. Hutchison (1984, 1989a) proposed a plate tectonics classification of the basins using the schemes of Bally and Snelson (1980) and Kingston *et al.* (1983). According to this classification, the Malay, Penyu and West Natuna Basins are either intracontinental rift or "wrench/shear" basins. As Hutchison (1989a) pointed out, some of the terms used for the basins are purely geographical and do not reflect our understanding of the origin of the Basins. The structural trend of the Penyu and West Natuna Basins is E–W to ENE–WSW whereas the Malay Basin is elongate in the NW–SE direction (Fig. 1.1). In contrast, the extensional basins in the Gulf of Thailand are predominantly N-trending structures. It is difficult to explain the contrasting structural trends in these basins using a simple rifting or wrench model. Harder *et al.* (1992) explained it in terms of a rotating stress model, in which the continuing indentation of India into Eurasia caused the rotation of the maximum principal stress directions from E–W to N–S.

The map in Fig. 2.5 shows that the extensional basins fall broadly into two groups based on their locations:

1. Basins that are *peripheral* to Sundaland ("Circum Sunda basins", Thamrin, 1985), *i.e.* including the fore-arc and back-arc basins associated with the Burma-Sunda-Java arc-trench system, and

2. Basins in the *interior* of Sundaland *i.e.* including the intermontane basins in Thailand and the offshore basins in the Gulf of Thailand and Natuna Sea area.

The time of basin initiation is not known for certain because the biostratigraphic evidence from the lacustrine synrift sediments, which seldom contain fossils, are unreliable. Figure 2.6 shows the stratigraphy of major basins in Southeast Asia compiled from the literature. The oldest sediment in the Gulf of Thailand and offshore Peninsular Malaysia appears to be slightly younger than those in the back-arc basins of Sumatra. Most of the peripheral basins in Sumatra and the

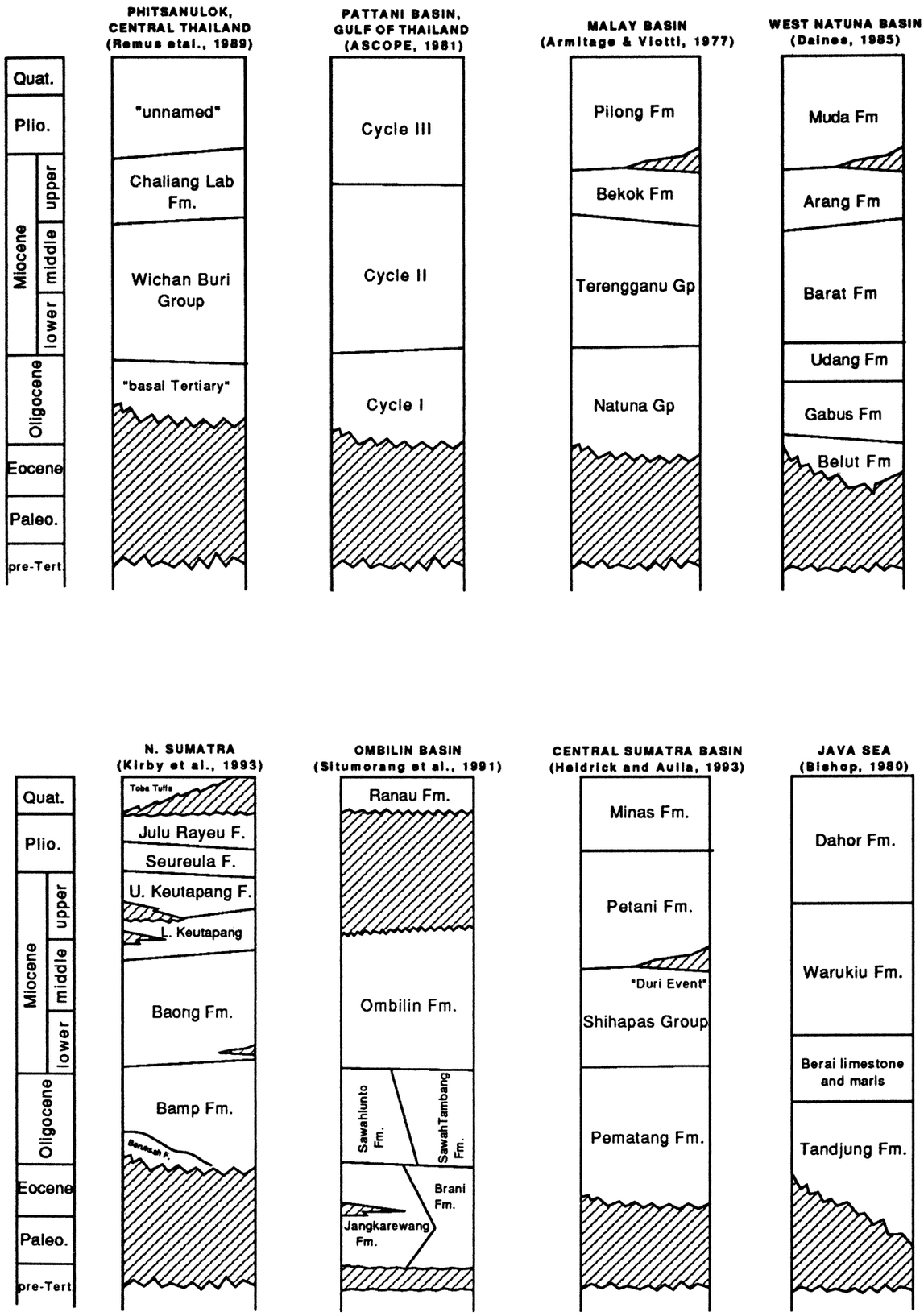

Figure 2.6. Stratigraphy of extensional basins in Sundaland. (A) Interior cratonic basins: Thai, Malay, West Natuna Basins. (B) Peripheral basins: Sumatra and Java back-arc basins.

Java Sea probably began forming in Paleocene–Eocene times but the intracontinental basins, such as the Malay, West Natuna and Thailand Basins, seem to have formed somewhat later, during the latest Eocene to early Oligocene. Sedimentation in most basins was, generally, lacustrine in pre-Oligocene times (Gibling, 1988; Williams *et al.*, 1995) but, some basins that were partly connected to the open sea, *e.g.* the Malay and West Natuna Basins, became more marine during the later part of their development (Beddoes, 1980; Daines, 1985).

2.3.1 Origin of Extensional Basins

The tectonic origin of the extensional basins in Sundaland is still poorly understood. Some of the proposed causes of basin formation are:

1. Back-arc extension resulting from subduction and oblique convergence along the Sumatra-Java Trench (Kingston *et al.*, 1983; Hutchison, 1989a; Daly *et al.*, 1991),

2. Formation by "pull-apart" along major left-lateral strike-slip faults by extrusion tectonics (Tapponnier *et al.* 1982, 1986),

3. Formation by combination of back-arc rifting and wrench faulting (Hamilton, 1979; Crostella, 1981).

4. Rifting following a prolonged thermal event accompanied by alkaline intrusives and, later, granite magmatism (Hutchison 1989a, his fig. 5.15).

5. Extension in response to stress field related to the collision of India and Eurasia (Harder *et al.*, 1992; Huchon *et al.*, 1994).

6. Formation of Gulf of Thailand and Malay Basins by dextral shear along pre-existing NW-striking faults (Packam, 1993; Polachan *et al.*, 1991).

7. Development of Sumatran "back-arc" basins as pull-aparts along NW-striking strike-slip faults resulting from oroclinal bending of the Andaman-Sumatra-Java Arc (Hutchison, 1992a).

From the existing models, it is apparent that the main disagreement between workers is with regard to whether the intracontinental basins in Sundaland were formed by back-arc extension (Ismail *et al.*, 1994) or by pull-apart along strike-slip faults (Polachan and Sattayarak, 1989). Back-arc extension may be applicable to the peripheral basins such as the central and southern Sumatra basins, which were also controlled by strike-slip faulting *i.e.* formation by a pull-apart mechanism (Situmorang and Yulihanto, 1985; Moulds, 1989). However, a back-arc origin for the interior basins such as the Malay and West Natuna Basins is considered unlikely because these basins are remote from the subduction zone. The Malay Basin is ~1000 km away from the Sumatra trench.

The development of Tertiary extensional sedimentary basins in Southeast Asia is interpreted, usually, in terms of the extrusion tectonics hypothesis (Tapponnier *et al.* 1982, 1986). According to the hypothesis, the indentation of India into Eurasia caused strike-slip faulting and extrusion of continental blocks away from the collision zone. The implication for Southeast Asia is that pull-apart basins developed along major "indentation-linked" strike-slip faults (Woodcock and Fischer, 1986) such as the Wang Chao, Three Pagodas, and Red River Faults. Daines (1985) and Polachan and Sattayarak (1989) have used this model to explain the formation of the West Natuna and Thailand Basins. The Thai, Malay and West Natuna Basins were envisaged to have formed along NW-trending left-lateral faults — the Wang Chao and Three Pagodas Faults — emanating from the eastern syntaxis of the collision zone (Fig. 1.2). Daines (1985) named the zone of extensional basins from the Gulf of Thailand to Natuna the "Malay–Natuna–Lupar Shear Zone" (Fig. 2.7). Wood (1985) also extended the shear zone, which he called the "Natuna Shear" (Wood, 1985, his fig. 22), into west Kalimantan (Borneo). There is no evidence to suggest that these shear zones exists. We know

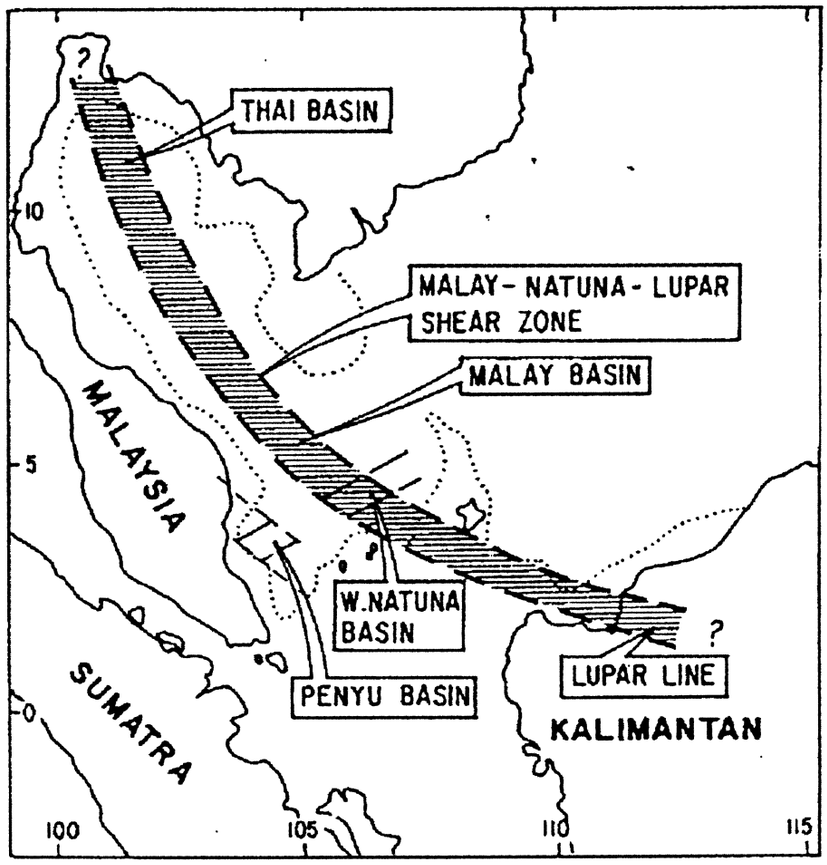

Figure 2.7. Sketch map of the "Malay–Natuna–Lupar Shear Zone" proposed by Daines (1985). The shear zone is shown by Daines to transect the Natuna basement ridge, which is a major structural discontinuity between the northern Sunda Shelf and West Borneo basement.

that the Gulf of Thailand, Malay and Natuna Basins are separate extensional basin systems with different orientations and are separated by major basement structural discontinuities (ASCOPE, 1981). In particular, the Natuna Ridge or "Swell" (Haile, 1973) is long known to be a positive structural feature throughout the Tertiary evolution of the area.

Ongoing debate regarding the India-Eurasia collision centres upon whether the indentation of India is accommodated by underthrusting beneath Tibet, by lateral extrusion, or by crustal thickening. Dewey *et al.* (1989) have discussed the evidence against underthrusting or significant lateral extrusion and concluded that the indentation of India into Eurasia is accommodated mainly by crustal thickening in Tibet. Recent seismicity on the strike-slip faults in the region (Dain

et al., 1984; Allen *et al.*, 1984; Peltzer and Tapponnier, 1988) suggests right-lateral motion, consistent with the predicted overall dextral shear regime east of the collision zone (Dewey *et al.*, 1989). Holt *et al.* (1991) also showed evidence for distributed dextral shear and clockwise rotation in the area.

The picture seems to have been quite different during the Tertiary. Tapponnier *et al.* (1986) have presented field and aerial photographic evidence for left-lateral motion on the Red River, Wang Chao, and Three Pagodas Faults during the mid-Tertiary. Recent field studies by Lacassin *et al.* (1993) give minimum estimates of Oligocene-Miocene left-lateral displacements of ~330±60 km on the Red River Fault but only ~35 ±20 km on the Wang Chao Fault. Left-lateral motion on the Wang Chao Fault has been dated as ~30 Ma (Maluski *et al.*, 1993) whereas that of the Red River Fault is ~35–24 Ma (Scharer *et al.* 1990, 1993, 1994). These studies suggest, therefore, that there had been significant left-lateral motion along some of the major NW-trending strike-slip faults during Oligocene-Miocene times, probably, in an overall dextral shear regime. Right-lateral slip on faults such as the Red River must have been a relatively recent, *i.e.* Quaternary, phenomenon (Allen *et al.*, 1984).

Several major, NW-trending, apparently left-lateral, faults also transect Peninsular Malaysia but neither their history nor their ages are known for certain. Left-lateral offsets of geological boundaries by the faults are in the order of 20 km (Tjia, 1972). The ages of the faults have been said to be anywhere between late Cretaceous to early Tertiary (Tjia, 1972; Burton, 1973). Field evidence (Burton, 1973) suggests that the Lebir Fault may have controlled the deposition of the Gagau Group, which is of ?upper Jurassic to lower Cretaceous age, whereas the Bukit Tinggi Fault may have influenced sedimentation in the Batu Arang Coal Basin, which has been dated palynologically as Oligocene–Miocene (Ahmad Munif, 1993). It is reasonable to conclude, therefore, that the NW-trending strike-slip faults were active during Jurassic/Cretaceous, and were reactivated during the Tertiary. The observed left-lateral displacements on these faults could be the

result of clockwise rotation of blocks about vertical axes while the entire region was deforming in an overall dextral shear regime brought about by the indentation of India into Eurasia (Dewey *et al.*, 1989). Dewey *et al.* (1989), Molnar and Lyon-Caen (1989), and England and Molnar (1990) have shown evidence for block rotation associated with strike-slip faults in eastern Tibet. The main implication of these observations is that the faults probably existed before the India-Eurasia collision, and were reactivated features.

Another major unresolved problem in Southeast Asia concerns the paleomagnetic data. Plate tectonic reconstructions of the region (Audley-Charles *et al.*, 1988; Hutchison, 1989a; Jolivet *et al.*, 1989; Rangin *et al.*, 1990; Daly *et al.*, 1991) have shown that in Late Cretaceous times, prior to the India-Eurasia collision, the southern margin of Eurasia was oriented WNW. The area has since rotated clockwise by more than 50° to its present position as India pushed northwards into Eurasia pass Sumatra and Burma, as supported by recent palaeomagnetic data (Otofuji *et al.* 1990; Huang and Opdyke 1991, 1993; Funahara *et al.* 1993). In Sumatra, Peninsular Malaysia, and Borneo, the paleomagnetic evidence is less convincing or, even, contradicting. The data from regions south of Peninsular Thailand (except Sumatra but including western Borneo) (Schmidtke *et al.*, 1990; Fuller *et al.*, 1991) suggest anticlockwise rotation of Peninsular Malaysia and Borneo, contrary to the prediction of the extrusion model. More recent results from Borneo (Lumadyo *et al.*, 1993) suggest that Borneo has been in its present position since the Eocene, and that there has been no anti-clockwise rotation since that time, as found by the previous studies. Various *ad hoc* explanations have been suggested to explain the discrepancies: *e.g.* unreliable measurements because of poor dating, remagnetization, and block rotation associated with shear deformation (Yan and Courtillot, 1989; McCabe *et al.*, 1993; Richter *et al.*, 1993). Complex vertical-axis rotation history could have occurred in such a highly faulted region undergoing transpressional tectonics; the sense of rotation of fault-bounded blocks depends on their orientation with respect to the transport direction (Garfunkel and Ron, 1985; Beck, 1989). In southern China, for example, Gilder *et al.*

(1993) observed local anticlockwise rotations associated with left-lateral motion along major faults. Hence, the mid-Tertiary deformation of Sundaland may be the result of *distributed* simple shear deformation accommodated by motion on pre-existing fractures in the Mesozoic basement, rather than by localised extension along *discrete* strike-slip fault zones as supposed in the extrusion model (*cf.* Tapponnier *et al.* 1982).

2.3.2 Basin Inversion

The Tertiary extensional basins in Southeast Asia underwent a phase of tectonic inversion in late Miocene times. This regional tectonic event has been recorded in the peripheral basins of Sumatra and the interior basins of southern and northern Sunda Shelf (Letouzey *et al.*, 1990; Ginger *et al.*, 1993). Basin inversion is manifested by folding in the Neogene strata, resulting in the so-called "Sunda folds" (Eubank and Makki, 1981). The folds are, in many places, truncated by a regional late Miocene–Pliocene unconformity (ASCOPE, 1981; Daines, 1985). The geometry of the inversion structures on the southern and northern Sunda Shelf have been described in some detail by Letouzey *et al.* (1990) and Ginger *et al.* (1993).

Locally, especially in Thailand, the regional inversion event was accompanied by basaltic magmatism. In the Phitsanulok Basin, for example, the regional unconformity is associated with basaltic lavas, dated at 10 Ma (middle-late Miocene) (Chinbunchorn *et al.*, 1989). Late Miocene diorite stocks have been reported from the margins of the Chao Phraya Basin (Achalabhuti, 1975). These occurrences of basaltic magmatism suggest a relatively widespread igneous activity in the region. Flower *et al.* (1992) documented two phases of basaltic magmatism associated with fracture intersections throughout Indochina, Thailand, and China, one at ~15 Ma and another at 0.5 Ma.

Structures resulting from basin inversion form an important type of hydrocar-

bon traps in Southeast Asian basins. Several workers have proposed a mechanism of right-lateral strike-slip faulting (dextral wrenching) in the basement as a cause of the inversion in the Malay and West Natuna Basins (Hamilton, 1979; Daines, 1985; Packam, 1993; Ginger *et al.*, 1994), while others (Letouzey, 1990) favours a simple mechanism of shortening. As yet, the cause of basin inversion is still poorly understood. Many authors believe that the inversion may related to stresses transmitted from plate boundaries (Letouzey *et al.*, 1990). Possible causes of inversion that have been suggested are:

1. Opening of the Andaman Sea during late Miocene times (Daly *et al.*, 1991).

2. Collision of microcontinental fragments along the northern Borneo margin in association with sea-floor spreading in the South China Sea (Hutchison, 1992a).

3. N–S compression produced by collision of Sulawesi and Reedbank along the eastern and northern margins of Sundaland, coupled with the resistive force in the south due to northward subduction along the Sunda arc (Letouzey *et al.*, 1990).

Chapter 3

Structure I: Penyu Basin

The Penyu Basin forms the western part of an E- to NE-trending basin system that extends from the east coast of Peninsular Malaysia to the South China Sea (Fig. 1.1). Its continuation into the Indonesian side of the border is known as the West Natuna Basin. The two basins have always been regarded as separate, although they appear to be structurally contiguous (Fig. 1.4). Unlike the West Natuna Basin, however, the Penyu Basin has not been well studied, probably because it is smaller and, hence, is thought to have a low potential for hydrocarbons. The Penyu Basin is ideal for studying extensional basin structures because its shallow pre-rift basement surface has been relatively well-imaged by seismic reflection. A detailed study of the Basin may help us understand better the evolution of similar basins in the region.

The Penyu Basin is bounded to the north by the Pahang Platform, which is the offshore continuation of the Eastern Belt granitic terrain of Peninsular Malaysia, and to the south by the Singapore Platform, which is part of the northern Sunda Shelf — the submerged part of Sundaland continental basement. The Basin becomes shallower westwards towards the Peninsular Malaysian coastline beneath Quaternary sediment of the Pahang River Delta. The exact timing of basin formation is unknown, but analogy with the West Natuna Basin (Daines, 1985) suggests that it was formed, probably, during the Late Eocene to Early Oligocene times (~40–35 Ma).

This chapter describes the stratigraphy and structure of the Penyu Basin,

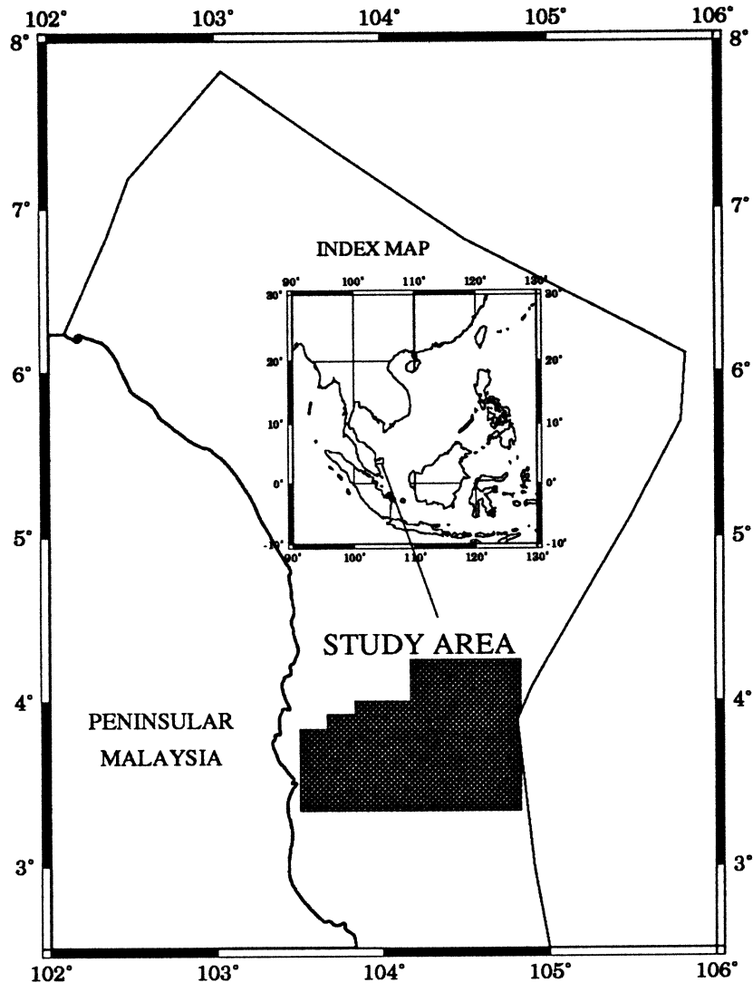

Figure 3.1. Map showing the location of Penyu Basin study area.

based on analysis of seismic reflection and well-stratigraphic data (Figs. 3.1 and 3.2). The only previous study of the Basin was a master's thesis by Ngah (1975), based on a limited dataset consisting of late 1960s and early 1970s vintage seismic data. As a result, the major basin-bounding faults were not very clearly resolved. High quality data, acquired during the 1981–1990 period through hydrocarbon exploration, provide the opportunity to re-examine the Basin's structure in more detail. A total of ~3500 line km of processed seismic data was used in this study. The aims of this study are to:

1. Map the major basin-bounding faults and study the fault styles and basin geometries

2. Identify main marker horizons in the seismic data and subdivide the basin

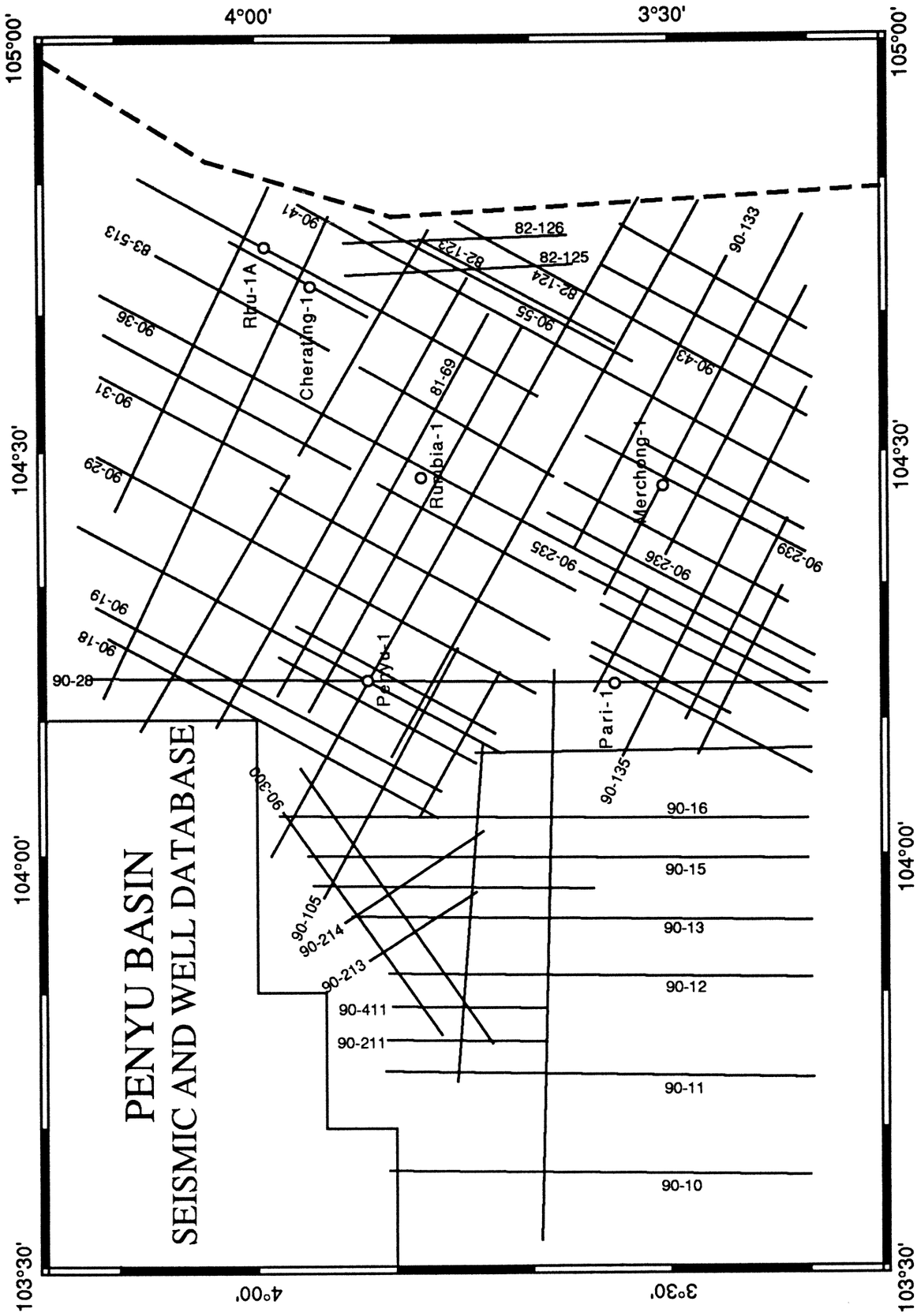

Figure 3.2. Location of seismic lines and exploration wells used in the study of the Penyu Basin. The seismic data are industry processed and migrated, 60-fold seismic reflection data, with 12.5 m common-depth-point interval, displayed at a horizontal scale of 1:50000 and a vertical scale of 5 cm s^{-1} two-way travel time. The processing steps are described in the text. Labelled lines are those shown in the figures in the chapter.

fill into stratigraphic units

3. Map stratigraphic horizons in two-way travel time (TWTT), and carry out depth conversion using available velocity data.

4. Examine fault patterns and geometries and interpret the kinematic evolution

The study shows that the development of the Penyu Basin, by roughly N–S extension, was controlled by two sets of intersecting faults: (1) NW-trending faults, which appear to have had significant strike-slip histories during the synrift extensional phase and, later, in the postrift phase when the faults were reactivated. (2) ENE-trending faults, which appear to be mainly dip-slip faults, indicating roughly N–S extension. The strong influence exerted by the NW-trending fractures on the geometry of the Penyu Basin suggests that basement weaknesses had been a major control on its development.

3.1 Seismic Data

The marine seismic reflection data used in the study were acquired by various contractors to PETRONAS between 1981 and 1990 using an airgun source (4084 in^3) and a 3 km-long streamer with 120 hydrophone groups spaced 25 m apart, towed 8 m below the sea surface. The common-depth-point (CDP) spacing is 12.5 m, giving a 60-fold data coverage. The data were recorded for 6 s two-way travel time (TWTT) with a sampling rate of 2 ms.

Processing was done commercially by DIGICON Singapore in 1991 using a conventional industry processing flow. Table 3.1 summarizes the processing parameters which are taken from the header of the seismic sections. After pre-processing, which included amplitude recovery and static corrections, the shotpoint data were sorted into CDP gathers for later stacking. Pre-stack processing involves deconvolution (essentially, to reduce noise and multiples), velocity analysis, normal-moveout correction, and muting. After stacking, deconvolution was carried out

to eliminate strong multiples that were not fully attenuated by pre-stack deconvolution. The data have been migrated using a finite-difference method based on stacking velocities obtained from velocity analysis.

For structural and stratigraphic interpretation in this study, the seismic sections are displayed at a horizontal scale of 1:50000 and a vertical scale of 5 cm s^{-1} TWTT. Interpretation was carried out manually using overlays on paper sections to map the major seismic markers and faults. The interpreted seismic sections were then digitized to generate structural contour maps and to perform time-depth conversion with the computer.

	PROCESSING SEQUENCE	
1.	Demultiplex	:At 2 ms sample rate to 6 s record length
2.	Resample	:To 4 ms with anti-alias filter applied
3.	True Amplitude Recovery	:Spherical divergence correction and exponential gain of 4 dB/s from 0 – 3.5 s
4.	Static Corrections	:Source and streamer depths = +8 m
5.	Trace Editing	
6.	Instrument Dephasing	
7.	Deflat	:Wavelet extraction and shaping
8.	Common Depth Point Gather	:60 fold, CDP interval 12.5
9.	Deconvolution	
10.	Velocity Analysis	:At 2.0 km interval
11.	Dip Moveout	
12.	Velocity Analysis	:At 1.0 km interval
13.	Normal Moveout Correction	
14.	First Break Mute	
15.	Inner Trace Mute	
16.	Common Depth Point Stack	:60 fold, CDP interval 12.5
17.	Deconvolution	
18.	Migration	:Finite difference method, layer thickness = 40 ms, using 100% stacking velocities
19.	Tau-P Filter	:Coherence enhancement
20.	Time-Variant Filter	
21.	Time-Variant Scaline	

Table 3.1. Summary of processing sequence for Penyu Basin seismic data, taken from the header of the seismic sections. Processing was done by DIGICON Singapore in 1991.

3.2 Major Structures

This section summarizes the major structural features identified in the Basin. A more detailed discussion of the structures follows later in the Chapter. Figure 3.3 is a simplified structural map of the Basin, showing the major basin-bounding faults and subbasins. Four main subbasins, or grabens, have been defined: Kuantan, Pekan, Rumbia, and Merchong Grabens. The grabens are bounded by two main sets of faults: one trending ENE–WSW (azimuth ~70°–80°) and another trending NW–SE (~100°–130°). The two largest faults are the ENE-trending Kuantan Fault, which is the border fault to the Kuantan Graben, and the NW-trending Trans-Penyu Fault which, judging from its straight map trace, appears to be an important structural discontinuity in the Basin.

Figure 3.4 is a map of the Top-Basement Unconformity, showing the main sediment depocentres in the Basin, the deepest of which is the Kuantan Graben with a total sediment thickness exceeding 8 km. This E-trending half-graben is ~20 km wide and 50 km long, and is highly asymmetrical because of the pronounced tilt of the hangingwall towards the Kuantan Fault. The Kuantan Graben is separated from the Rumbia Graben by the eastward protrusion of the Pahang Platform. The shallower western part of the Graben comprises two synthetic, northward-dipping half-grabens separated by a tilted fault block (Fig. 3.6).

The Pekan Graben, in the southwestern corner of the Basin, is a relatively small half-graben, with a maximum of only about 4 km of sediment. Its margin is determined by relatively short (<20 km) normal faults that alternate in polarity along strike (Fig. 3.6) — a characteristic feature of the East African rifts (Rosendahl, 1987) and seems to be typical of young rift zones. As a rift basin evolves, its segmented border faults may become continuous as they merge during growth (*e.g.* Trudgill and Cartwright, 1994). The Pekan Graben appears to be the conjugate half-graben to the Kuantan Graben to the north, formed by roughly N-S extension. Because its border faults are preserved as short segments,

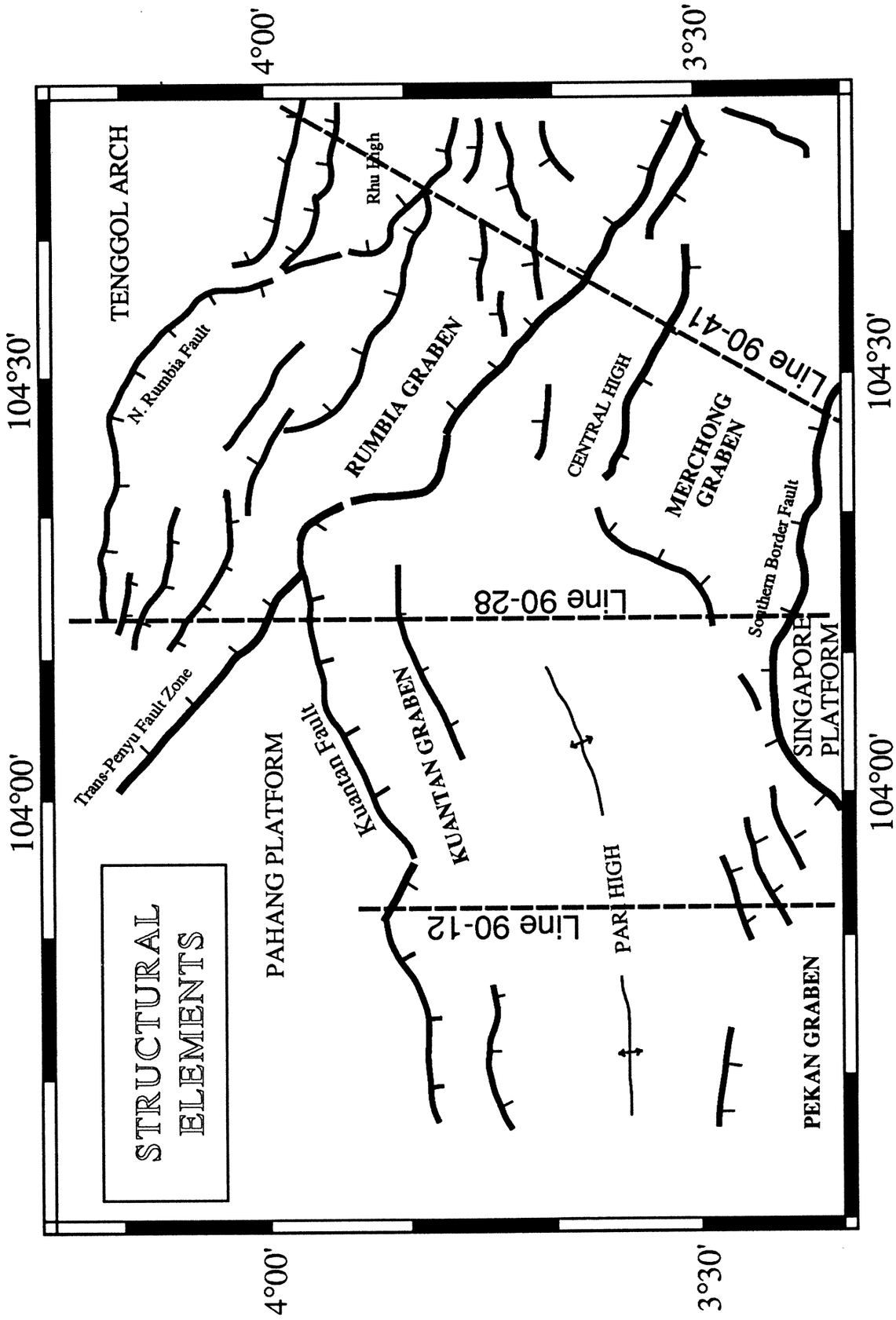

Figure 3.3. Simplified structural map of Penyu Basin showing the main grabens, border faults and intrabasin highs. (Compare with Fig. 3.4)

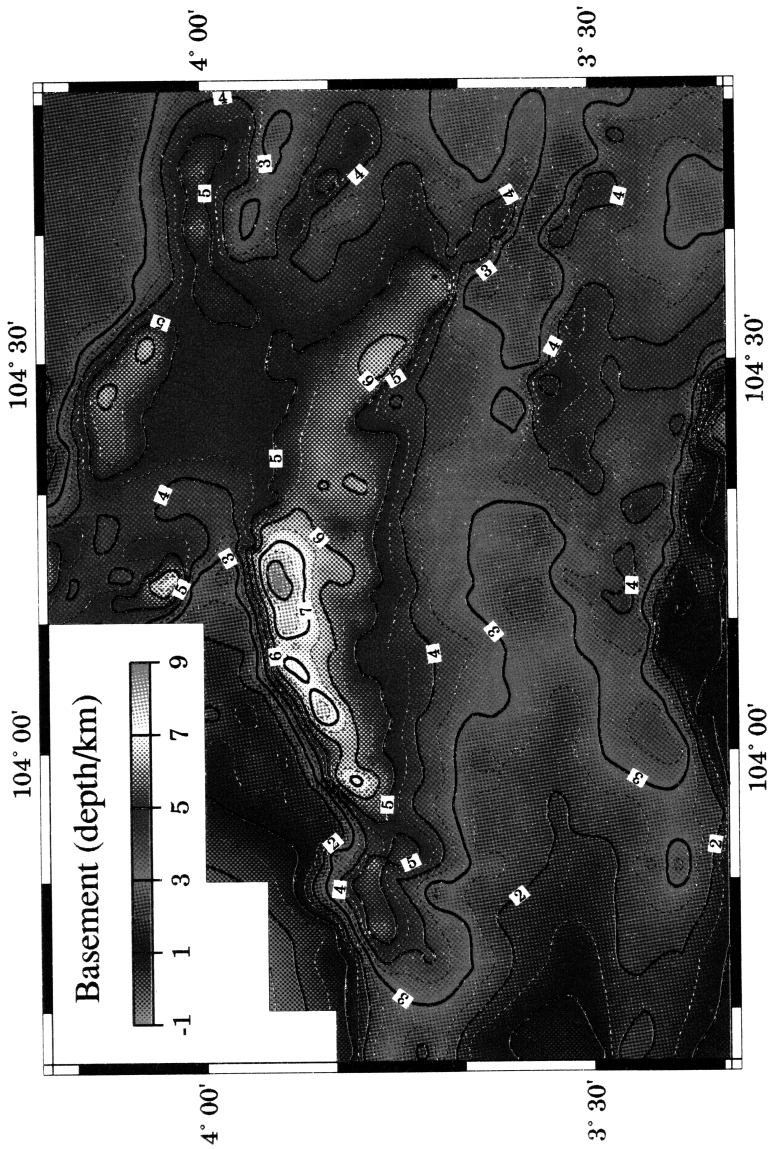

Figure 3.4. Depth of Horizon 8 (Top-Basement Unconformity), Penyu Basin. The depth to Horizon 8 is given by $Z_8 = \sum_{i=1}^{8} V_i \, \Delta t_i / 2$ where V_i and Δt_i are, respectively, the interval velocity and two-way-time thickness of the seismic unit between horizons i and $i - 1$ (see Appendix A.1 for interval velocities). (Compare with Fig. 3.31).

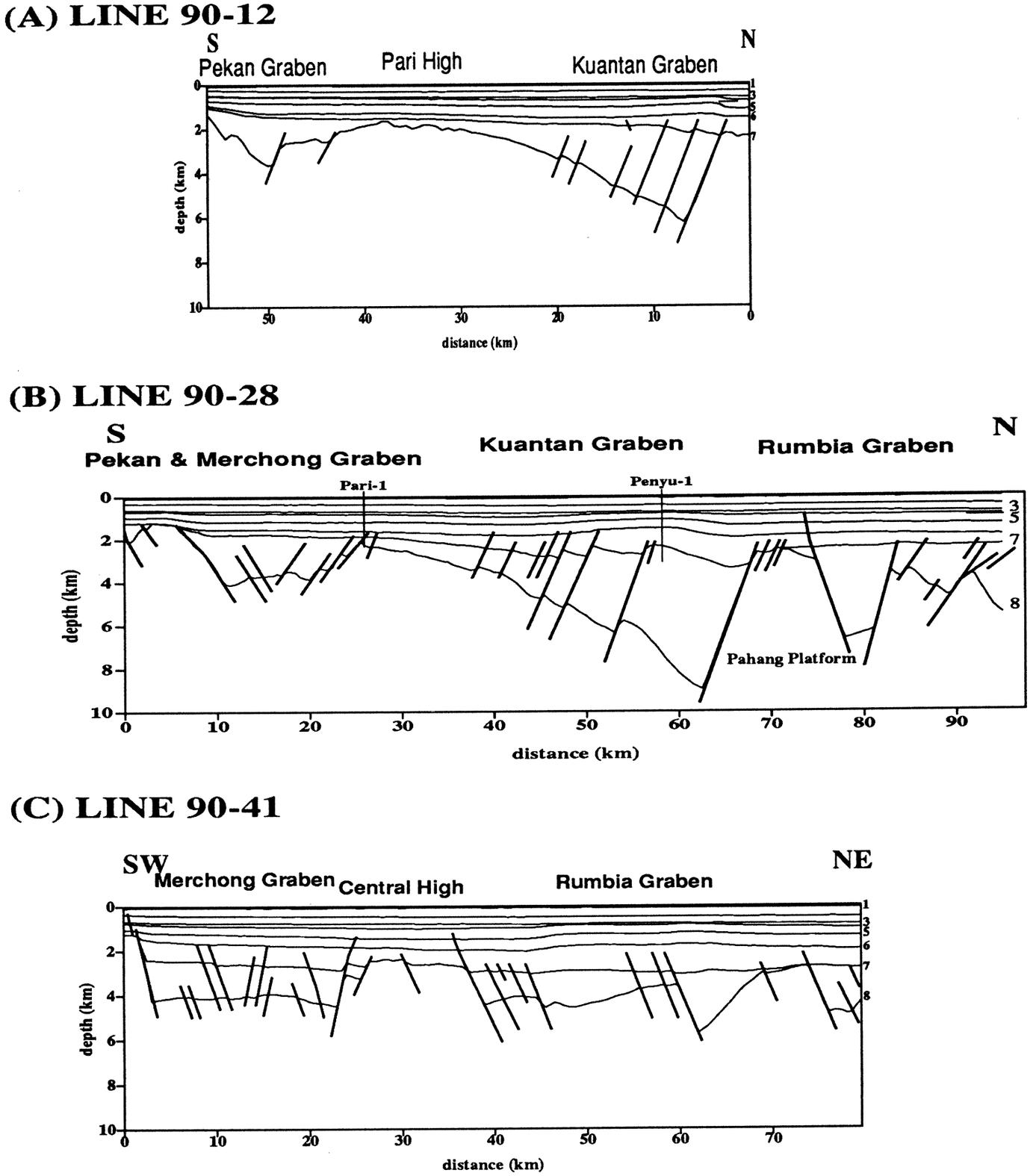

Figure 3.5. Representative geoseismic sections along three seismic lines shown in Fig. 3.3. (A) Line 90-12 (B) Line 90-28 (C) Line 90-41. Numbers on the right of each panel represents the horizon number.

the Pekan Graben probably represents a relatively immature stage of extension compared to the Kuantan Graben.

The Rumbia Graben strikes NW-SE and is bounded to the southwest by the Trans-Penyu Fault. Its northeastern margin is less pronounced; it is defined by a series of NW-trending arcuate normal faults. As will be shown later, these arcuate normal faults have shallow dips and listric geometries. The Merchong Graben, in the southeastern corner of the Basin, also strikes roughly NW–SE but has a rectangular map shape, bounded to the NE and SW by steep border faults. Seismic evidence shows that the Trans-Penyu Fault and the Merchong Graben border faults have had significant strike-slip histories, as implied also by their remarkable linearity in map view.

In Fig. 3.5, a series of depth-converted geoseismic sections (their location shown in Fig. 3.2), highlights the basic geometries and styles of faulting in the various subbasins. We can see, basically, two subbasin systems separated by the Pari/Central High: in the south is the Merchong-Pekan Graben system and in the north is the Kuantan-Rumbia Graben system. Line 90-12 (Fig. 3.5A) shows the two east-trending half-grabens, Pekan and Kuantan, separated by an intrabasin ridge, the Pari High, which represents the "interference zone" (Rosendahl, 1987) formed by the hangingwalls of the two opposing half-grabens. Line 90-28 (Fig. 3.5B) is a section across the central, deepest part of the Basin, and transects three subbasins: Merchong, Kuantan, and Rumbia. Two wells have been drilled along this profile: one located on the Pari High and encountered basement, and the other located on the crest of a major inversion structure above the deepest part of the Kuantan Graben. The Merchong Graben, at the southern end of the profile, is bounded on both sides by major faults, while to the north of the Pahang Platform, the Rumbia Graben comprises a series of narrow fault-bounded troughs. The complex faulting in that part of the Basin appears to be the result of divergent strike-slip faulting along the Trans-Penyu Fault. Lastly, Fig. 3.5C shows the contrasting geometries in the eastern part of the Basin. The Merchong

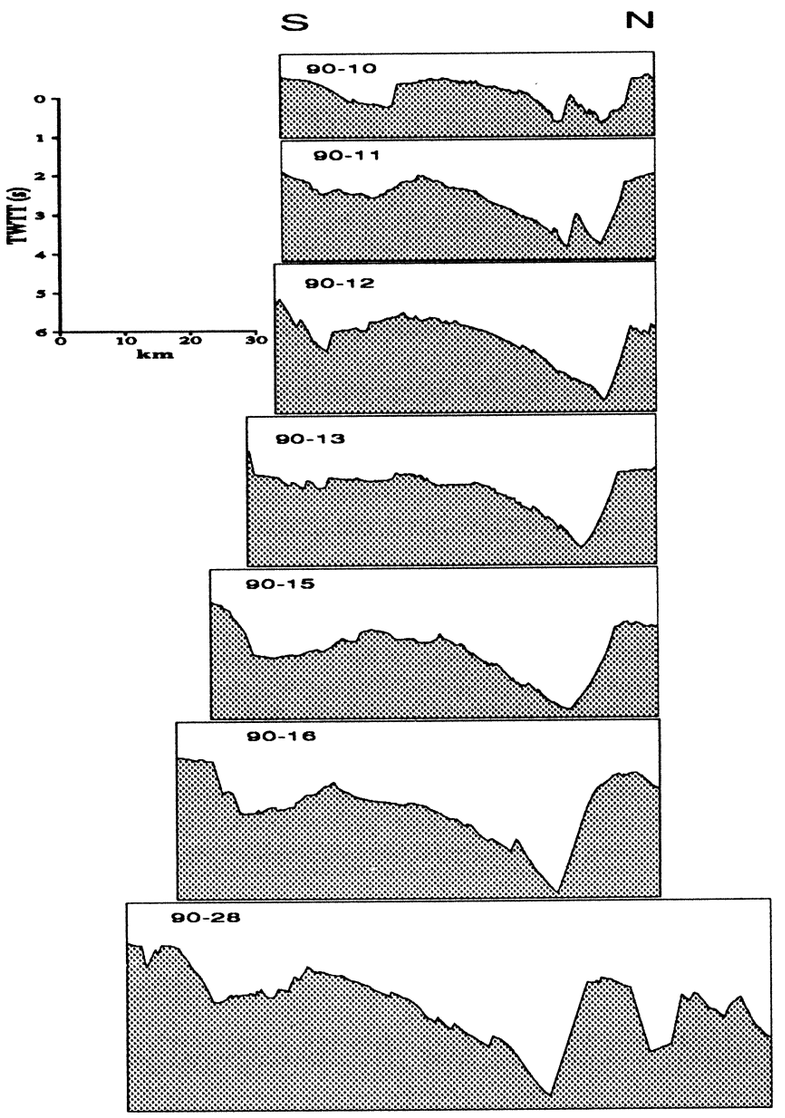

Figure 3.6. Series of N–S profiles highlighting the variation in basement topography, and the geometry of subbasins in the western part of the Penyu Basin. Note the switching of border fault polarity in the Pekan–Merchong Graben. *e.g.* compare Lines 90-10 and 90-15. Vertical scale in seconds TWTT.

Graben in the south shows remarkable symmetry, with steep bounding faults, while the Rumbia Graben to the north shows the more typical half-graben tilt-block geometry.

3.3 Stratigraphy

The stratigraphy of the Penyu Basin is based on the interpretation of seismic data, incorporating lithological and biostratigraphical information from the wells. Using the well-established principles of seismic stratigraphic analysis (Mitchum *et al.*, 1977), the basin fill is subdivided into mappable units, demarcated by marker horizons. These marker horizons were identified on the basis of their lateral continuity and tectono-stratigraphical significance. Laterally continuous, basin-wide reflectors are necessary so that stratigraphic units can be traced over the entire basin. They are surfaces associated with reflection termination and stratigraphic onlap and, therefore, are important stratigraphic markers. Figure 3.7 is from Line 90-36 at the southern side of the Merchong Graben. The figure illustrates the typical geometry in that part of the Basin, characterised by closely spaced, slightly listric, north-dipping basement faults overlain by synrift sediment wedges. Shown also are the main reflectors and unconformities, picked out as prominent reflection terminations. Most prominent of these are Horizon 8 (Top-Basement), Horizon 6 (Top-Synrift II), and Horizon 2. Note the onlap of strata within the upper part of the post-rift succession onto the southwestern margin of the Basin.

Some marker horizons represent abrupt changes in the internal reflection characteristics, which are related to changes in the depositional environment (Fig. 3.8). For example, a shale-dominated sequence deposited in a "quiet" lacustrine or shallow marine environment tends to show parallel and continuous, high-amplitude reflections. In contrast, coarse-grained sediments deposited in "high-energy" fluvial environments may not show any coherent internal reflections, and are described

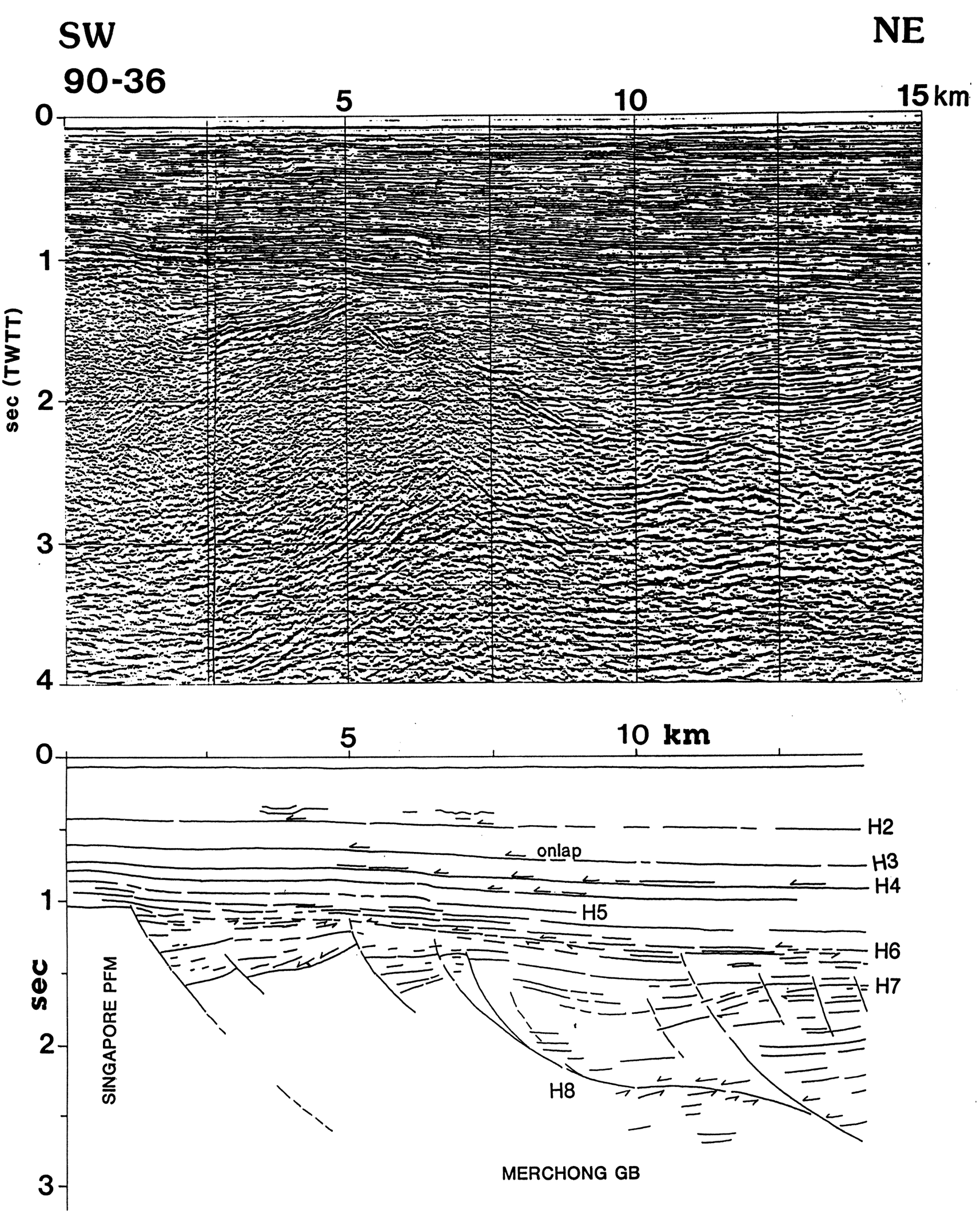

Figure 3.7. Line drawing of part of Line 90-36, from southwestern part of the Merchong Graben, showing the structural style, main horizons and reflector geometry and characteristics.

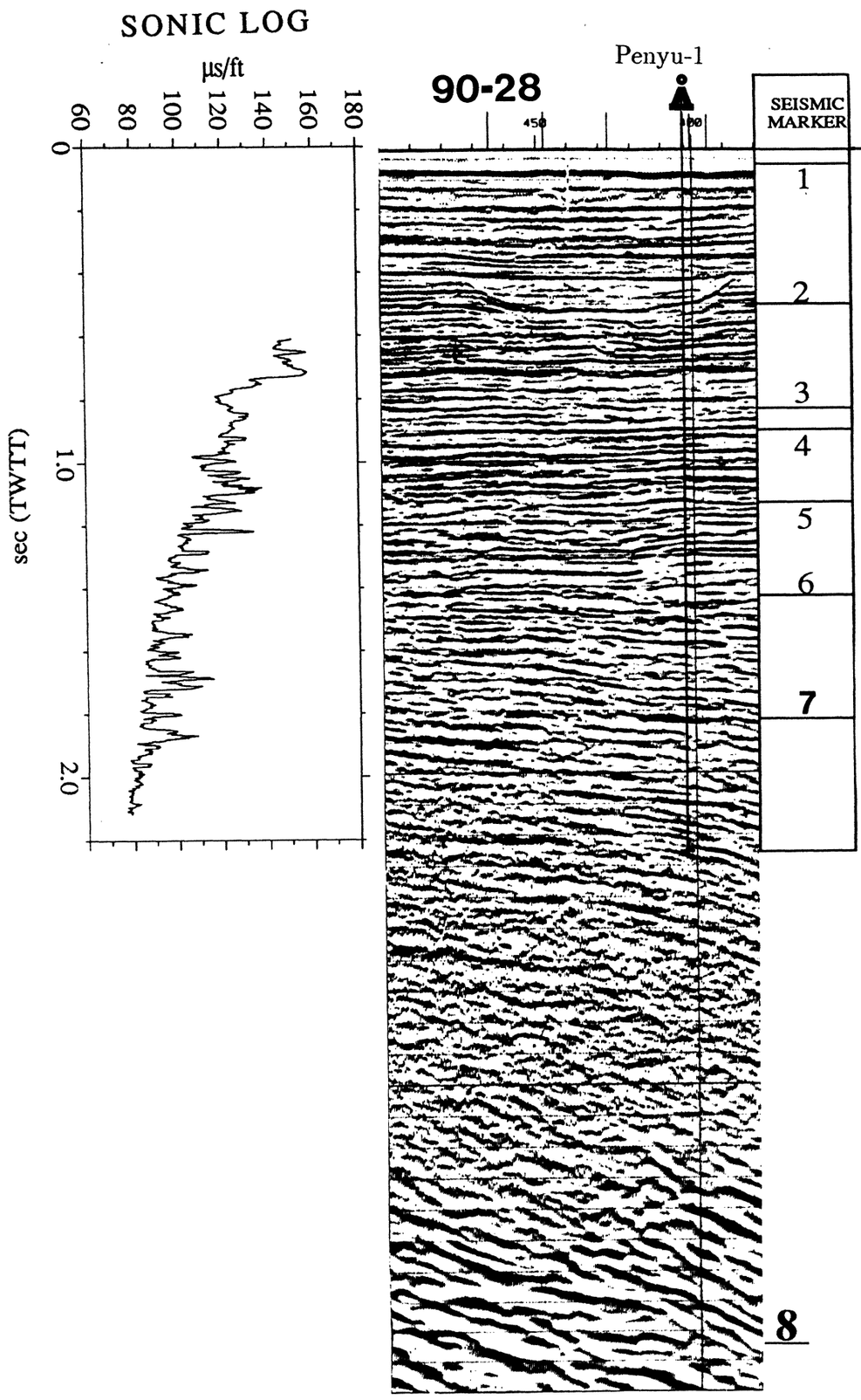

SEISMIC FACIES

high frequency, parallel reflections; very continuous, occasional channel-like features

variable, high frequency, semi-continuous, parallel reflections

unconformity

continuous, parallel reflections in late postrift strata

highly reflective, continuous parallel reflections in early postrift strata

discontinuous, partially reflective late synrift strata

T.D.

discontinuous, poorly reflective synrift strata

low-frequency, high-amplitude reflections, typical in some parts of the basement

top- basement reflector

STRATIGRAPHIC SUMMARY

AGE	BIOZONES: palynology	BIOZONES: foraminifera	PALAEOENVIRON.	REMARKS
Plio-Pleistocene	poor data	no data	shallow marine	
		Vulvulina pennatula		top of coaly sequence
U. Mio - L. Plio		Ammonia		deepening
?L-M Miocene	Almuspollenites verus	Ammonia/ Trochammina	intertidal	transgression
		Miliammina	littoral to lower estuarine	regional unconformity
lower Miocene	Callophylum			
	Zonocostites ramonae	poor fauna	supratidal freshwater to estuarine	base of coaly sequence
	Casuarina			
Oligocene	?Magnastriatites howardii		fluvial lacustrine	onset of brackish conditions
	Algal Cyst I and II	barren		

Figure 3.8. Seismic, sonic, and stratigraphical log from Penyu-1 well, located at the deepest part of the Penyu Basin, showing the general relationship between seismic reflection characteristics, log response and paleoenvironments. Depths in sonic log and stratigraphic summary have been converted to seconds two-way travel time based on well-velocity data. Two-way time, t_{twt}, in seconds is given by $t_{twt} = 0.732z + 0.203$ where z is log depth in km. Biostratigraphy and general paleoenvironmental interpretation based on paleontological analysis by Bates and Ong (1991).

as being reflection-free or "transparent". Depositional environment interpretation from seismic facies was aided by correlation with lithological and biostratigraphical information at well locations. Because the wells in the Penyu Basin are widely spaced (Fig. 3.2), interpolation between them is rather speculative. Interestingly, similar lithologies and depositional environments seem to persist in most wells, even though some are >30 km apart (Fig. 3.17, p. 69).

Some marker horizons were identified by erosional truncation of underlying strata. These horizons, therefore, represent erosional unconformities resulting from tectonically or eustatically induced base-level changes during basin evolution. Their recognition is important for understanding the tectono-stratigraphic development of the Basin. Erosional unconformities are recognized by angular reflection termination, commonly enhanced by seismic facies changes across the unconformities, brought about by a marked change in the depositional environment. Below, the stratigraphic units and their defining unconformities are described.

3.3.1 Seismic Units and Unconformities

In a previous study, Ngah (1975) defined three major stratigraphic units (Fig. 3.9). The youngest unit, Unit A consists of Pliocene to Recent marine deposits, mainly soft mud, showing weak and transparent reflections. Unit B is Middle to late Miocene in age, and consists of coastal deposits of sandstone, mudstone and, commonly, lignite. This unit is characterised by very strong and continuous reflections. Unit C, of Oligocene to early Miocene age, consists of continental deposits, overlying granitic and metamorphic basement. It shows relatively weak or transparent reflections.

Ngah's study suggests that sedimentation in the Penyu Basin was almost exclusively continental and mainly lacustrine, with increasingly marine influence upwards. A recent unpublished study by TEXACO (1992) have also resulted in a three-fold subdivision of the stratigraphy (Fig. 3.9). In that study, the synrift

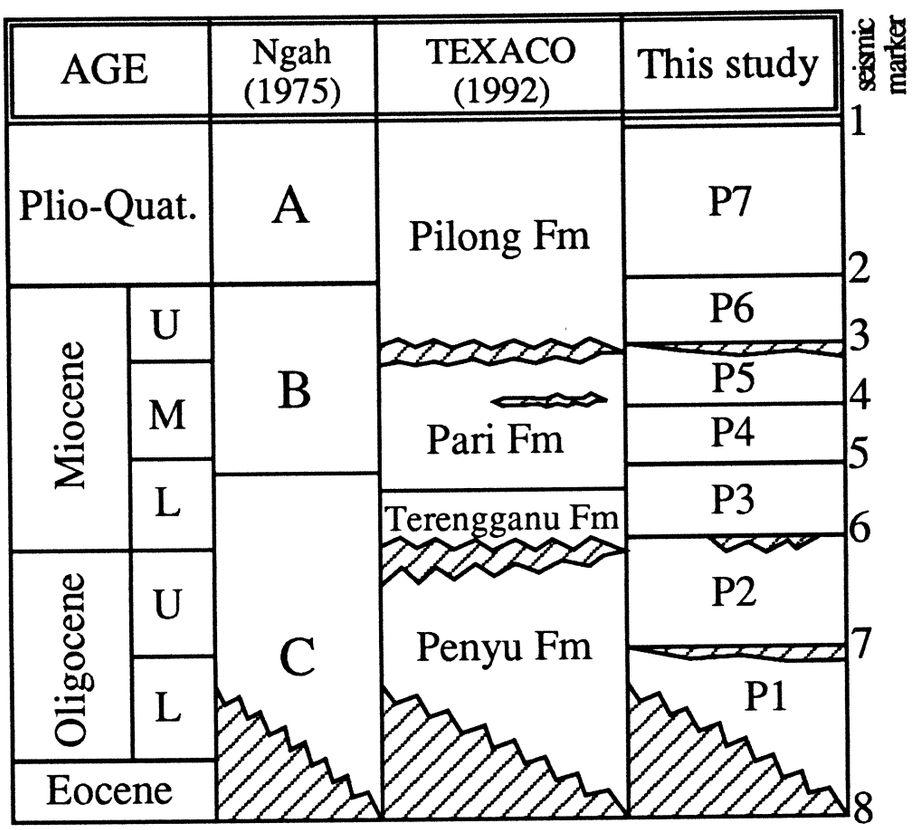

Figure 3.9. Comparison of the stratigraphic schemes used in the study and the earlier schemes defined by Ngah (1975) and TEXACO (1992).

clastic wedges, formed during the main phase of fault-controlled sedimentation, were assigned to the "Penyu Formation". A regional unconformity at the top of the Penyu (corresponding, roughly, to the top of the Oligocene) marks the end of a tectonic event in the late Oligocene. A laterally extensive lower Miocene shale, the "Terengganu Formation", occurs at the base of the Penyu Formation, and is believed to be equivalent in age to the "Barat Shale" in the West Natuna Basin and to the "Terengganu Shale" in the Malay Basin. The overlying "Pari Formation" (lower–upper Miocene) consists of nonmarine to marginal marine sediments deposited during the post-rift stage. The youngest unit, of Pliocene–Recent age, was assigned to the "Pilong Formation", following the nomenclature of Armitage and Viotti (1977) for the southern Malay/West Natuna Basin.

Seismic Unit	Reflection characteristics	Inferred Environment
POST-RIFT II		
Unit P7	Parallel and continuous, high-amplitude reflections	low-energy shallow marine sedimentation with minor relative sea level fluctuations
Unit P6	Less continuous parallel reflections, some chaotic and mounded reflections, and channel-form features (5–10 km wide) with reflection-free infill	transgressive high-energy sedimentation, nearshore to coastal environments; channels formed by erosion of underlying strata during relative rise in sea level above Mid-Miocene Unconformity
POST-RIFT I		
Units P3,P4,P5	Very continuous, parallel, high-frequency reflections; convergent reflections towards the crests of inversion structures	Relatively quiet environment, probably coastal plain sediments (coaly sequences); thinning of sedimentary units due to syn-sedimentary growth of inversion structures
SYN-RIFT II		
Unit P2	Like Unit P1 but are, in some places, more laterally continuous, generally parallel and of higher amplitude; only rarely affected by faulting	As in P1; quiet environment, probably alluvial plain/lacustrine sedimentation during late synrift inversion stage
SYN-RIFT I		
Unit P1	Discontinuous and poorly reflective, some parallel reflections, commonly faulted; overall divergent reflectors representing syndepositional half-graben fills	"high-energy" nonmarine sedimentation during extensional faulting
PRE-RIFT (BASEMENT)	generally reflection-free, although some high-amplitude reflections suggest folding of stratified rocks	mainly igneous rocks, minor sedimentary rocks and/or metasediments

Table 3.2. Seismic stratigraphic subdivision of Penyu Basin fill and their characteristic reflections. Youngest to oldest from top to bottom. General paleoenvironmental interpretation based on paleontological analysis by Bates and Ong (1991) and Rexilius *et al.* (1992).

Based on the new high-quality seismic data used in this study, a refinement of the previous stratigraphic schemes is proposed. The basin fill is now subdivided into seven seismo-stratigraphic units, P1 to P7 (Table 3.2). Figure 3.9 shows the approximate correlation of the present scheme with the earlier ones. The eight bounding seismic reflectors are shown alongside the stratigraphic units in Fig. 3.9. Of the eight, and excluding Horizon 8 (Top-Basement Unconformity), three are major intrabasinal, erosional unconformities that represent significant breaks in sedimentation during major tectonic events. The major unconformities are discussed below.

Horizon 8 (Top-Basement Unconformity) Horizon 8 marks an abrupt change in the reflection characteristics between the pre-rift rocks and the overlying basin fill (Fig. 3.10). Because the pre-rift rocks are dominated by igneous and metamorphic rocks, they are, generally, poorly reflective in most parts of the Basin. Horizon 8 is identified, usually, as a very strong pair of high-amplitude reflections (Fig. 3.8). Identification is difficult where the overlying sediment is also poorly reflective, or where the basement itself consists of layered, possibly sedimentary, rocks. In some places, such as the Merchong Graben, the discordance between pre-rift and synrift rocks is striking. Figure 3.10 shows part of Line 90-133 from the Merchong Graben, where stratified pre-rift rocks, of probable Mesozoic age, are truncated by the Top-Basement Unconformity.

The regional geology suggests that the basement is the offshore continuation of the Mesozoic geology of Peninsular Malaysia (Chapter 2). Pre-Tertiary sedimentary rocks, equivalent to the Tembeling/Gagau Groups, are believed to be present beneath the Tertiary basins of northern Sundaland (Hutchison, 1989a). The discordant reflections in the pre-rift rocks is apparent in Line 90-133 (Fig. 3.10) because the line is oriented NW–SE, roughly perpendicular to the regional strike of Mesozoic and older rocks of Peninsular Malaysia. Basement rocks penetrated in two wells prove that sedimentary rocks do occur in the basement. Well Pari-1, drilled on the Pari High (Fig. 3.5B), encountered calcareous siltstone at 2164 m.

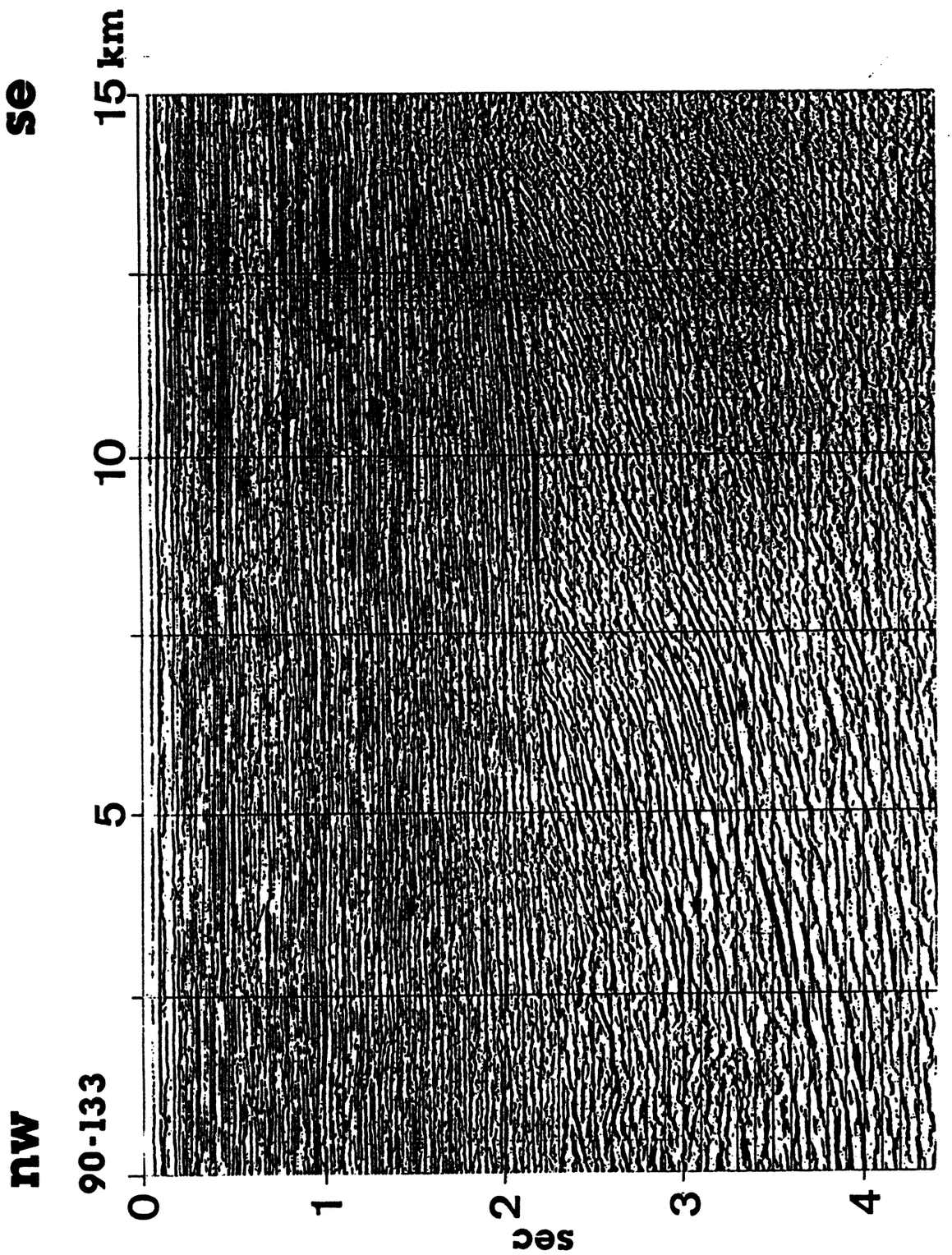

Figure 3.10. Prominent reflections in the pre-Tertiary basement, Penyu Basin, indicating the existence of stratified sedimentary rocks of, probably, Mesozoic age (Line 90-133). Top-Basement Unconformity indicated by double high-amplitude reflection at ~2.2 s on the SE side of profile. Note that the discordance between basement and basin fill becomes less pronounced northwestwards, but the basement can still be identified by its relatively low frequency reflections.

Core samples of the siltstone showed bedding planes dipping at 50°– 60° to the horizontal, in marked contrast to the subhorizontal bedding normally observed in the overlying Tertiary sediments. Well Rhu-1A, was drilled on a southwesterly tilting intrabasinal fault block ("Rhu High") encountered tuffaceous sandstone at 2989 m.

Horizon 7 (Mid-Oligocene Unconformity) This unconformity is defined in the Rumbia Graben by truncation of the hangingwall rollover anticline in the synrift fill (Fig. 3.11). It shows also a marked contrast in the reflection characteristics between the synrift and post-rift sediments. The synrift sediment exhibits divergent, somewhat discontinuous, reflections, whereas the postrift shows relatively continuous, parallel reflections. The synrift sediment tends also to be poorly reflective. Horizon 7 marks the end of fault-controlled, extensional phase of basin development in the Rumbia Graben.

Horizon 6 (Top-Oligocene Unconformity) This unconformity marks a major change in the reflection characteristics, from poor reflections in high-energy late-synrift sediments to parallel, continuous reflections in the overlying postrift sediments. Palynological evidence (Rexilius *et al.*, 1992) suggests that the unconformity coincides with the start of marine incursions in the Basin, which resulted in a coastal plain/swamp type of environment conducive for the development of coal-bearing deposits. Horizon 6 corresponds to, roughly, the top of the Oligocene, and is probably correlatable with the base of the transgressive *Terengganu Shale* in the southern Malay Basin (Madon, 1992) and to the *Barat Shale* in the West Natuna Basin (Daines, 1985). Thus, it seems to have a more regional significance, even though its erosional nature is not very pronounced. It marks the complete cessation of rifting in the Basin which was accompanied, in places, by mild wrench-related compressional tectonics.

Figure 3.12 shows an example of a wrench-induced structure formed at the

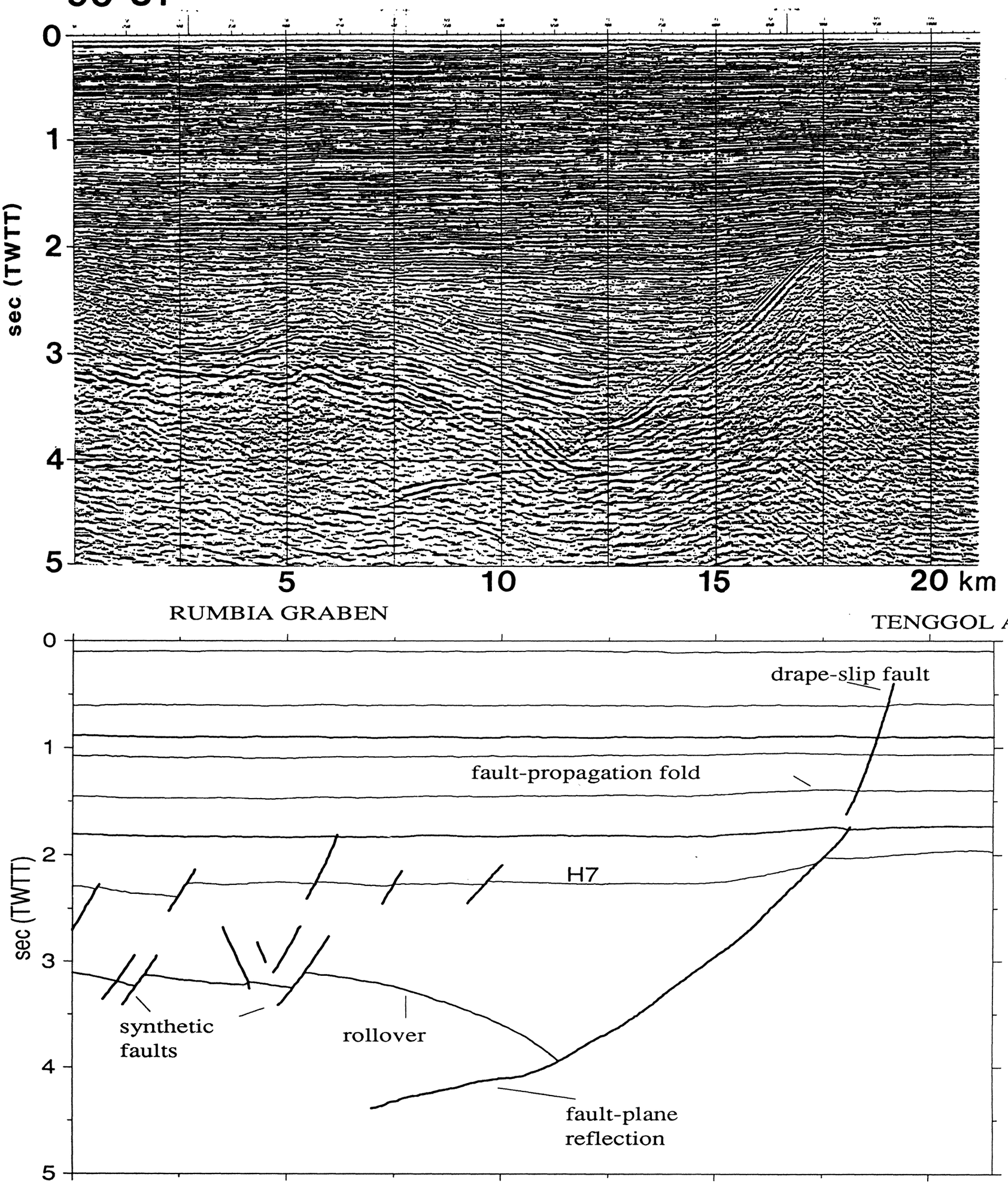

Figure 3.11. Line 90-31 showing listric border fault and the Top-Synrift I (Mid-Oligocene) Unconformity represented by Horizon 7. Note the truncation of hangingwall rollover in the synrift sediment. Slight folding of postrift sediment is associated with the propagation of the border fault into the post-rift section during a later inversion phase.

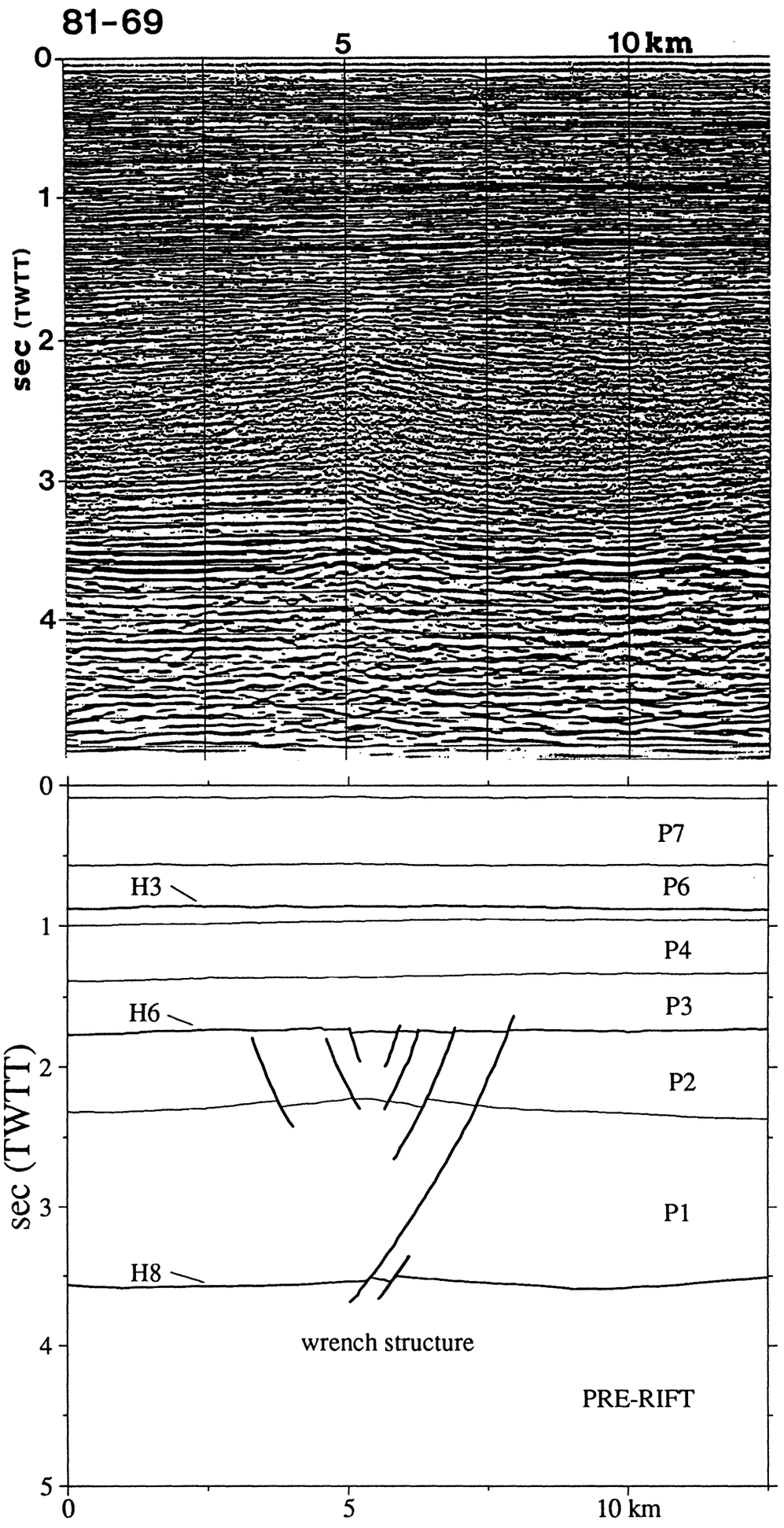

Figure 3.12. Line 81-69 showing, in the center, the Top-Oligocene Unconformity (Horizon 6) marked by crestal erosion of a "flower structure" associated, probably, with a basement wrench fault.

end of the rifting phase. The figure shows slight erosion of Synrift II strata on the crest of the "flower structure" by the Top-Oligocene Unconformity. Wrench-reactivation of the basement fault could have been caused by an early phase of tectonic inversion (Section 3.5).

Horizon 3 (Mid-Miocene Unconformity) This unconformity is a very prominent intrabasinal unconformity, characterised by crestal erosion of inversion anticlines that were formed by folding of Postrift I and older strata (Fig. 3.13). Abrupt changes in the reflection characteristics across the unconfomity are sometimes observed. In Line 82-124 (Fig. 3.13), the unconformity separates strata showing irregular and discontinuous high-amplitude reflections from ~50 ms of transparent seismic facies above it. Away from the crestal region, the unconformity appears to be parallel and conformable with the underlying strata, with subtle toplap relationships (Fig. 3.14). This suggests that the inversion structures were formed below sea level and that subaqueous erosion on the crest had occurred simultaneously with deposition on the flanks (Fig. 3.15). The decrease in thickness of the sedimentary units towards the crest also implies syn-depositional deformation. The age of this unconformity is middle Miocene and is probably related to the regional unconformity in the Malay and West Natuna Basins.

Other seismic reflectors identified in the study are tectonically less significant but were used to facilitate mapping the basin. Horizon 1 is the present-day sea floor, which is about 60–70 m below mean sea level. Horizons 2, 4, and 5 are relatively strong reflectors, identified by changes in the reflection characteristics but do not seem to represent significant tectonic events. Horizon 2 often marks a major change in seismic facies, from somewhat transparent and chaotic, channelised facies in Unit P6 to a continuous and parallel seismic facies in the overlying Unit P7 (Fig. 3.16). Palaeontological evidence suggests that the chaotic channelised facies represents nearshore or coastal plain deposits, whereas the continuously reflective facies represent low-energy shallow marine deposits, which may have resulted from a rise in relative sea level during the early Pliocene.

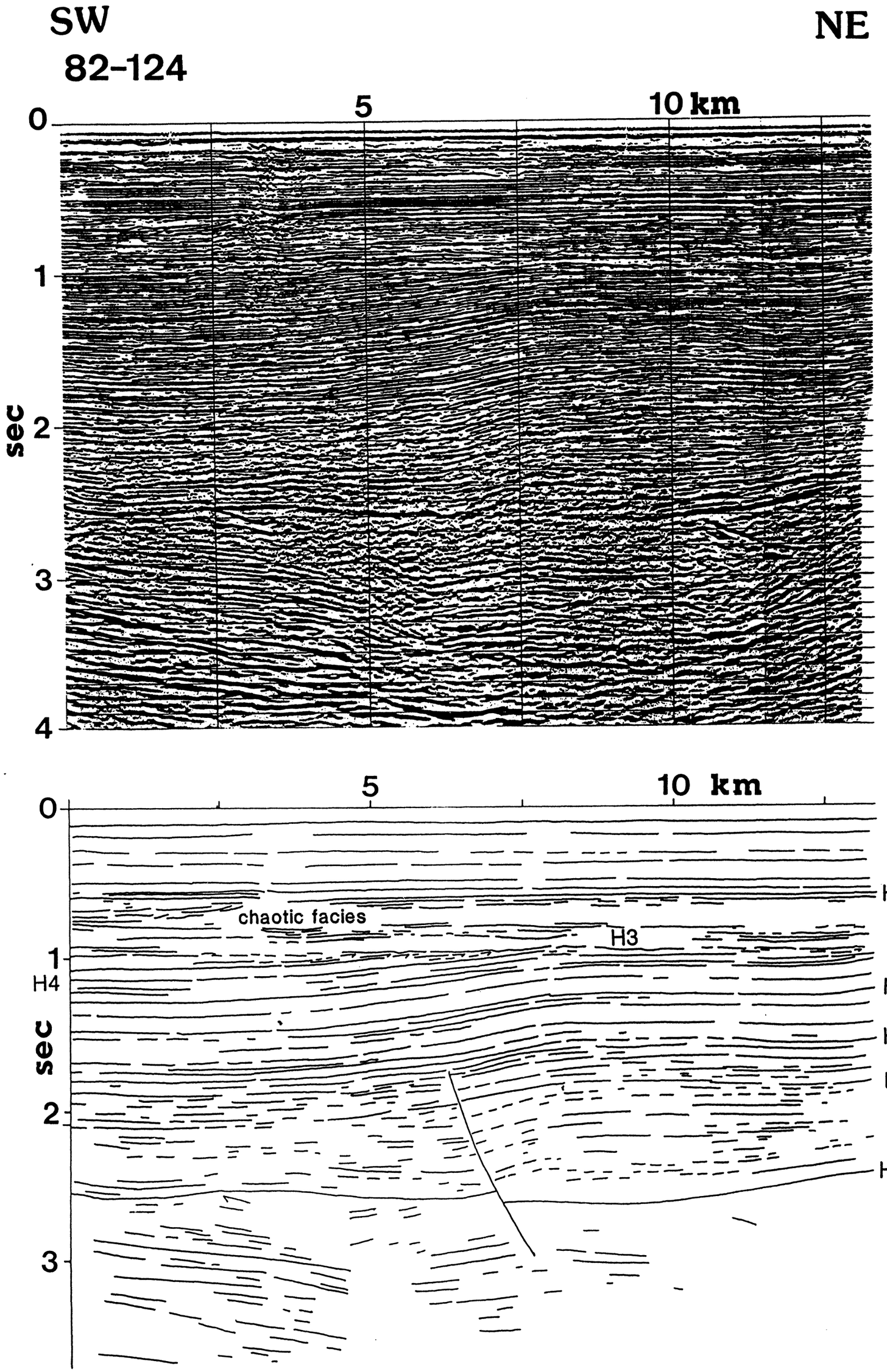

Figure 3.13. Middle Miocene Unconformity, Horizon 3, marked by erosion of inversion fold crests in the Post-rift I.

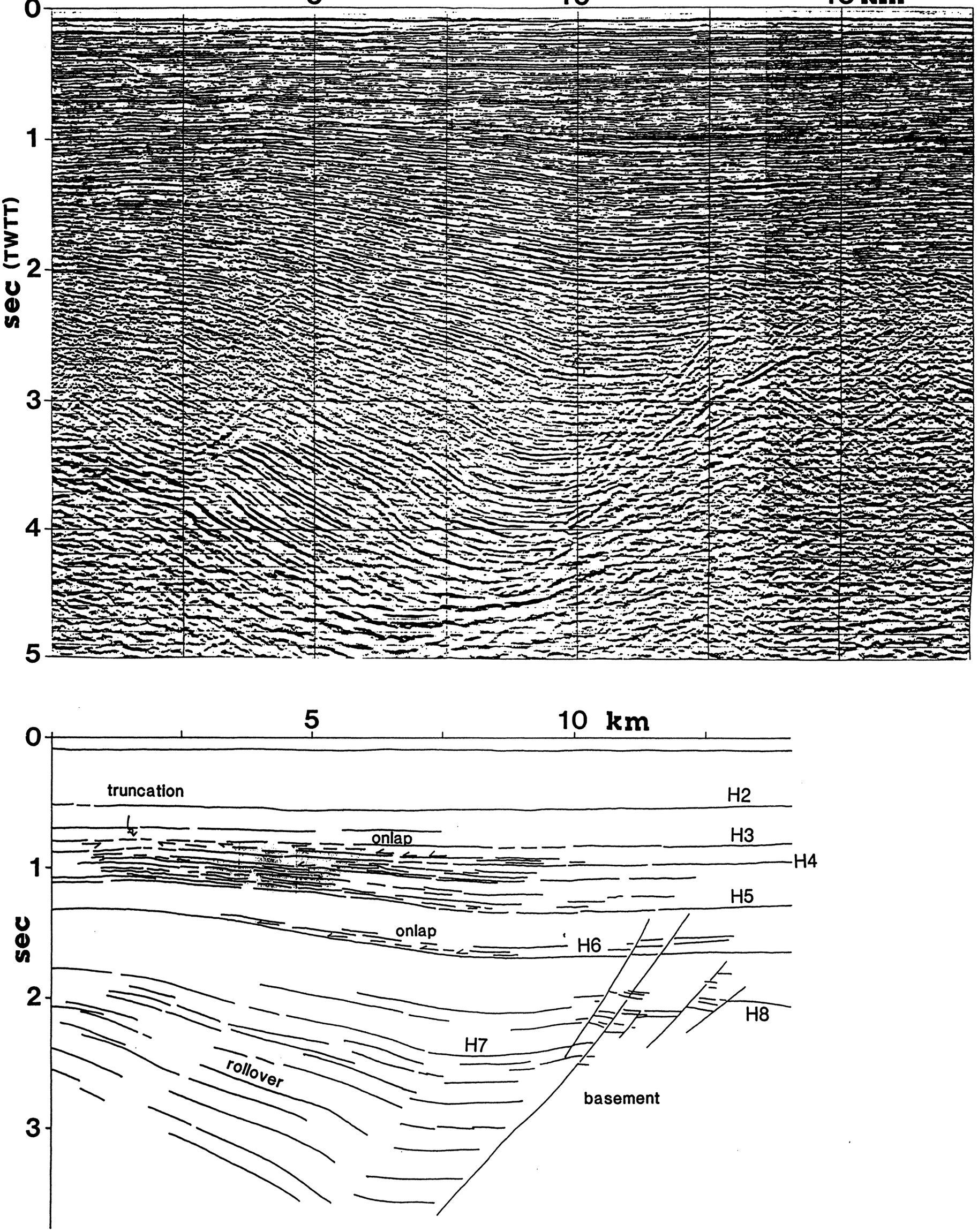

Figure 3.14. Line drawing of Line 90-28, showing the stratigraphic relationship associated with growth of inversion structure adjacent to the Kuantan Graben. Subtle onlap onto the inversion structure is indicated by the arrows. Note also the truncation on the structure at the Mid-Miocene Unconformity (Horizon 3).

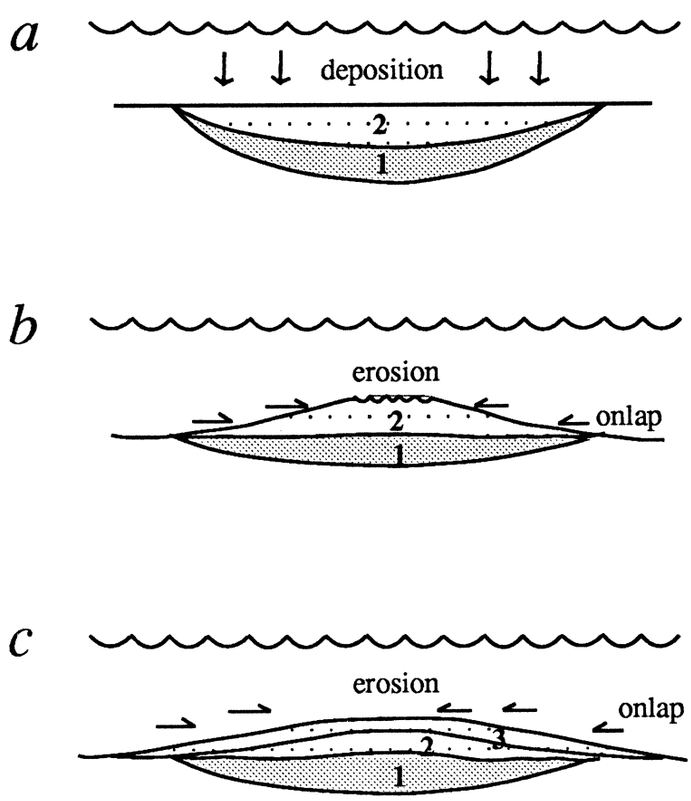

Figure 3.15. Cartoon illustrating the sequence of development of inversion structures and the relationship between erosion on the crest and simultaneous deposition on the flanks. (A) Deposition of units 1 and 2. (B) Deformation and inversion causes erosion on the crest, and deposition of the flanks. (C) Deposition of Unit 3 on a growing structure results in onlap and thinning of the unit towards the crest.

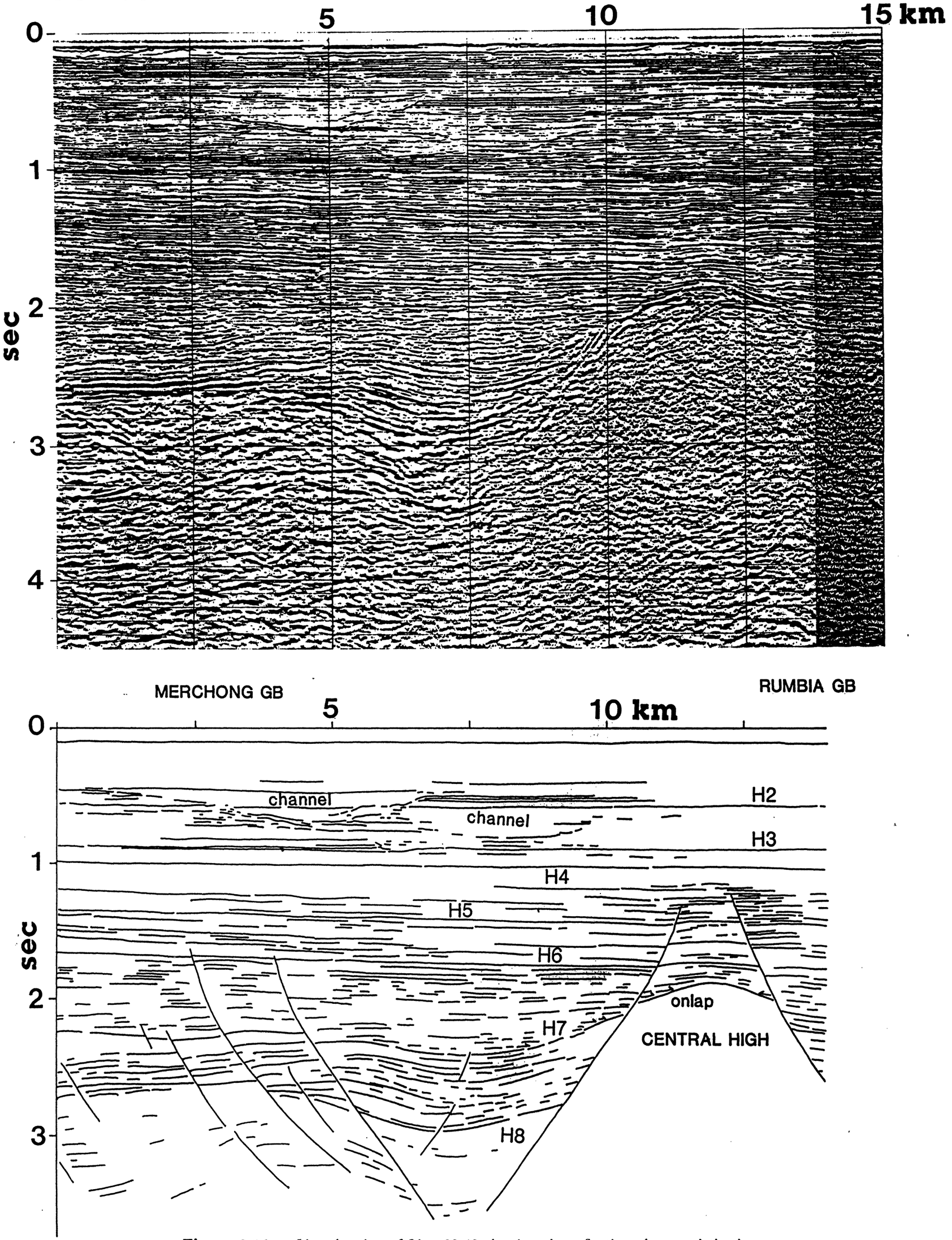

Figure 3.16. Line drawing of Line 90-43 showing the reflection characteristics in the synrift and postrift sediments. Note the large channel-like features above the Mid-Miocene Unconformity, contrasting with the underlying "regular" seismic facies. Note, on the right, the stratigraphic onlap on the basement high.

3.3.2 Lithology and Palaeonvironments

The lithology and inferred paleoenvironments of the Penyu Basin sediments were compiled from unpublished well-completion logs and drilling records. Lithological information are from well-cuttings description whereas the biostratigraphic and paleontological information is based on the analysis by Bates and Ong (1991). Because core data are lacking, only a very general interpretation of the depositional environment can be made.

Figure 3.17 shows a schematic N–S stratigraphic cross-section through wells Pari-1 and Penyu-1, located along Line 90-28 shown in 3.5B. Pari-1 is located on a basement high and, therefore, penetrates the Pari High basement ridge. Penyu-1, on the other hand, is located exactly on the crest of a major inversion anticline in the Kuantan Graben, where the sedimentary fill is thickest. The basement at Penyu-1 is at least 5 km below the total depth (T.D.) of the well (2681 m). As in the neighbouring Malay and West Natuna Basins, the sediment in the Penyu Basin are virtually entirely siliciclastic, comprising interbedded shale, siltstone and sandstone, with abundant coal in the middle. The basal succession consists of interbedded sand-shale sequences deposited in fluvio-lacustrine environments. The sediments are devoid of marine fossils, but occurrences of fresh water palynomorphs, such as *Pediastrum* and *Botryococcus*, indicate lacustrine conditions. The presence of mangrove and back-mangrove pollen suggests a weak brackish influence. The palynological results of Rexilius *et al.* (1992) suggest that Units P1 and P2 are of Oligocene age and, therefore, represent the synrift phase of basin development when the basin was undergoing active extension. These units consist of, essentially, grey shales, siltstones and relatively minor very fine to medium grained sandstones. Unit P1 thickens considerably towards Penyu-1, reflecting the influence of the Kuantan Fault on the subsidence of the Graben during Synrift I stage. Unit P2 also increases in thickness from Pari-1 to Penyu-1, although not as much. It represents the later stages of extension in the Basin (Synrift II).

The top of Unit P2 (Horizon 6) is marked by the onset of brackish-water con-

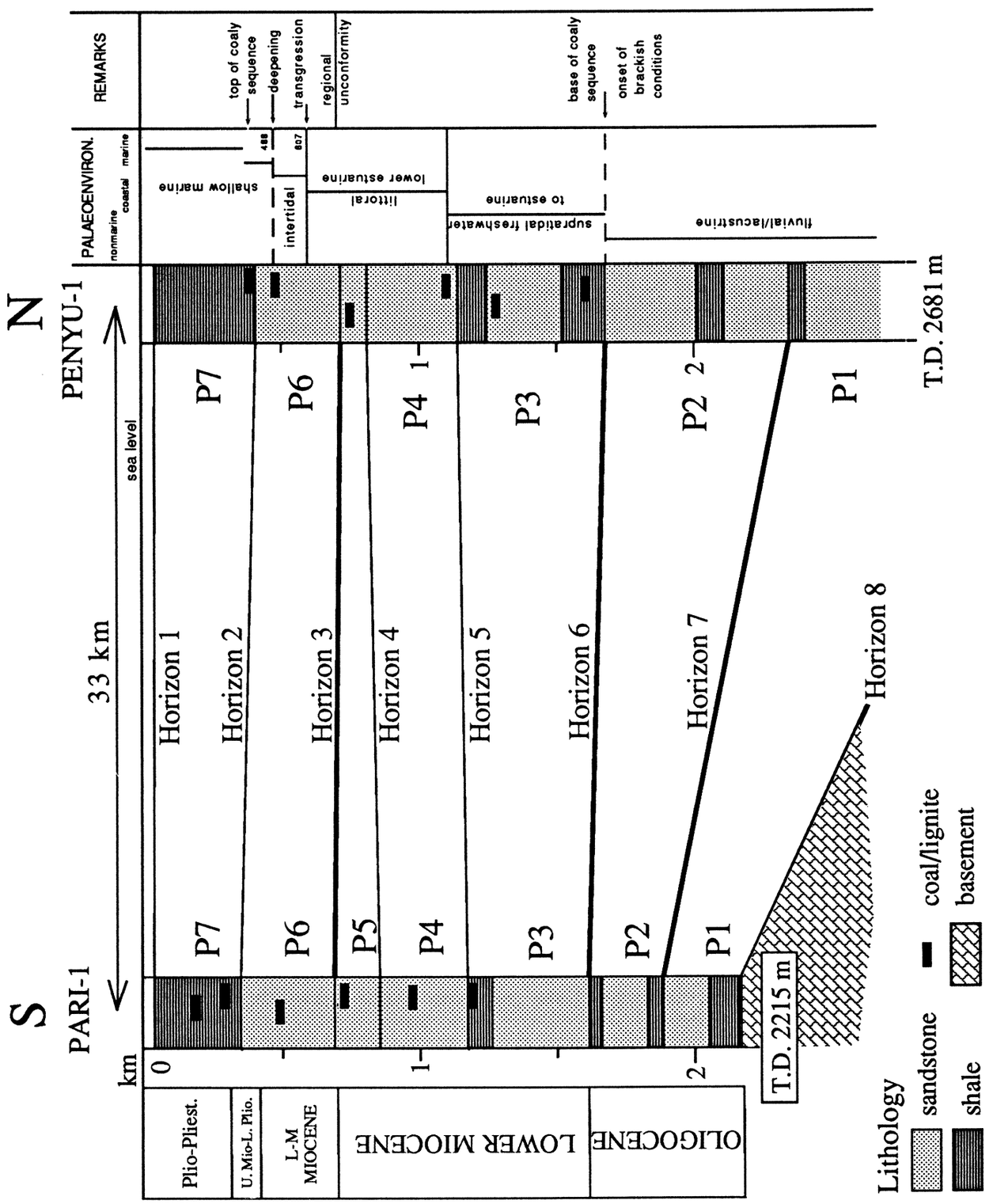

Figure 3.17. Schematic cross-section based on correlation between Pari-1 and Penyu-1. Lithology based on well completion logs, whereas paleoenvironments are based on analysis of Bates and Ong (1991).

ditions in the Basin as a result of marine incursions. In Penyu-1, the overlying Unit P3 contains abundant coaly horizons, indicative of waterlogged swamp environments. Brackish-water palynomorphs in this sequence suggest that the coals formed in a coastal plain setting, which means that the Basin was near sea level by this time. The occurrence of coal in Pari-1 is shifted vertically relative to that in Penyu-1, suggesting that the effect of the marine incursion had reached there slightly later, because it was located on an intrabasin high and may have been above sea level while Penyu-1 was already subsiding. Brackish depositional conditions in Unit P3 are indicated by occurrences of mangrove-type pollen and, occasionally, foraminifers. Units P3, P4 and P5 represent, collectively, the "Postrift I" stage that ended with tectonic deformation during the basin inversion phase. Unit P6, above the Mid-Miocene Unconformity, represents deposition during a major mid–late Miocene marine transgression in the area. Deposition occurred in intertidal and coastal environments. Finally, the overlying Unit P7 consists of mainly poorly-consolidated claystones and minor siltstones deposited in a shallow open marine environment, as indicated by the abundance of benthonic foraminifers.

Lithological and palaeontological evidence suggest that the start of postrift subsidence in the Penyu Basin coincided with a change in depositional conditions. Whereas the synrift phase is characterised by nonmarine lacustrine environments, apparently, when the basin was above sea level, the postrift phase is characterised by deposition in a coastal plain setting, with marine incursions becoming more frequent during the later part of the Miocene. By that time, the Basin may have subsided almost to sea level. Fully marine conditions were established only in late Miocene times, following a major late Miocene transgression.

3.4 Extensional Structures

This section describes the major extensional features in the Basin. The three main grabens – Kuantan, Rumbia, and Merchong – are discussed in turn, em-

phasizing the extensional structural styles and, then, interpreting their kinematic development.

3.4.1 Kuantan Fault

In the eastern part of the Basin, the Kuantan and Pekan Grabens form, essentially, an ENE-trending graben system dominated by normal faults resulting from, apparently, N–S extension. The major basin-controlling fault is the Kuantan Fault, a large normal fault that forms the northern boundary of the eastern part of the Basin. Minor faults in the hangingwall of the Kuantan Graben are mostly synthetic to the main bounding fault. This is the typical fault style in the Basin, whereby minor faults in the hangingwall tend to be synthetic, rather than antithetic, to the main bounding fault. Although antithetic faults occur, they are relatively rare and tend to form at the distal end of the hangingwall. In Fig. 3.18, for example, synthetic faults occur at the crestal part of the hangingwall rollover and appears to be the result of crestal collapse. No regularity in spacing of the minor faults is observed.

Fault/Area	Line	Dip	Dominant slip
Kuantan Fault (west)	90-10	54°, 55°S	dip-slip
	90-211	43°S	dip-slip
Kuantan Fault (main)	90-28	54°N	dip-slip
Trans-Penyu Fault	90-36	58°N	dip-slip
North Rumbia Fault	90-29	36°, 37°S	oblique-slip
	90-31	33°SW	oblique-slip
	83-513	36°SW	oblique-slip
Cherating-Rhu Faults	90-41	40°, 48°, 47°NE	dip-slip
Merchong Graben Faults (W)	90-36	42°– 44°NE	dip-slip
Merchong Border Fault (N)	90-41	63°SW	oblique-slip
Southern Border Fault (S)	90-41	68°NE	oblique-slip

Table 3.3. Fault dips calculated from selected dip lines that are approximately perpendicular to the mapped fault trace (Fig. 3.3).

The Kuantan Fault is the largest half-graben border fault, with a horizontal

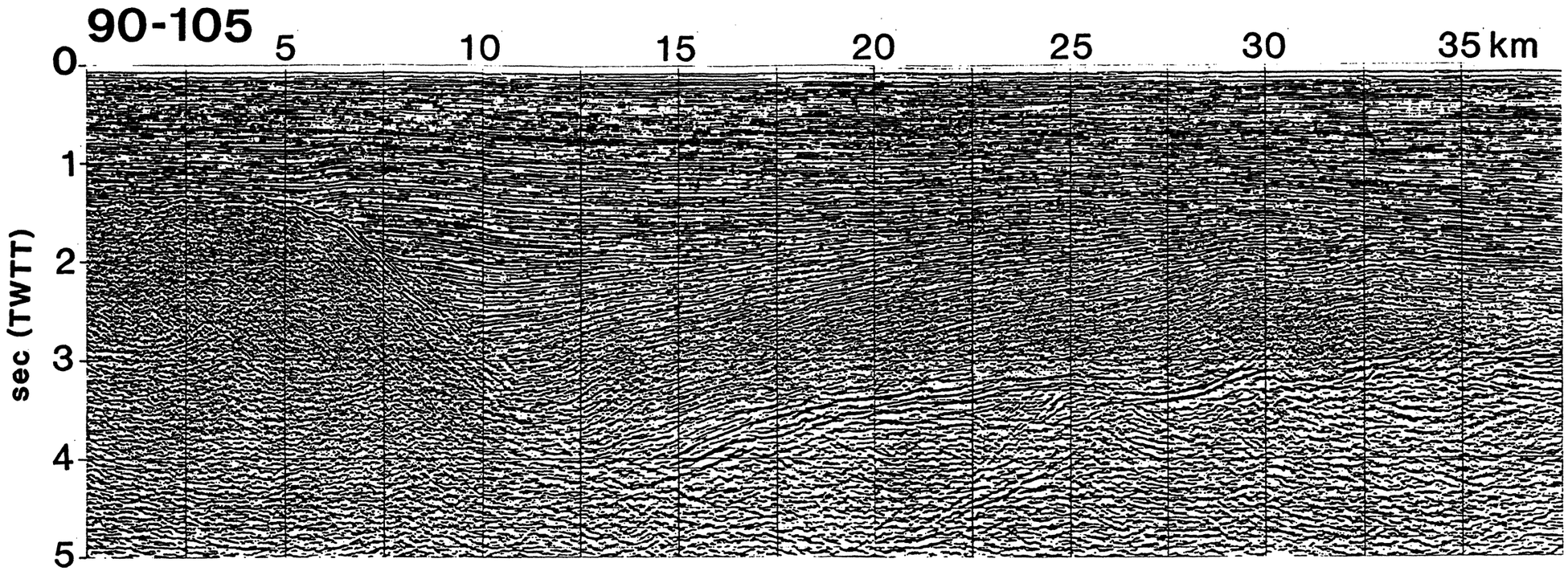

Figure 3.18. Line 90-105 across the Kuantan Fault. Note the synrift sediment geometry, hangingwall rollover, and crestal antithetic faults. The partially eroded footwall scarp suggests that the Fault had been inactive long before it was buried by postrift sediment.

displacement of up to ~6.5 km. The displacement on the fault decreases from west to east as the Kuantan Graben becomes narrower. This suggests that the Fault was probably initiated at the centre of the Basin and had propagated westwards during extension. A series of profiles across the Graben (Fig. 3.19) shows that the geometry of the Fault vary considerably along strike. The Fault is planar in Line 90-211, listric in Line 90-214, and even has a ramp-like feature in Line 90-213. In Line 90-411, the Fault has several branches that appear to be splays off a low-angle sole fault, suggesting perhaps the influence of older ?thrust during extension (Faccenna *et al.*, 1995).

The dips of major faults were measured along selected profiles, which were depth-converted using the available velocity data (Appendix A.1). The data (Table 3.3) suggest that the majority of faults have dips greater than 40°, as would be expected for extensional normal faults (Jackson and White, 1989). The Kuantan Fault, in particular, has a relatively steep dip of ~55°. The Kuantan Fault was mapped in a previous study by Ngah (1975) as a single curvilinear fault. Because of the closer seismic grid used in this study, we are able to resolve the Fault into at least two major segments, as illustrated in Fig. 3.3. An eastern segment forms the main bounding fault to the Kuantan Graben and is separated from a western segment by an overlap, or relay, zone. Figure 3.20 is an interpreted seismic line oriented roughly NE–SW through that overlap zone. The figure shows a relatively flat Pahang Platform passing abruptly southwestwards into a zone of high-angle normal-separation faults downthrowing basinwards. The upward-fanning geometry of the faults resembles a "flower structure" and suggest, possibly, a strike-slip origin for these faults. There is no evidence, however, that these faults extend either to the northwest or to the southeast. Hence, these high-angle normal faults could be transfer faults, which link the two segments of the Kuantan Fault across the overlap zone. Many studies have shown that extensional faults nucleate as discrete segments, which eventually link up as they overlap and coalesce (Peacock and Sanderson, 1994; Trudgill and Cartwright, 1994; Cartwright *et al.*, 1995). During advanced stages of fault growth, the overlap zones between fault segments

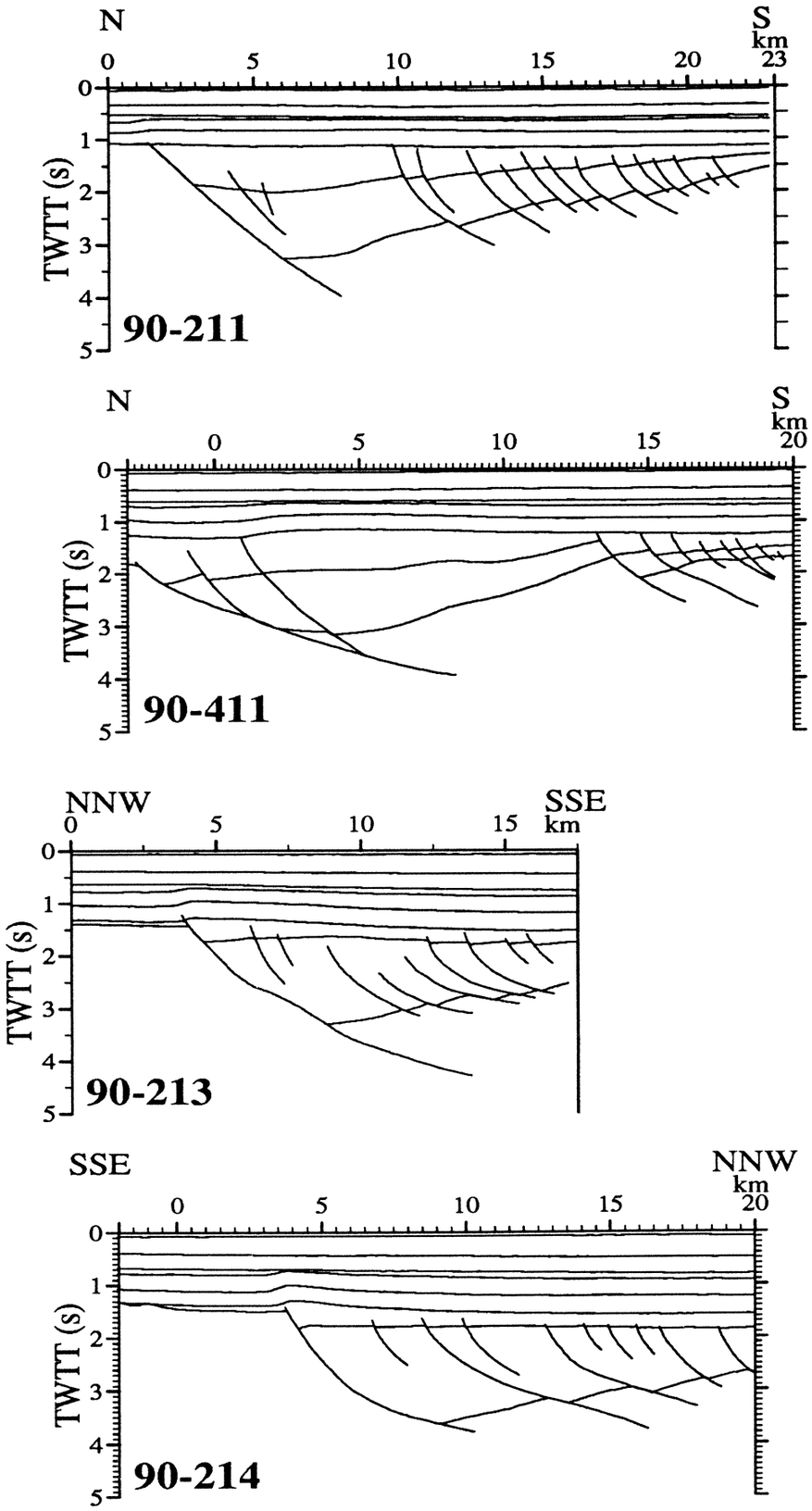

Figure 3.19. Seismic sections across the Kuantan Graben, from west (top) to east (bottom). The same horizontal scale in km is used for easy comparison. Note the variable fault geometry along strike. *Line 90-214 is shown at a smaller scale in foldout overleaf.*

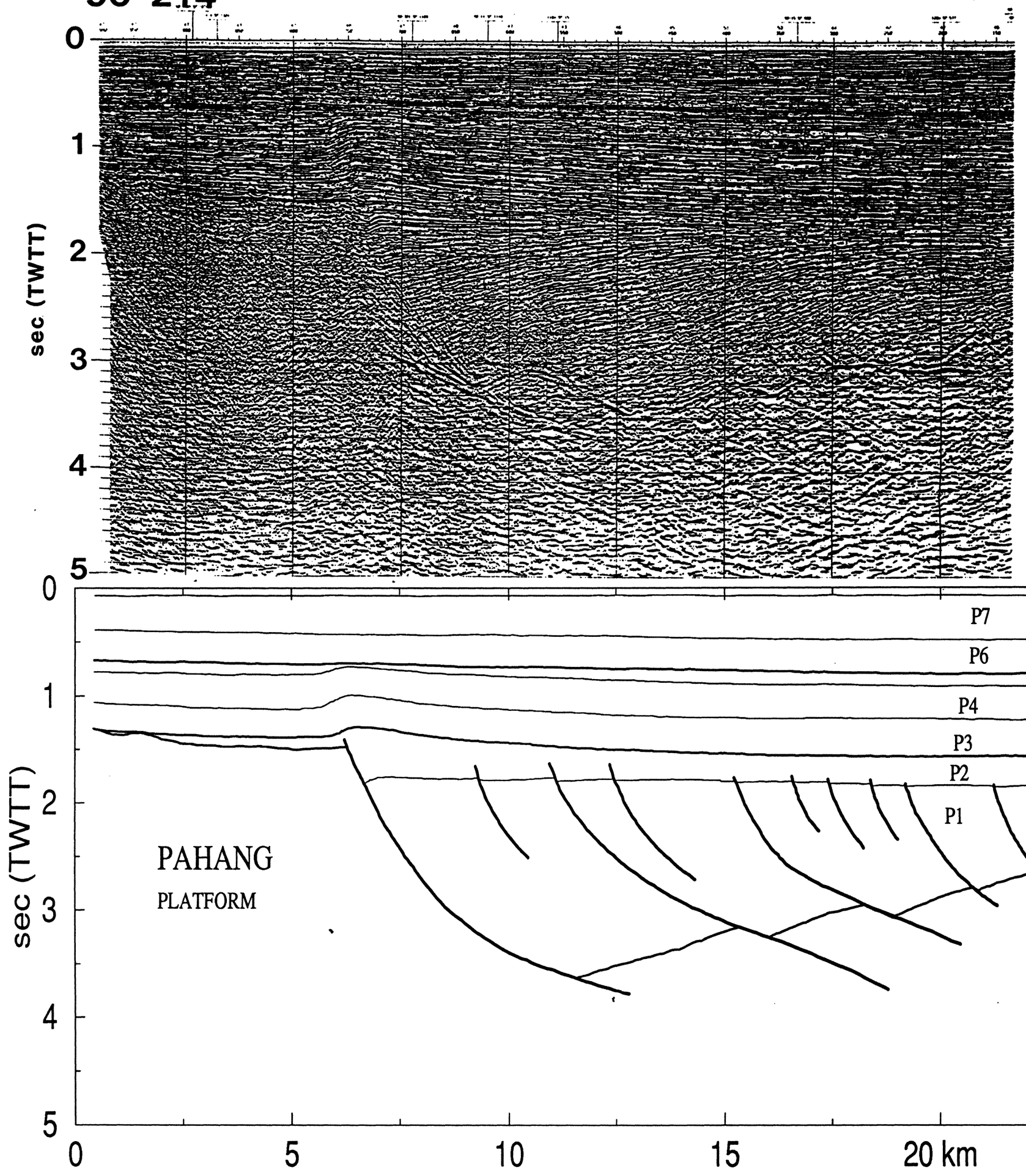

Figure 3.19 (cont.) Top: Seismic line 90-214 across the Kuantan Graben, showing a series of hangingwall faults that are synthetic to the main bounding fault to the northwest. Bottom: Interpretation of the line. Notice the small fault-propagation fold at above the footwall scarp, indicating reactivation of the border fault.

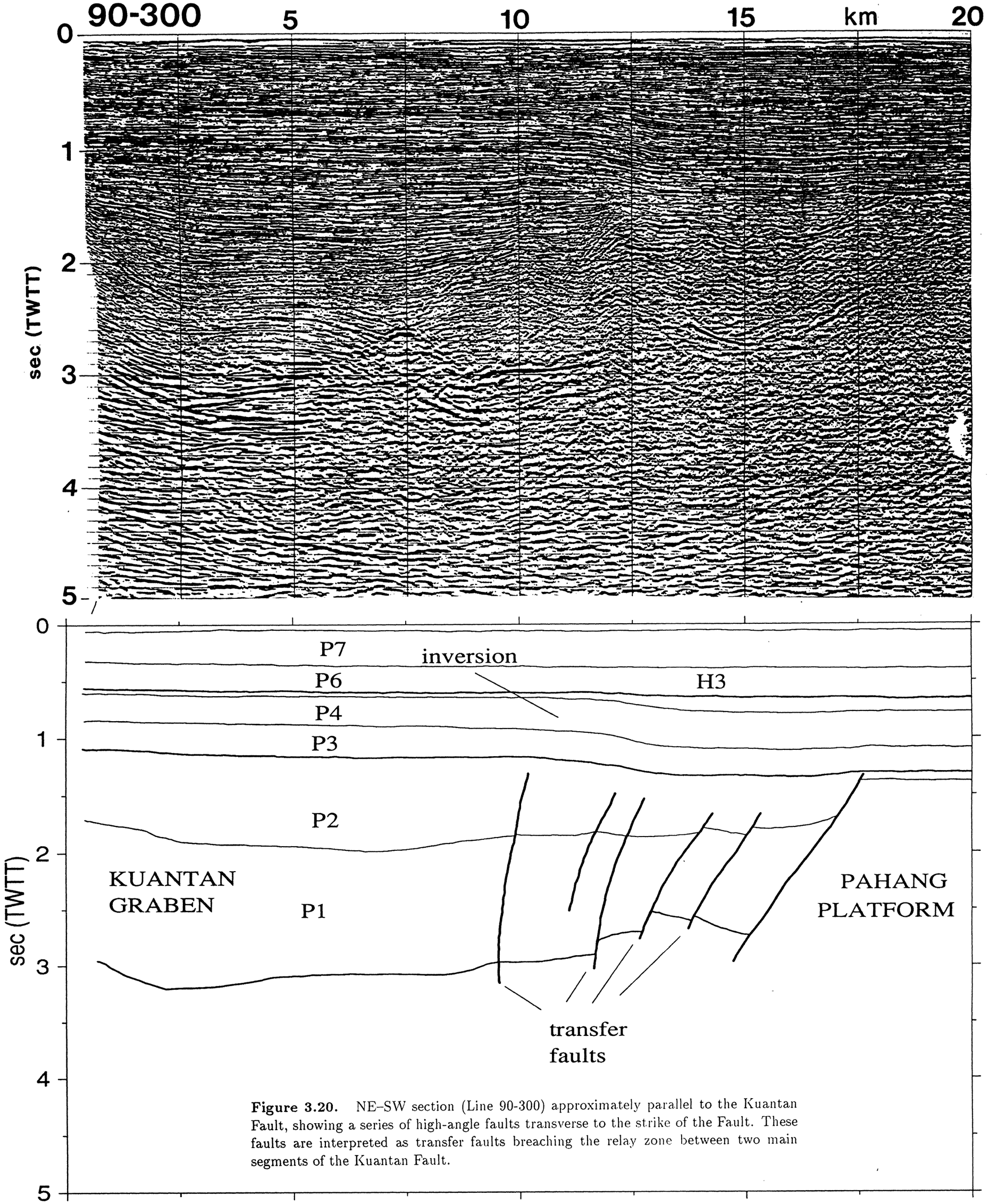

Figure 3.20. NE–SW section (Line 90-300) approximately parallel to the Kuantan Fault, showing a series of high-angle faults transverse to the strike of the Fault. These faults are interpreted as transfer faults breaching the relay zone between two main segments of the Kuantan Fault.

may be breached by transfer faults. It is also probable that the transfer faults in the Kuantan Fault Zone developed along pre-existing NW-trending basement weaknesses.

Assuming that the Kuantan Fault evolved as an elliptical fault, according to the fault growth model (Barnett *et al.*, 1987; Walsh and Watterson, 1988; Cowie *et al.*, 1993), a relationship can be found between the displacement and length of the Fault. According to the theory of fault growth, the displacement of a fault, $\mathcal{D}$, is proportional to its length, $\mathcal{L}$, and is given by (Walsh and Watterson, 1988)

$$\mathcal{D} = a\mathcal{L}^b$$

The constant a is a parameter determined by rock property and tectonic environment and b is the scaling factor which governs how fast the fault lengthens as its displacement increases. The value of b is still a topic of debate. Various authors favour different scaling factor, ranging from 0.9 (Dawers, 1993) to 1.5 (Marrett and Allmendinger, 1991; Gillespie *et al.*, 1992) to 2.0 (Walsh and Watterson, 1988).

In Fig. 3.21, the displacement and length of 17 faults in the Penyu Basin were plotted on a log-log scale with data compiled from various sources. For comparison with the published data, the horizontal displacement (heave) of the Penyu Basin faults was converted to down-dip displacement by assuming a constant dip of 60°. Although the individual dataset spans a limited range of displacement and length, when taken as a whole, they represent five orders of magnitude and plot in a straight line. This suggests a power-law scaling relationship between fault displacement and length, as predicted by the fault-growth model (Cowie and Scholz, 1992). The Penyu Basin faults also plot within the overall trend, which suggests that they obey a similar fault-growth model. Because the Penyu Basin data is limited, it is not enough to give a unique scaling factor. The overall trend shown by the dataset in Fig. 3.21, however, suggests a scaling factor, b, of about 1.6.

The fault growth model is a useful concept because it explains an important observation in normal fault systems. If normal faults obey a universal scaling law,

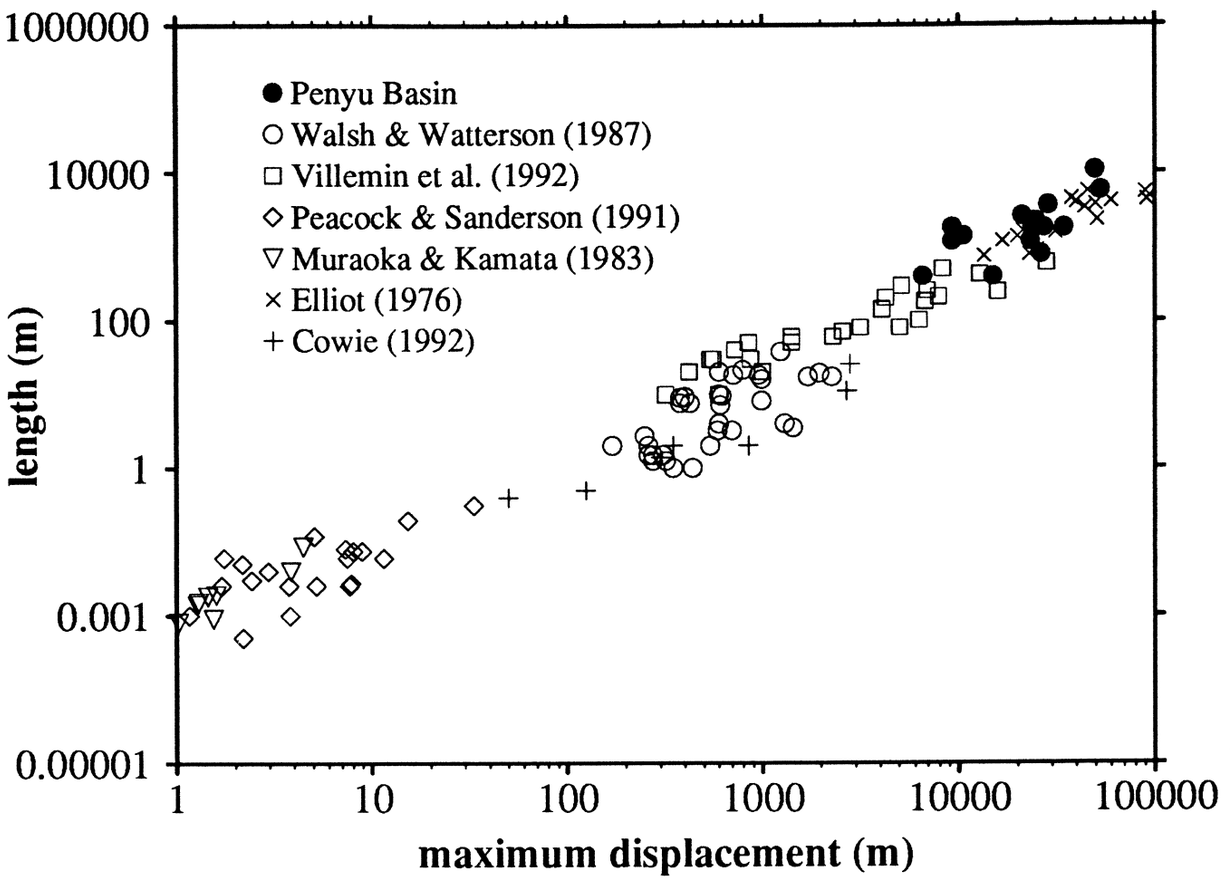

Figure 3.21. Log-log plot of fault displacement *vs* length: comparison of Penyu Basin data with some published data.

say $b = 1.6$, a departure from the straight line in Fig. 3.21 would imply that other processes may be involved in the growth of the faults. For instance, if two, initially unconnected elliptical faults grew such that their tip lines interact and eventually coalesce, the resulting fault would be longer than the ideal fault growth model would suggest. This fault will plot above the overall trend in Fig. 3.21 and give an inaccurate picture of its growth.

Peacock and Sanderson (1994) show that large faults grow by linkage of smaller segments, which is sometimes reflected in the along-strike displacement profile. Figure 3.22A shows the plot of displacement (heave) measured along strike in the eastern segment of the Kuantan Fault. An ideal fault would show decreasing displacement from the centre of the fault to the tip line at either ends. The presence of two displacement maxima in Fig. 3.22A, however, implies that the eastern Kuantan Fault may have been formed by two coalescing fault segments.

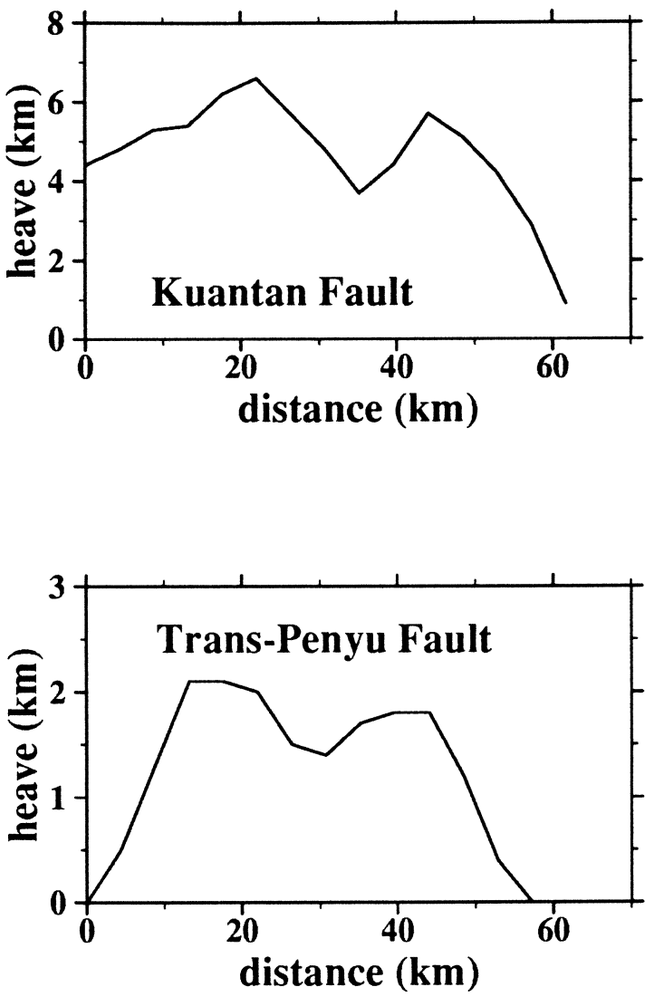

Figure 3.22. Plot of displacement (heave) versus arbitrary distance in km along the western segment of the (A) Kuantan Fault. (B) Trans-Penyu Fault. Presence of minima in the curves about halfway along strike suggests that the faults may have evolved by segment linkage (*cf.* Peacock and Sanderson, 1994).

It would seem reasonable to assume that the western segment of the Fault was formed by a similar process. Figure 3.22B is the displacement profile for the southeastern part of the Trans-Penyu Fault, which also suggests fault growth by segment linkage. It should be emphasized, however, that the ideal fault-growth model assumes that the fault is initiated in a homogeneous isotropic medium, which is rarely the case in natural systems. Pre-existing planes of weakness (*e.g.* old faults) may exert a strong influence on the growth and linkage of faults.

Figure 3.23 shows schematically the evolution of the Kuantan Fault by segment lengthening and linkage during progressive extension. The main part of the Fault may have nucleated at the deepest part of the Basin, where displacement had

been greatest, while smaller segments nucleated to the west (1). Further extension causes the segments to eventually link up (2) and form the two main strands of the Kuantan Fault, which are separated by a relay ramp. During advanced stages of extension, the relay ramp is breached by NW-trending transfer faults, whose location may have been influenced by pre-existing basement weaknesses. A major basement weakness along what is now the Trans-Penyu Fault may have prevented propagation of the Fault further eastwards. Part of the strain at this junction is accommodated by the initiation of an oblique-slip "release fault" (*cf.* Destro, 1995).

An interesting feature of the Kuantan Graben is that the hangingwall-basin fill is also highly faulted (Fig. 3.19), apparently as the result of propagation of the synthetic hangingwall extensional faults into the sediment cover. The hangingwall faults exhibit listric profiles as they continue upwards into the overlying sediment. Notice that the faults tend to die out before reaching the Top-Synrift Unconformity, suggesting that the faulting may be related to the rifting phase. The listric geometry is believed to be the result of simultaneous extension and sedimentation, as illustrated in Fig. 3.24, based on the experimental results of Vendeville and Cobbold (1988).

Although most faults seem to terminate near the Top-Synrift Unconformity, which marks the end of the extensional phase, some faults, such as the Kuantan Fault (Line 90-105, Fig. 3.18) and the northern Rumbia Graben border faults (Line 90-29, Fig. 3.25), have propagated upwards into the postrift strata. These faults cut the younger stratigraphic units up to Horizon 2, but no apparent change in the thickness of those units is observed across the faults. This suggests that the apparently young age of faulting is not the result of tectonic reactivation of the basement faults. Because the post-rift phase is one of gradual subsidence with apparently no tectonic activity, the young faults could be the result of differential compaction of the sedimentary layers during postrift subsidence. This type of fault has been termed "drape-slip fault" by Bertram and Milton (1989, p. 251).

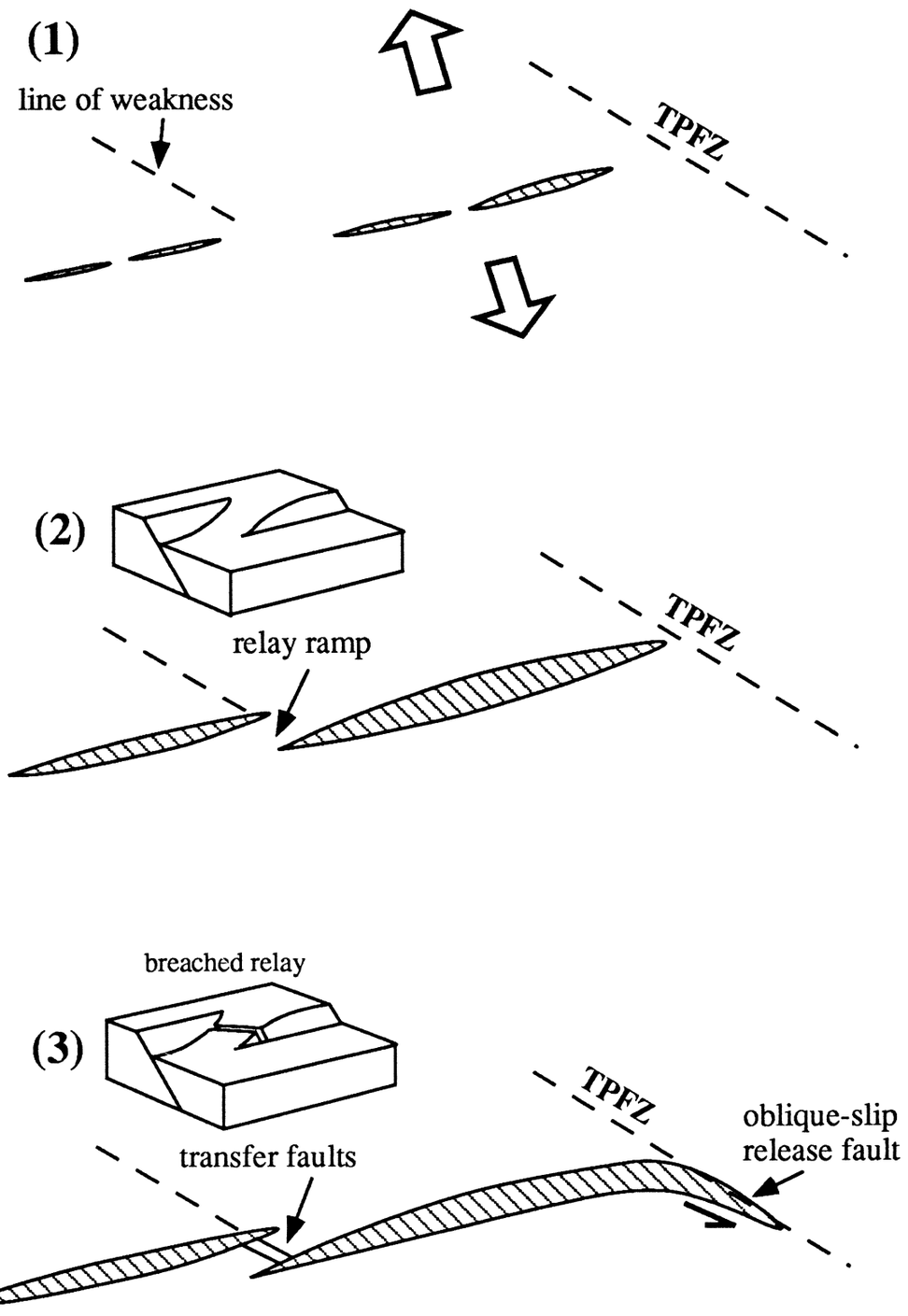

Figure 3.23. Model for the evolution of Kuantan Fault. (1) Incipient faults developed as segments in response to N–S extension. (2) Segments joined to become larger faults as extension progresses. Relay ramp develops as the fault tips interact. (3) Transfer fault breaches the relay ramp. The presence of major line of weakness (Trans-Penyu Fault) causes oblique slip fault to develop in the east. Block diagram shows schematically the geometry of the relay zone.

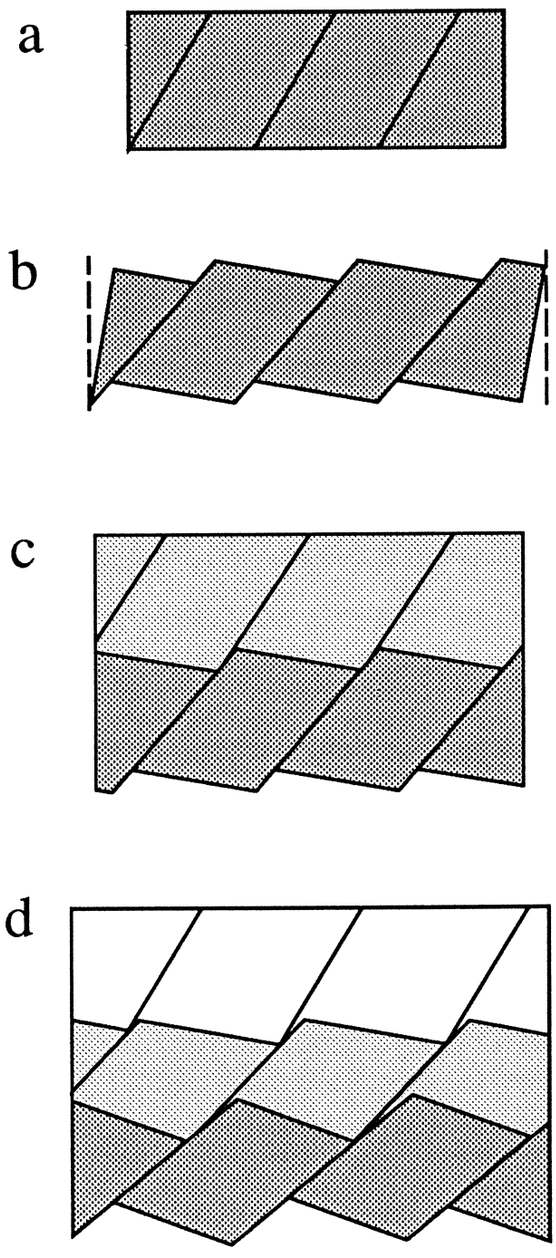

Figure 3.24. Model of listric faulting caused by syn-extensional sedimentation (After Vendeville and Cobbold, 1988). (A) Initiation of faults dipping at 60°. (B) After an increment of extension, the dips of faults decrease as the blocks rotate. (C) Sedimentation of new layer and propagation of faults up section, dipping at 60°. (D) Another increment of extension and sedimentation, causing rotation of older faults and propagation up the section. The result is an overall listric fault. Note that compaction of the older layers may enhance the listricity of the fault.

The occurrence of fault-propagation folds suggests that some parts of the Kuantan Fault have been reactivated during the tectonic inversion phase (see Section 3.5). For example, in Line 90-105 (Fig. 3.18), the Fault has propagated upwards into Unit P3 in front of a small fold which had developed above the foot-wall scarp. Notice that the fold is truncated at the Mid-Miocene Unconformity (Horizon 8). Fault-propagation folds are observed also in the other lines shown in Fig. 3.19. The basin inversion phase, which took place in middle Miocene times, is discussed further in Section 3.5.

3.4.2 Rumbia Graben

The Rumbia Graben, in the eastern part of the Basin, has a more complex geometry and shows contrasting structural styles along its length. The southeastern part of the Graben is characterised by regularly-spaced (10–12 km apart), NW-trending normal faults forming domino-style tilted blocks. In the northwest, however, the structure is dominated by low-angle and, commonly, listric faults which appear to be linked at depth with the Trans-Penyu Fault. These structures seems to be secondary splay faults resulting from strike-slip reactivation of the Trans-Penyu Fault. The southwestern margin of the Rumbia Graben is marked by the remarkably linear Trans-Penyu Fault. This fault was traced by Ngah (1975) further to the northwest for about 100 km, almost reaching the Peninsular Malaysian coastline. The Fault dips steeply to the northeast at ~55°, and appears to represent a major structural discontinuity across the Basin. Horizontal displacement along the southeastern part of the Trans-Penyu Fault suggests that it may have formed as smaller fault segments that linked up during the evolution of the Basin (Fig. 3.22B). Because it is straight and parallel with the major strike-slip faults on Peninsular Malaysia, the Fault may represent a reactivated basement fault.

Evidence for significant strike-slip motion on the Trans-Penyu Fault is found in the northeastern part of the Rumbia Graben. Figure 3.26A is a correlation of faults in Lines 90-18 and 90-19, which are oriented perpendicular to the axis of the

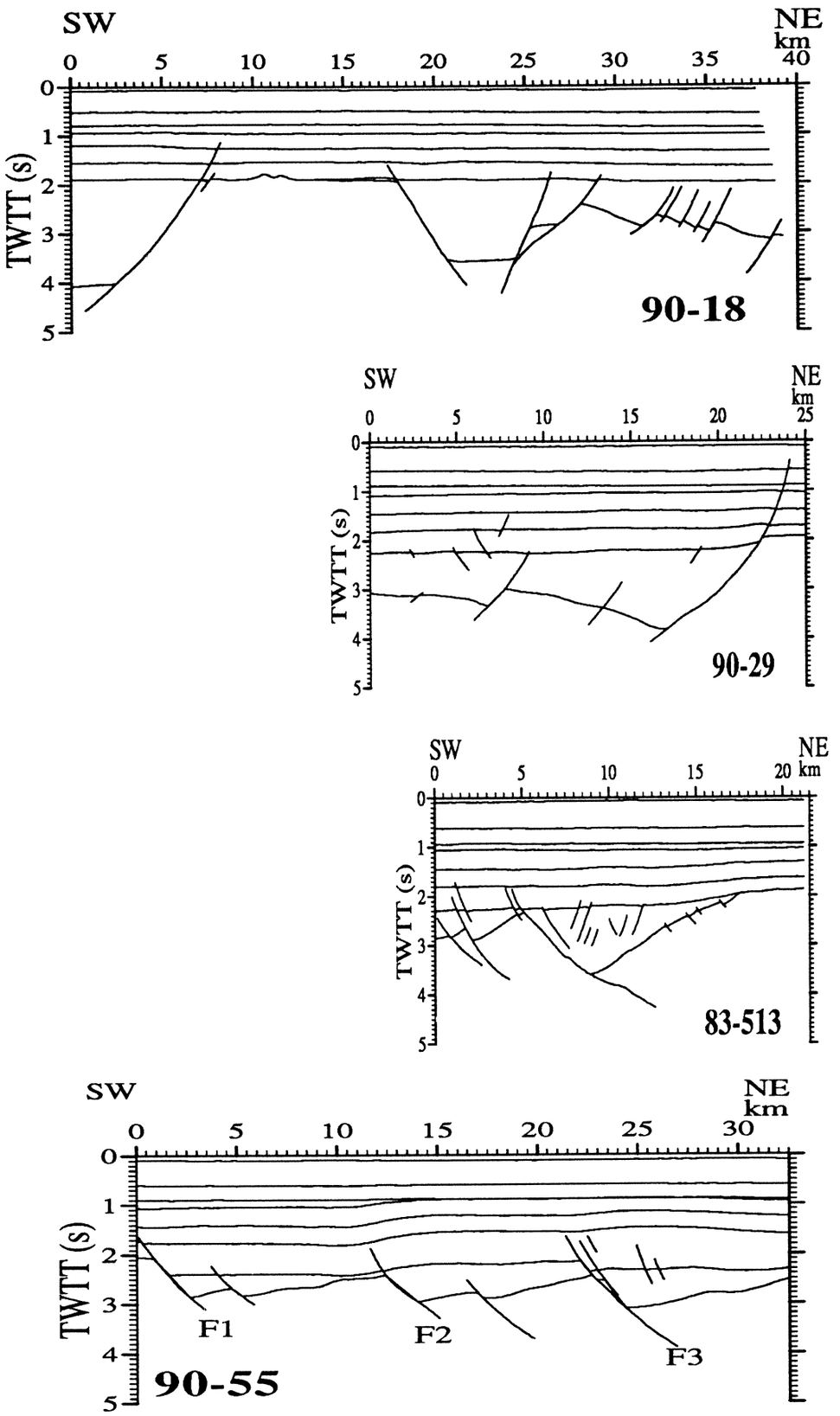

Figure 3.25. Selected NE–SW cross sections across the Rumbia Graben, showing the contrasting fault geometries and styles along strike, from NW (top) to SE (bottom). Line 90-55, at the bottom, shows tilted fault-blocks in the southeastern part of Graben, exemplifying the typical of domino-style of extensional faulting. Note the regular spacing of the main border faults (F1, F2, and F3). The same horizontal scale in km is used for easy comparison. *Foldout overleaf shows Line 83-513 at a smaller scale.*

Figure 3.25 (cont.) Top: Seismic line 83-513 from the Rumbia Graben, showing the prominent fault-plane reflection between 7 and 12 km, dipping northeastwards and forming the border fault to a half-graben. Bottom: Interpretation of the line, showing the main half-grabens and faults.

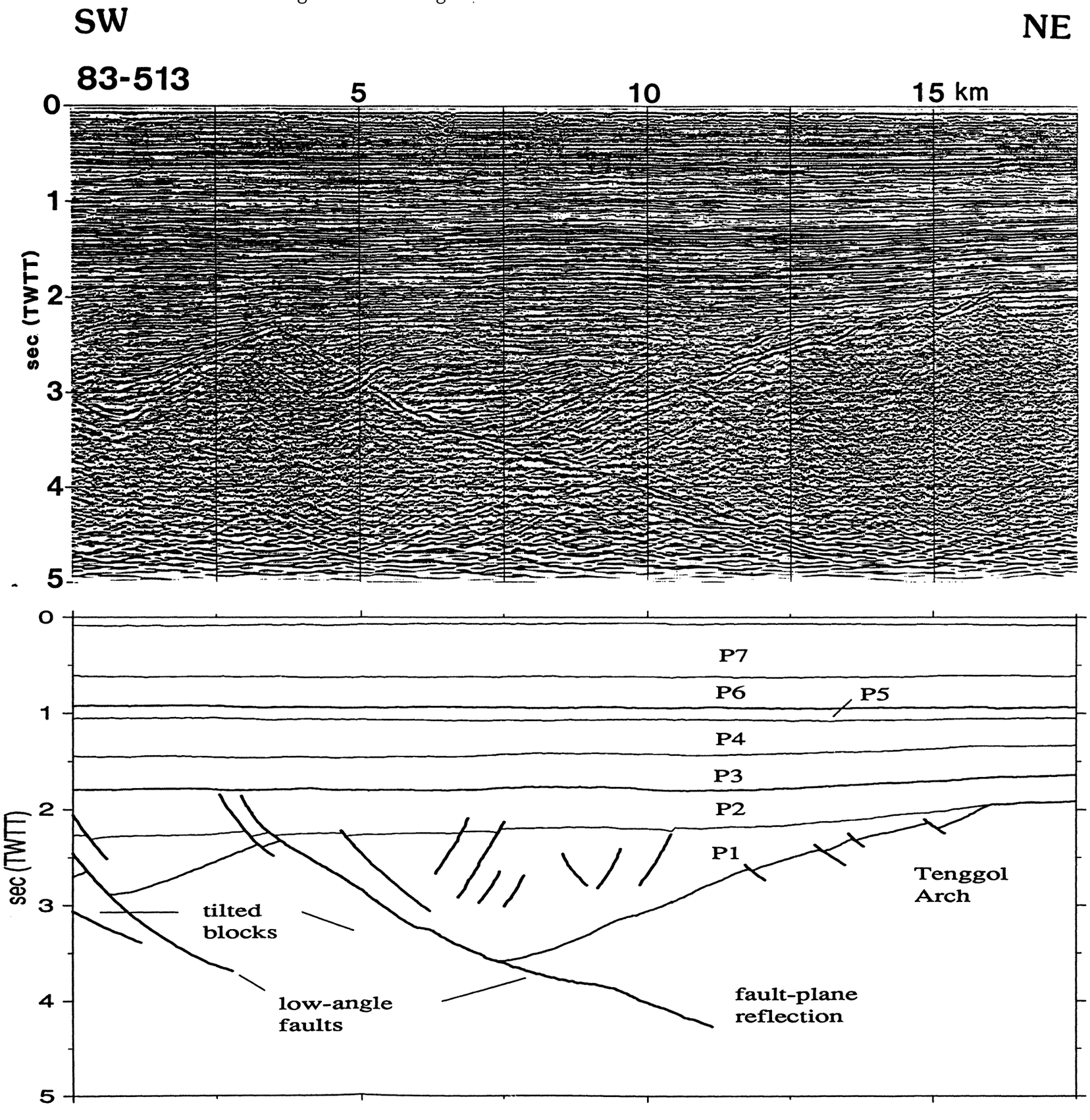

Graben. The figure shows a series of closely spaced, SW-dipping faults, antithetic to the Trans-Penyu Fault. The shallower dips of these smaller faults suggest that they may be linked to the Trans-Penyu Fault at depth. A reconstruction of the geometry of the faults is shown in Figure 3.26B. The SW-dipping faults are interpreted as splays of the Trans-Penyu Fault, which form a releasing geometry in response to strike-slip reactivation. The 3D geometry of the whole system resembles a negative flower structure, with the Trans-Penyu Fault acting as the master oblique-slip fault along which pull-aparts grabens developed.

Futher to the southeast, in the main part of the Rumbia Graben, large and strongly arcuate half-graben border faults having dips as low as 31° and 35°(Table 3.3). Lines 90-29 and 83-513 (Fig. 3.25) show two major faults with opposite polarity; one downthrowing to the SW and the other to the NE. An interesting feature of these faults is that they appear to be listric rather than planar.

In some lines, fault-plane reflections can be traced into the basement down to about 4.5 s two-way time. The true-scale geometry of the fault can thus be determined from depth-converted sections by assuming an appropriate velocity for the basement. Figure 3.27 is a depth-converted section of Line 83-513 that was shown previously in Fig. 3.25. The velocity of the sedimentary layers used in the conversion is based on stacking velocites and well velocity surveys (Appendix A.1). A number of possible basement velocities was used to show the uncertainties in the conversion of the fault plane. Very little difference in the fault profile is produced by the different basement velocities. According to the data of Ben-Avraham and Emery (1978), a velocity of 5.0 km s^{-1} (Appendix A.1) is probably the maximum for the Mesozoic rocks underlying the Sunda Shelf, and is therefore regarded as the most likely model. The average dip of the fault is 35° down to about 8 km depth.

The identification of listric normal faults in seismic sections is usually problematic because of the uncertainties in the depth-conversion of two-way-time seismic sections. The occurrence of wedge-shaped, syn-rift reflectors is not, by itself,

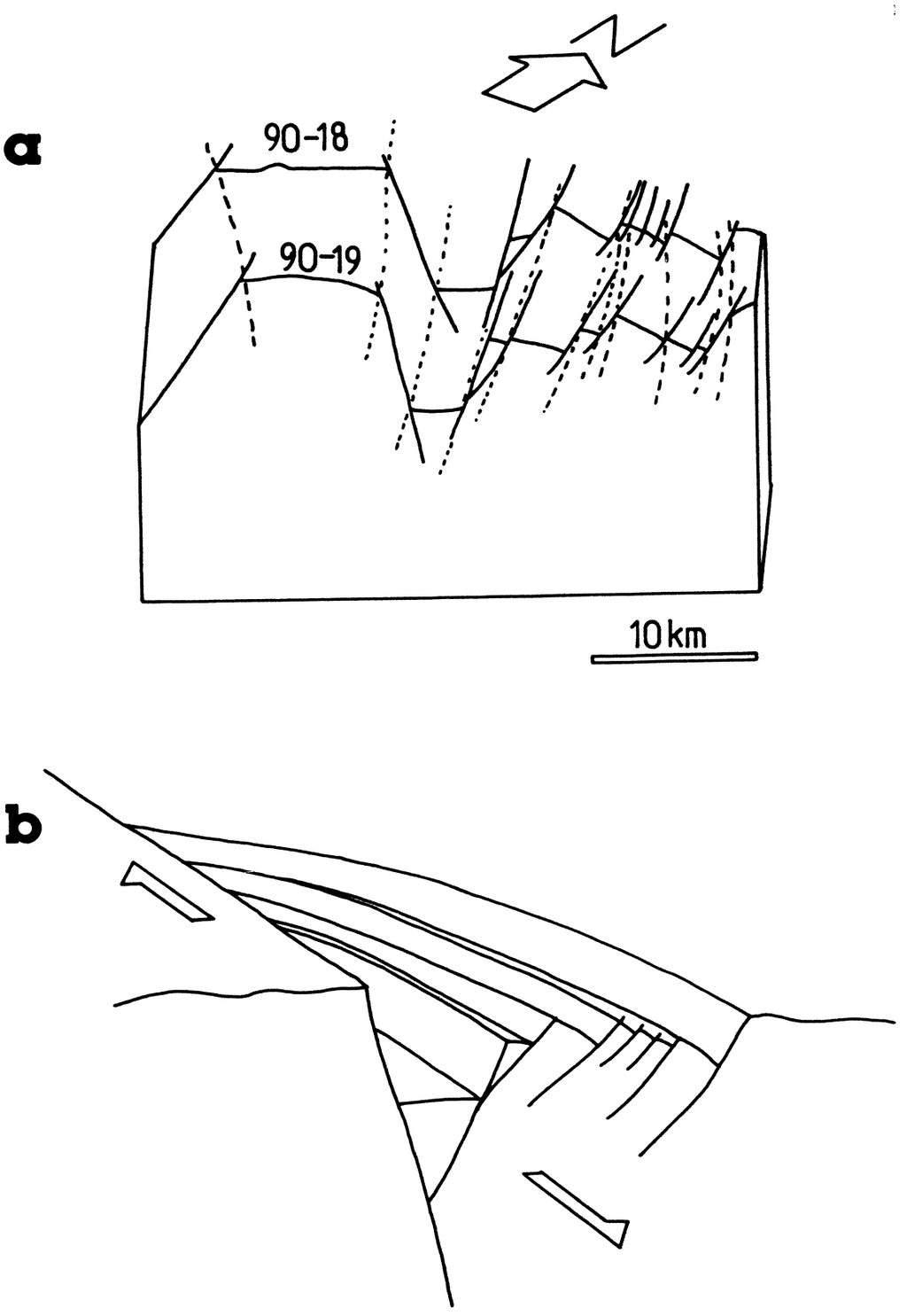

Figure 3.26. (A) Correlation of faults in Lines 90-18 and 90-19. (B) Schematic interpretation of the geometry of faulting as suggested by the reconstruction in (A).

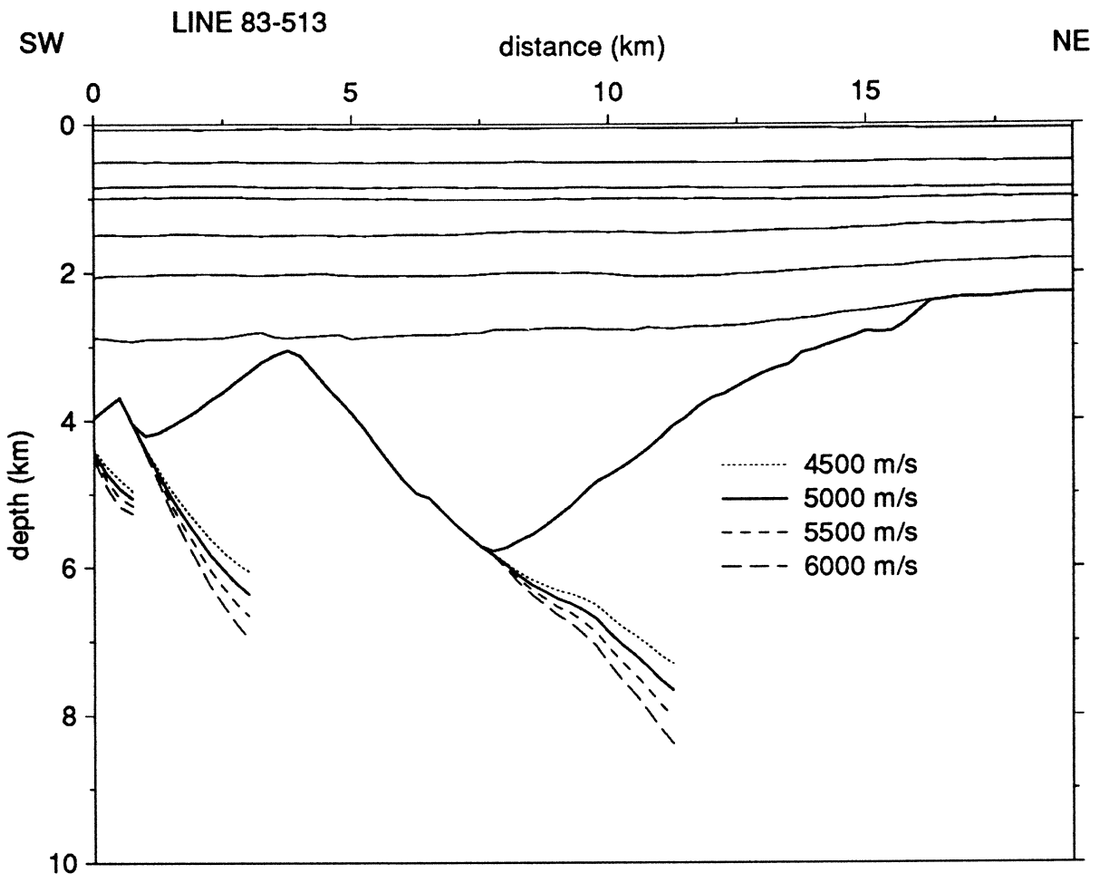

Figure 3.27. Depth-converted section based on Line 83-513 to show the fault geometry in the basement. Most likely basement velocity is 5000 km s^{-1}.

characteristic of listric faults because it can also result from planar domino-style faulting (Barr, 1987). In domino faulting, both the fault and the hangingwall beds rotate about horizontal axes during extension, resulting in planar wedge-shaped synrift reflectors. In the Rumbia Graben, the rotational nature of faults is not readily demonstrated (*cf.* Wernicke and Burchfiel, 1985) because of the lack of pre-rift reflectors which can be used as passive markers. The presence of hangingwall rollover, however, is commonly associated with listric normal faults (*e.g.* Shelton, 1984; Badley *et al.* 1984). Hangingwall rollover is caused by increasing bed rotation towards the bounding fault resulting from the curvature of the fault plane, while the footwall remains stationary. The fact that the northern Rumbia faults are low-angle and there is rollover of the hangingwall sediment suggest strongly that the faults are listric. Further evidence for the listric geometry of the fault is given by the fact that they are arcuate in map view (see Fig. 3.31).

3.4.3 Merchong Graben

The Merchong Graben, in the southwestern corner of the Basin, is characterized by steep bounding faults to the northeast and southwest, and by its symmetry and flat basement topography (Fig. 3.28). The interior of the Graben is cut by a set of conjugate normal faults that dip towards the centre of the Graben. In map view, these faults define sigmoidal traces in the western part of the Graben (Figs. 3.31). Its rectangular shape, flat basin floor, steep walls, and linear bounding faults suggest strongly that the Graben formed as a pull-apart between two NW-trending strike-slip faults. The general geometry is similar to that of the Dead Sea pull-apart basin (Fig. 4.15, p. 138). These straight and steeply dipping (~65°) faults are parallel to the Kuala Lumpur – Endau Fault on Peninsular Malaysia, which are left-lateral strike-slip faults that was active in late Cretaceous–Tertiary times (Chapter 2). At the western end of the Graben (Fig. 3.35A), extension in a roughly NW–SE has resulted in conjugate normal faults forming a narrow rift zone (Fig. 3.29).

The northern border fault (NMF in Fig. 3.28) shows signs of having been reactivated during the postrift phase. This is best observed in Line 90-41 (Fig. 3.28), where the fault has propagated into the postrift strata and show a convex-upward profile. Another fault lie basinwards, parallel to the NMF and has a similar geometry. The three-dimensional geometry of the faults, shown schematically in Fig. 3.30, is that of an upward-diverging fault system resembling a positive flower structure. The Fault shows variable curvature along strike; convex upwards in the southeast but concave upwards in the northwest. The apparently helicoidal geometry is similar to that produced experimentally by Naylor *et al.* (1986), and suggests that the NMF had been reactivated as a dextral wrench fault (Fig. 3.30). The Merchong Graben seems to have evolved from a transtensive to a transpressive phase, which involved reactivation of the earlier extensional structures.

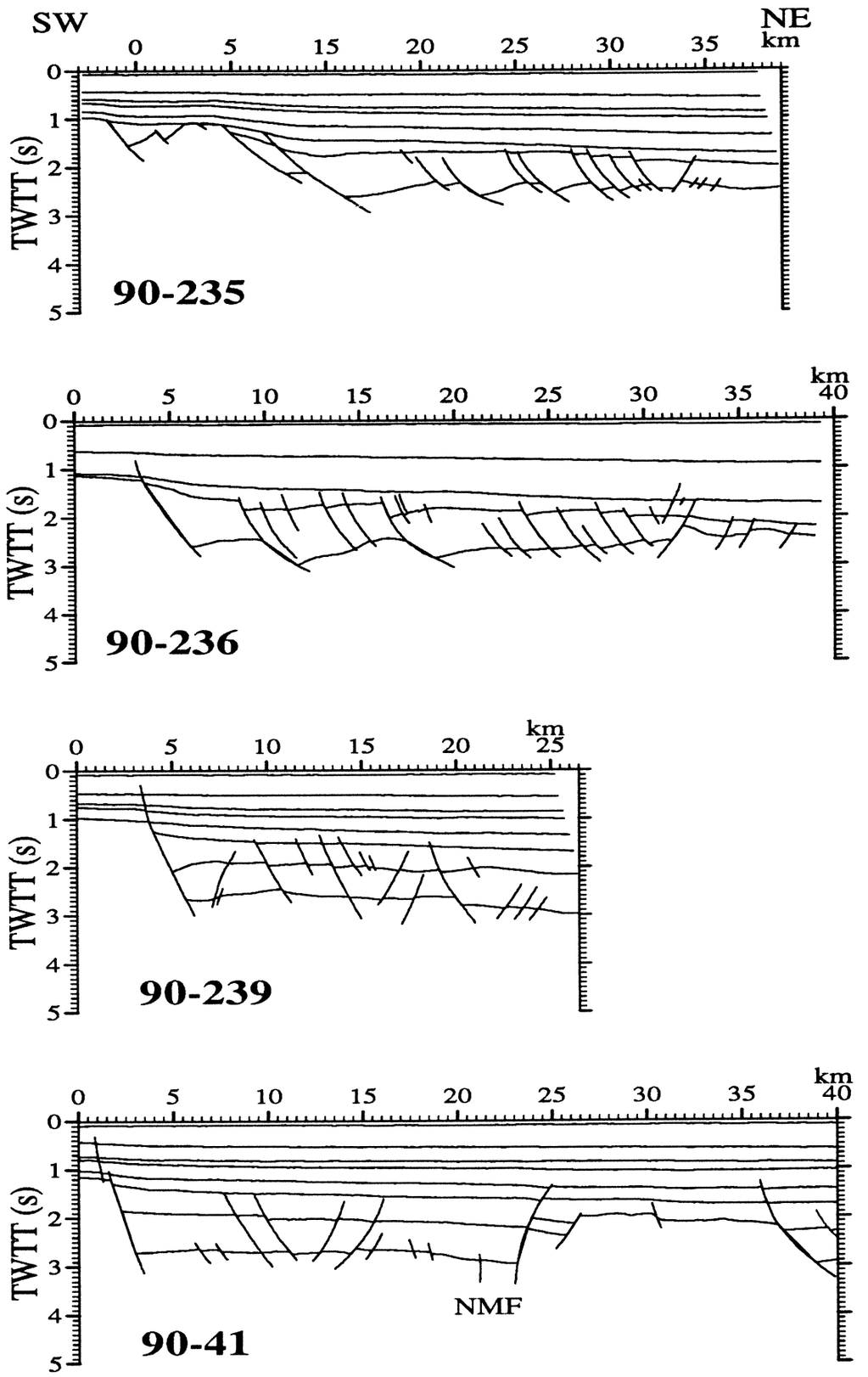

Figure 3.28. Selected NE–SW cross sections across the Merchong Graben, showing the contrasting fault geometries and styles along strike, from NW (top) to SE (bottom). The same horizontal scale in km is used for easy comparison. *Detail of Line 90-41 showing the geometry of the Merchong Graben given in foldout overleaf.*

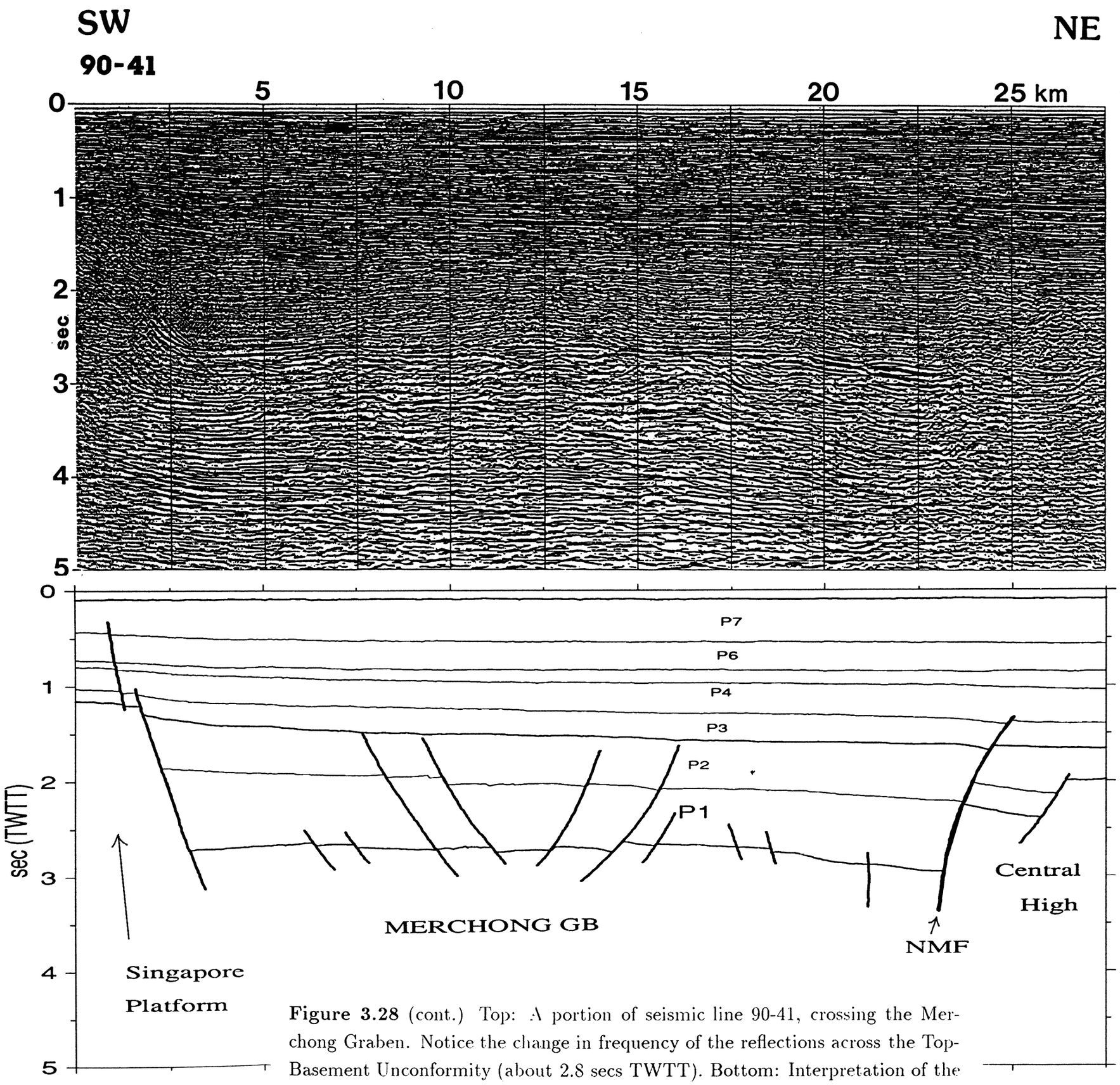

Figure 3.28 (cont.) Top: A portion of seismic line 90-41, crossing the Merchong Graben. Notice the change in frequency of the reflections across the Top-Basement Unconformity (about 2.8 secs TWTT). Bottom: Interpretation of the line showing the major faults and graben geometry. Note the curvature of the North Merchong Fault (N.M.F.).

Figure 3.29. Cross-section across the Merchong Graben. Line 90-135. NW–SE section of Merchong Graben, showing the numerous closely-spaced faults at the Western Boundary Fault Zone.

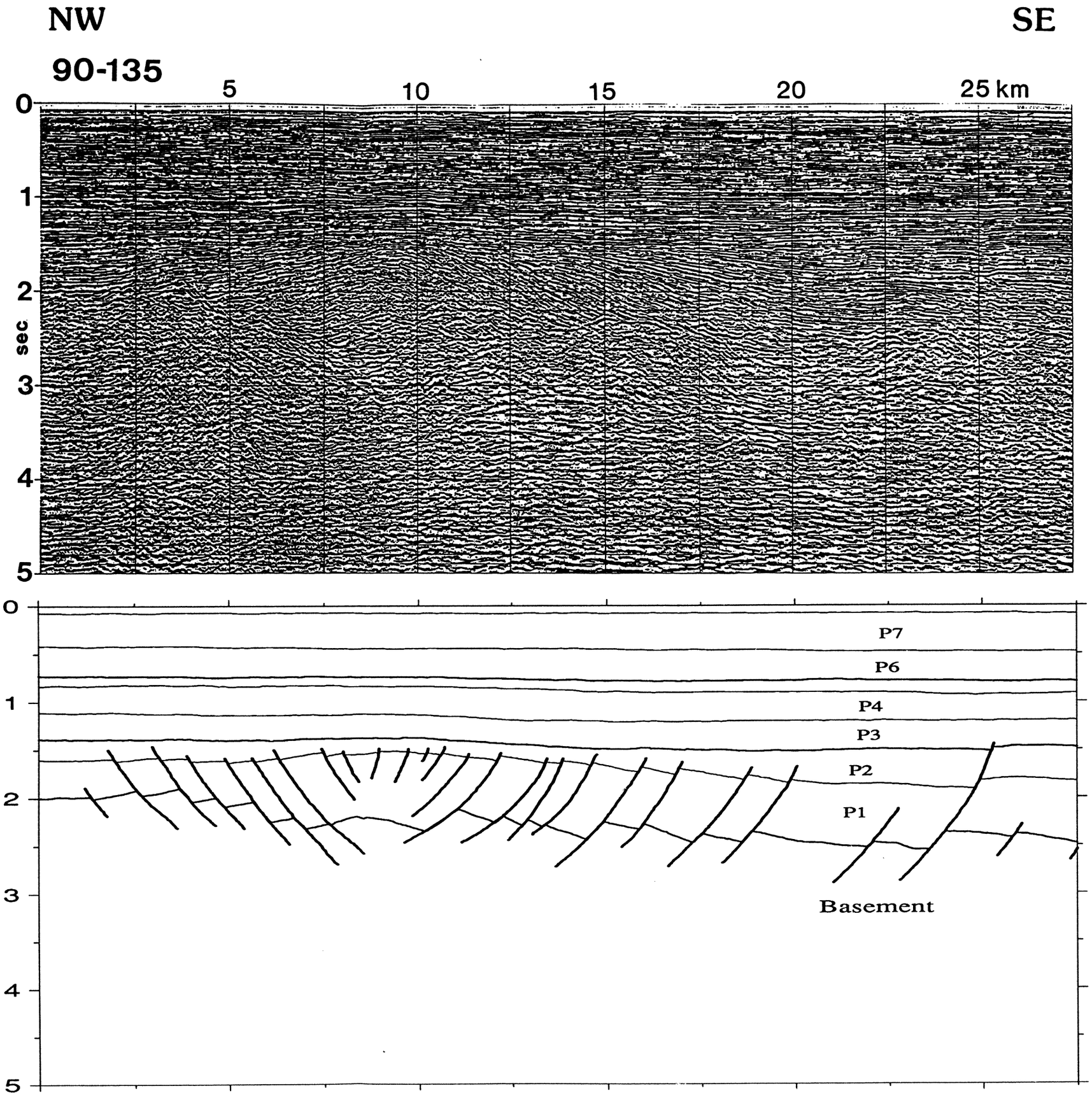

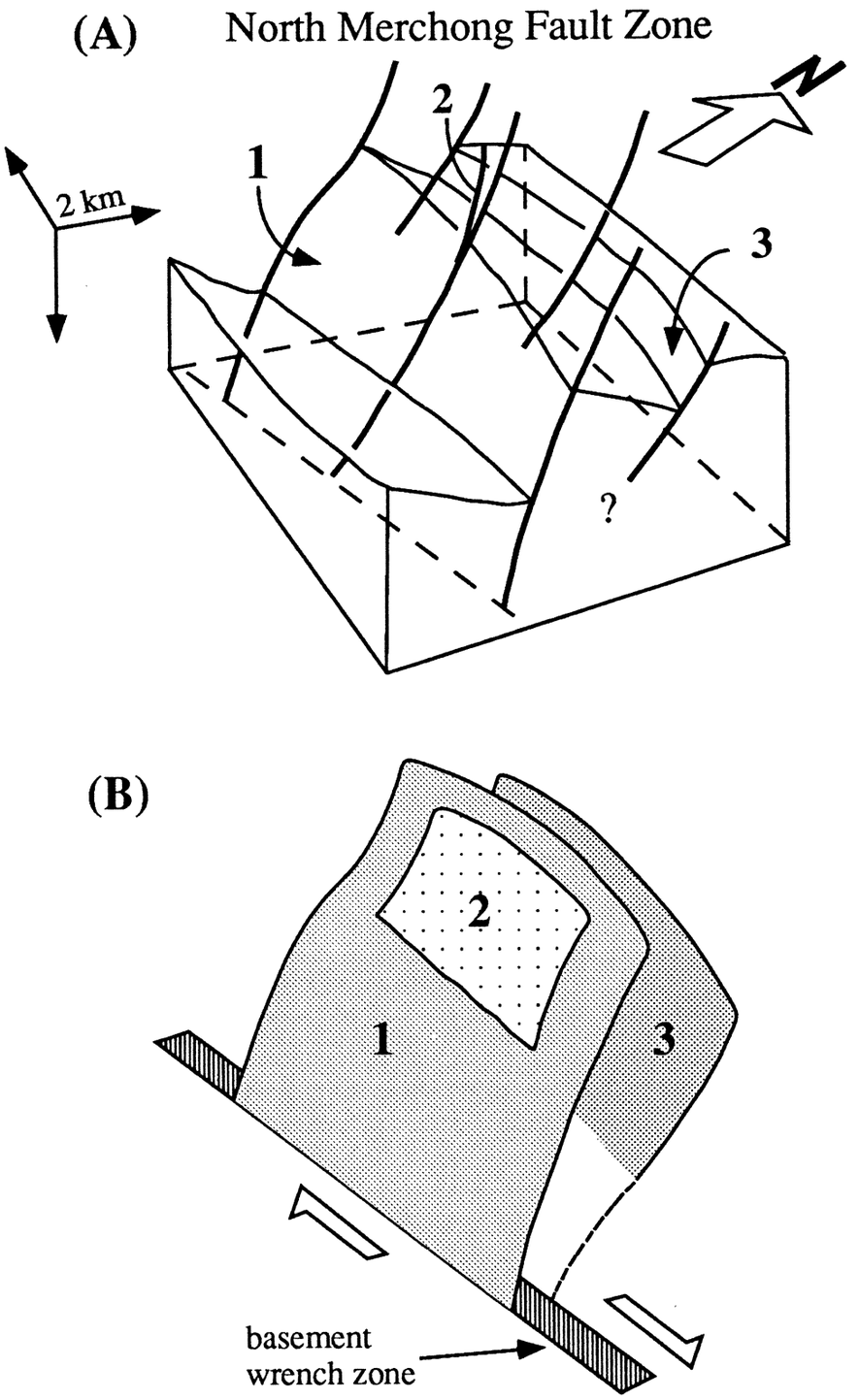

Figure 3.30. A) Block diagram showing the geometry of the North Merchong border fault zone based on correlation between successive NE–SW dip-lines. Three fault planes (1, 2, 3) are identified. Fault 2 is a small splay of Fault 1. The deeper part of Fault 3 is unclear from the seismic data, but its curvature suggests that it is linked with Fault 1 at depth. (B) Schematic diagram of the three faults in (A), illustrating the curved fault planes, linked as part of a major dextral basement wrench zone (*cf.* Naylor *et al.* 1986).

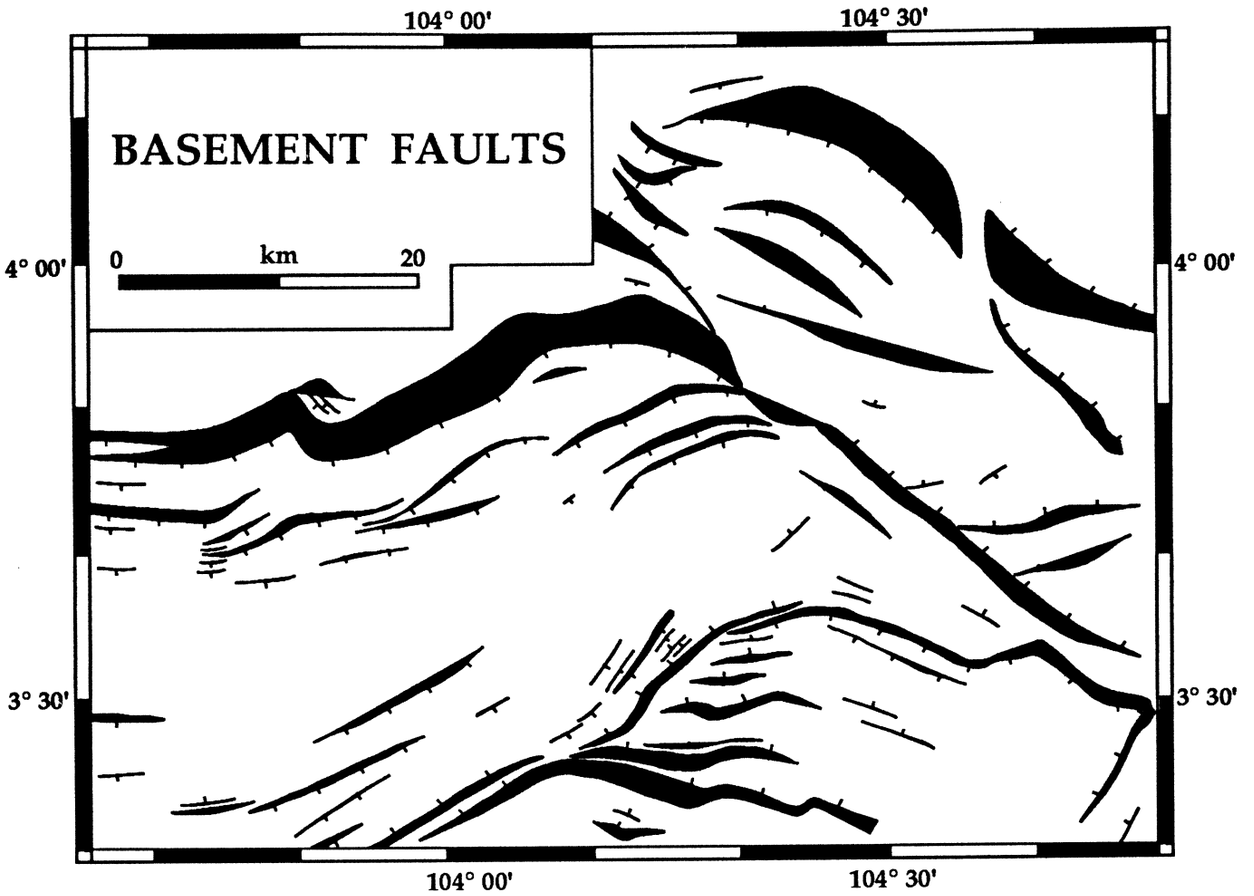

Figure 3.31. Basement faults in Penyu Basin. Barbs represent downthrown side. Note that "thicker" faults mean larger horizontal displacement (heave).

3.4.4 Kinematics of Extension

Figure 3.31 shows a map of faults identified from the seismic data. The map shows, essentially, two sets of fault: one trending ENE and another trending NW. The orientation of the faults, shown in Fig. 3.32, suggest roughly N–S extension, between 150° and 190°. This result is consistent with the regional stress regime associated with the indentation of India into Eurasia, which resulted in overall dextral shear of the region and, hence, E–W shortening and N–S extension. The rectilinear fault pattern in the Basin suggests that extension may have been strongly influenced by pre-existing basement structures. Especially striking are the linear NW-trending faults bounding the Rumbia and Merchong Grabens in the eastern part of the Basin. These faults have a similar orientation to known left-lateral strike-slip faults on land, which indicates that they originated along older faults. Seismic evidence has been discussed earlier to show that the Trans-

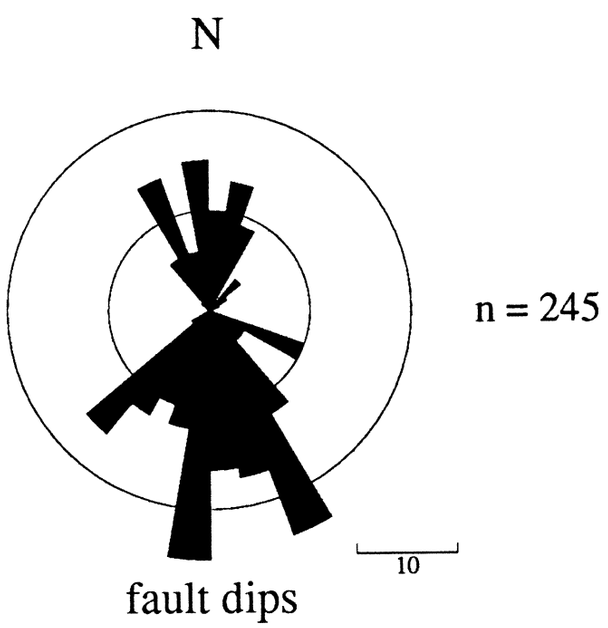

Figure 3.32. Rose plot of fault orientation, represented as the direction normal to the fault strike, *i.e.* dip azimuth. Each sector represents 10°, outer circle is n=20.

Penyu Fault and northern Merchong border faults had acted as strike-slip faults during basin development. The presence of these older faults may have resulted in the partitioning of extension to produce the resulting complex basin geometry.

Besides fault orientation, hangingwall dip direction is also a useful indicator of the regional extension direction in half-graben basins. Hangingwall dip analysis (Scott *et al.*, 1994) is based on a simple assumption that the hangingwall of a half-graben border fault dips in the direction of extension. The technique is particularly useful in areas where the seismic coverage is insufficient for detailed mapping of fault geometry. The hangingwall dips in the Penyu Basin were computed at the intersections of the seismic lines shown in Fig. 3.2. Because we are interested only in the azimuths, rather than the absolute magnitudes, of the

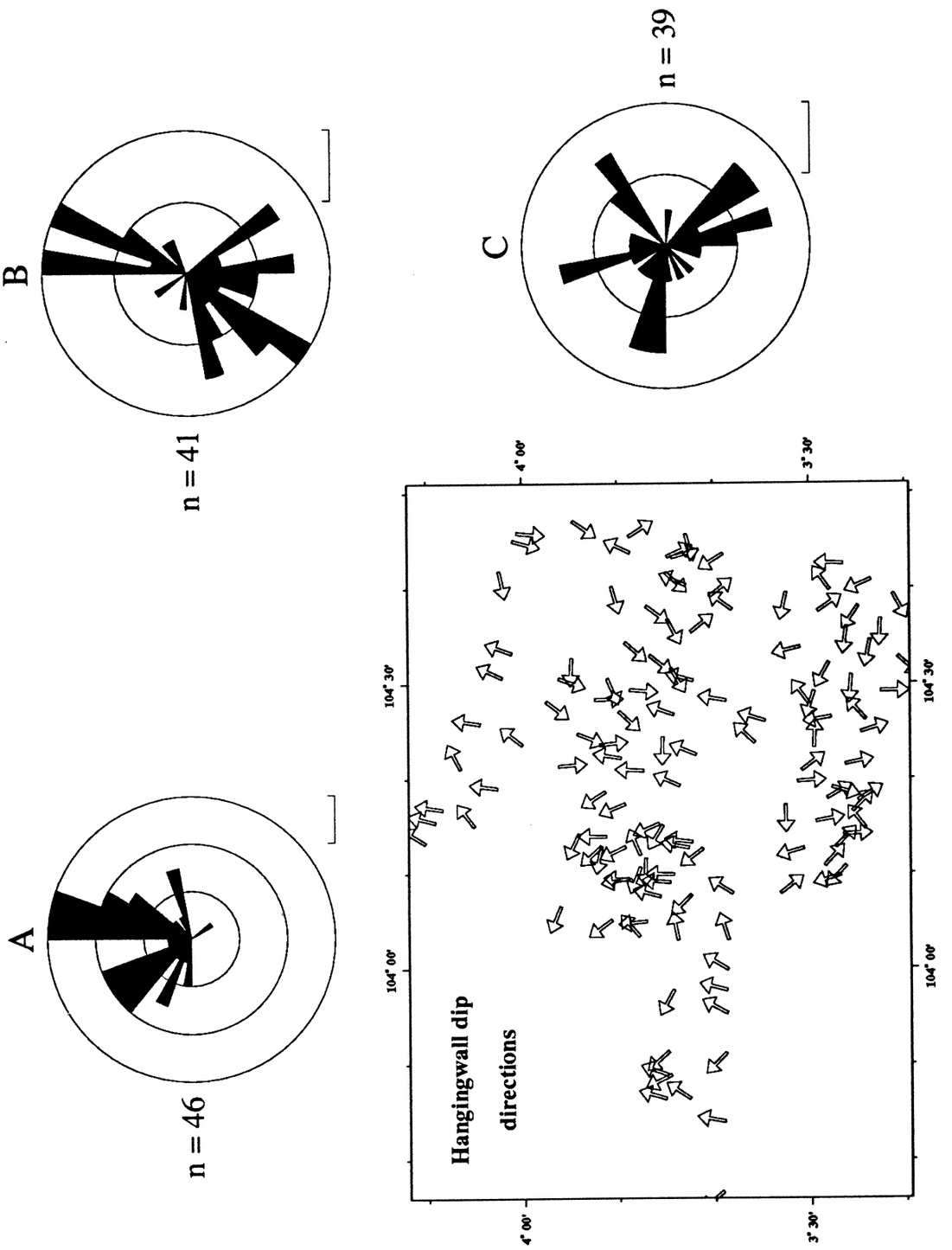

Figure 3.33. Map of hangingwall dip directions calculated at the intersections of seismic lines (method outlined in Scott *et al.* 1994), showing the general kinematics of the basin border faults. Rose plots for each graben are shown to illustrate the partitioning of the extension due to pre-existing basement inhomogeneities. A) Kuantan Graben. B) Rumbia Graben. C) Merchong Graben.

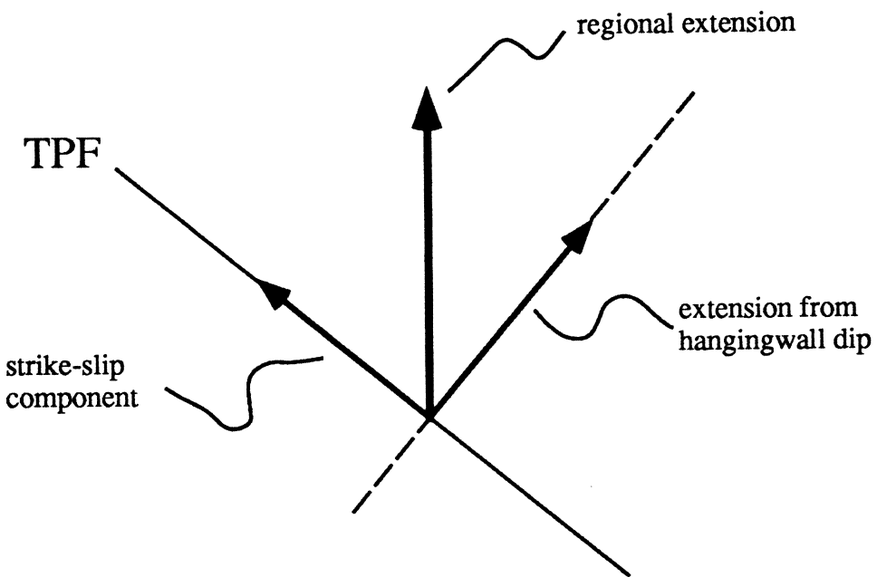

Figure 3.34. Partitioning of extension by Trans-Penyu Fault (TPF) into left-lateral strike slip and NE–SW dip slip.

hangingwall dips, the method works for both depth and time sections. Figure 3.33 is the result, in the form of an arrow-map showing the hangingwall dip directions and rose diagrams representing the three main subbasins. As indicated by the fault dip-azimuth data in Fig. 3.32, the Kuantan Graben shows roughly N–S extension. Its simple half-graben geometry seems to be the result of almost orthogonal extension. In the Rumbia Graben, the overall extension implied by the hangingwall dips is roughly NNE–SSW, probably the result of partitioning of the extension into left-lateral slip on the Trans-Penyu Fault (Fig. 3.34).

The Merchong Graben shows a complex hangingwall dip pattern because of local tilting of the numerous small fault-bounded blocks within it (Fig. 3.31). Figure 3.35 shows a model for the formation of the Merchong Graben. As in the Rumbia Graben, the oblique orientation of its bounding faults relative to the regional N–S extension may have resulted in partitioning of slip into NE–SW extension and left-lateral strike slip on both its northern and southern bounding faults (Fig. 3.35). This produces a sinistral shear couple and rotational shearing of the intragraben faults, forming the sigmoidal-shaped basinal faults observed in the western part of the graben (Fig. 3.35A). The intragraben faults may have

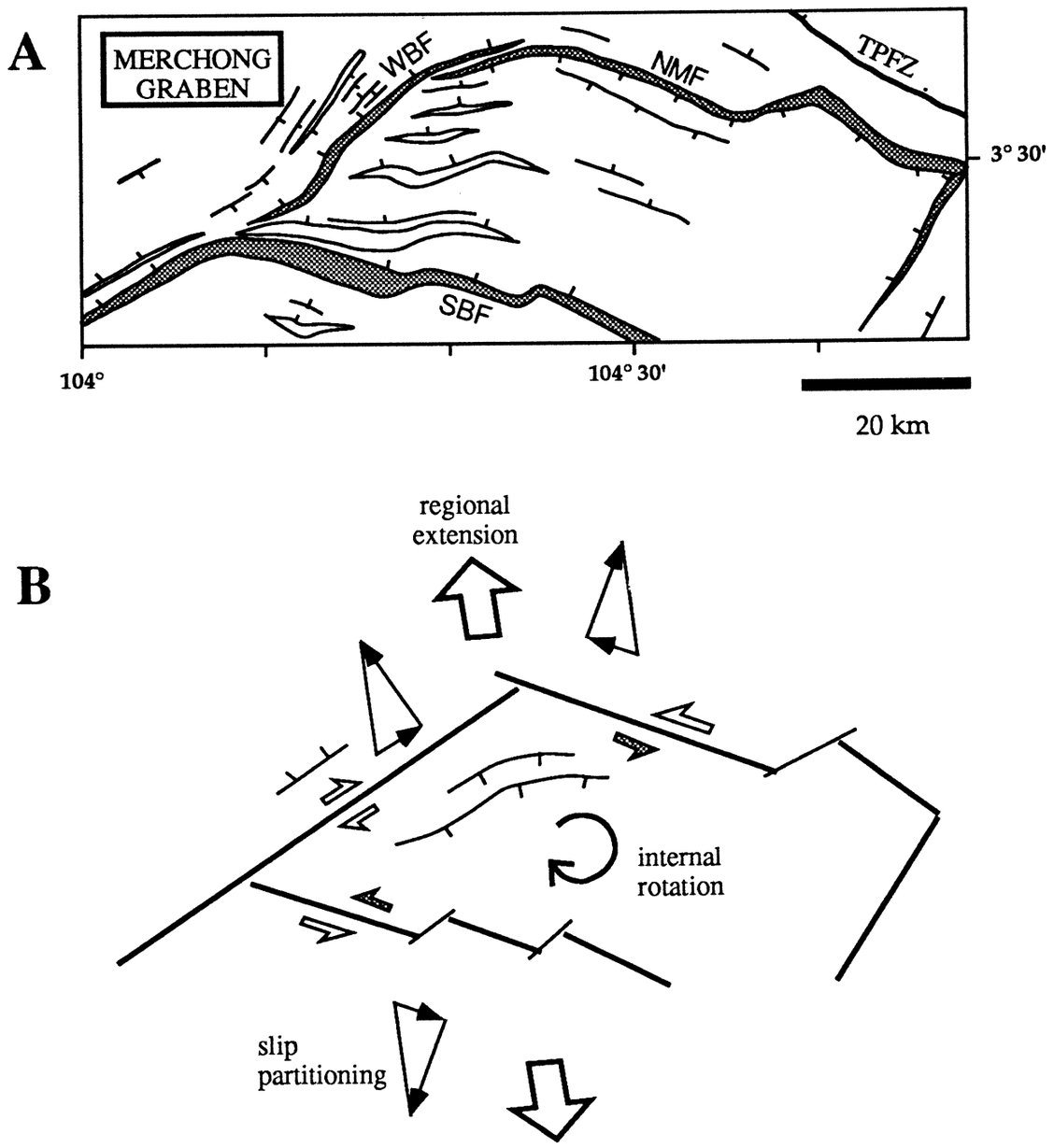

Figure 3.35. Kinematic development of Merchong Graben. (A) Map of major border faults: Trans-Penyu Fault (TPFZ), Western Boundary Fault (WBF), Northern Merchong Fault (NMF), and the Southern Boundary Fault (SBF). Note the sigmoidal intragraben faults. (B) Kinematic interpretation of the structural features in (A), discussed in the text.

developed as extensional fractures during graben initiation, and were subsequently rotated as a result of the sinistral shear on the system (*cf.* Schreurs, 1994).

The kinematic development of the Penyu Basin is shown schematically in Fig. 3.36. The Basin is envisaged to have formed in response to regional dextral shear, caused by the India-Eurasia collision (Chapter 2), which reactivated pre-existing subparallel NW-trending basement faults. Deformation is accommodated by clockwise rotation of the faults and crustal blocks between them. The resulting slip on the NW-trending faults is sinistral as the blocks rotate in response to the regional dextral shear (A). Secondary clockwise rotation of the blocks resulted in opening of isolated half-grabens at the fault intersections, probably assisted by E-trending basement inhomogeneities.

3.5 Inversion Structures

Inversion structures are the result of contractional deformation of originally extensional basins ("positive inversion") or extensional reactivation of thrust zones ("negative inversion") (Coward, 1994). "Basin inversion" refers specifically to the positive inversion of extensional basins as a result of compressional forces (*e.g.* Murphy, 1989). There is widespread evidence for basin inversion in the Penyu Basin. At least two phases of inversion have been recognized, based on the presence of compressional structures and associated erosional unconformities. The first inversion phase took place at the end of the Synrift II phase in late Oligocene times. It involved the strike-slip reactivation of basement faults as the result of late synrift tectonic movements. Structures formed during this phase are recognized as "pop-up" structures, which are often truncated at their crests by the Top-Oligocene Unconformity (Horizon 6) (Fig. 3.12, p. 62).

The second, more widespread, phase of basin inversion occurred during the early to middle Miocene, and is related to the regional inversion phase documented in the Malay and West Natuna Basins (Ginger *et al.*, 1993). The inver-

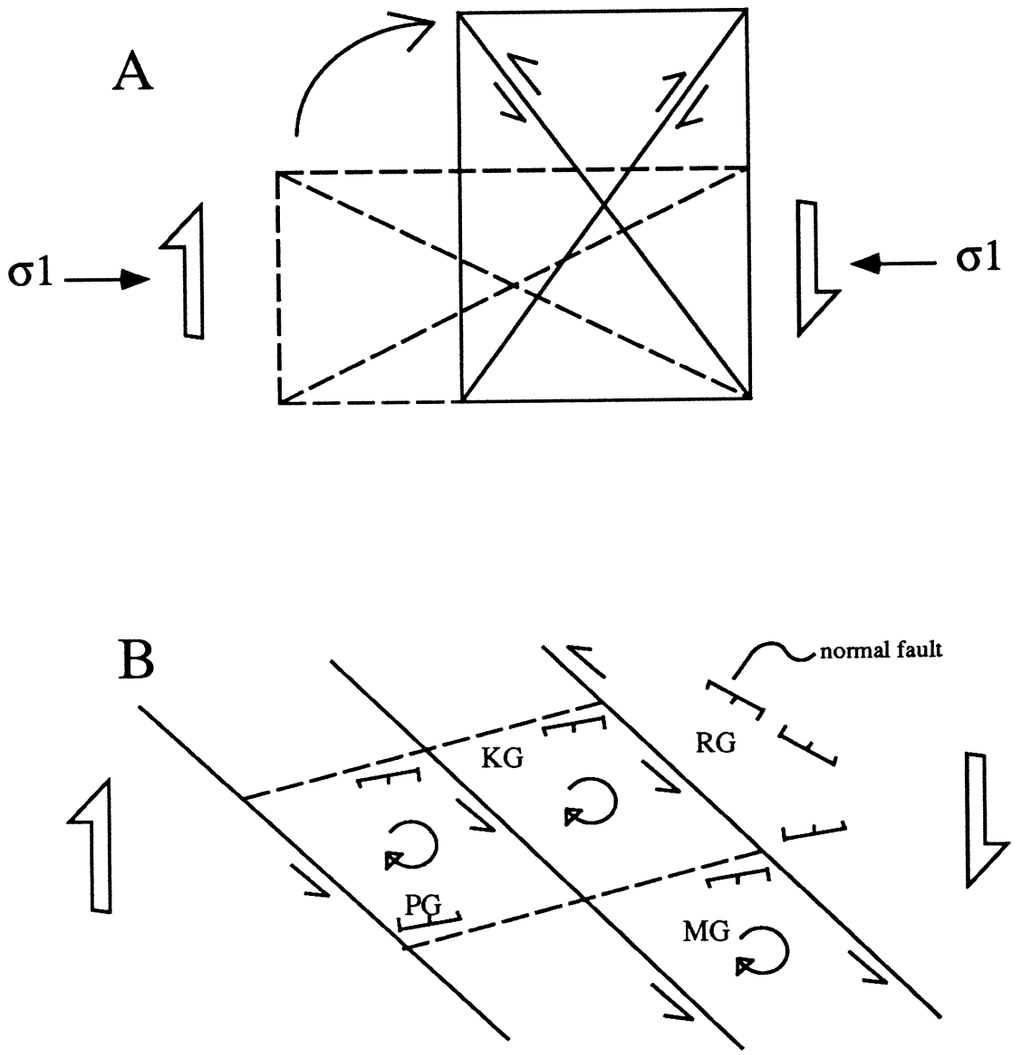

Figure 3.36. General model for the development of the Penyu Basin. (A) Schematic of dextral transpressional shear acting on rectangle with conjugate set of faults (dashed line). During deformation, the NW-trending fault rotate clockwise, resulting in left-lateral slip. (B) Basin developed as isolated extensional grabens as a result of internally rotating crustal blocks between the NW-trending faults. PG– Pekan Graben, KG– Kuantan Graben, MG– Merchong Graben, RG– Rumbia Graben.

sion resulted in the deformation of Postrift I and older strata, while the younger Postrift II strata above the Mid-Miocene Unconformity remained unaffected. A map view of the major inversion structures is shown in Fig. 3.42C (p. 110). The structures occur as elongate E-trending doubly-plunging anticlines, each ~25 km wide, located directly above the main half-grabens as a result of roughly N–S shortening. The largest of these structures occurs in the Kuantan Graben. This asymmetrical fold affects only Postrift I and older strata, and is centred over the deepest part of the graben (Figs. 3.5B). Its amplitude at Horizon 6 level is ~330 m, decreasing upwards to ~195 m at Horizon 4 level, which suggests that the structure is a "growth" feature formed during sedimentation of Postrift I strata (Fig. 3.7). The structure becomes narrower and smaller towards the west, as the Kuantan Graben gradually becomes shallower. There seems to be a direct correlation between the size of the inversion structure and that of the underlying half-graben. In the extreme west (Line 90-10), the structure is only ~2 km wide and has an amplitude of about ~150–300 m. Its asymmetry is closely related to the underlying normal fault which appears to have been reactivated and had propagated up-section into the post-rift strata. The crestal part of the structure is truncated by the Mid-Miocene Unconformity (Horizon 3).

The inversion structure in the western part of the Kuantan Graben appears to have developed by reactivation and propagation of the underlying border fault into the younger sedimentary cover. It is unclear whether the formation of this structure was accompanied by reversal of slip on the Kuantan Fault. The fact that the crest of the anticline is at some distance basinwards from the Fault (Fig. 3.7) suggests that fault reactivation was not significant. Inversion was achieved mainly by bulk shortening of the synrift fill and buckling of the postrift strata (Fig. 3.37A). This could be typical of "mature" half-graben border faults which may cease to be active long before inversion began. A high cohesion of the fault would tend to inhibit reactivation (Huyghe and Mugnier, 1992) (Fig. 3.37A). Furthermore, the steep dip of the Kuantan Fault would be unfavourable for reactivation (Fig. 3.38).

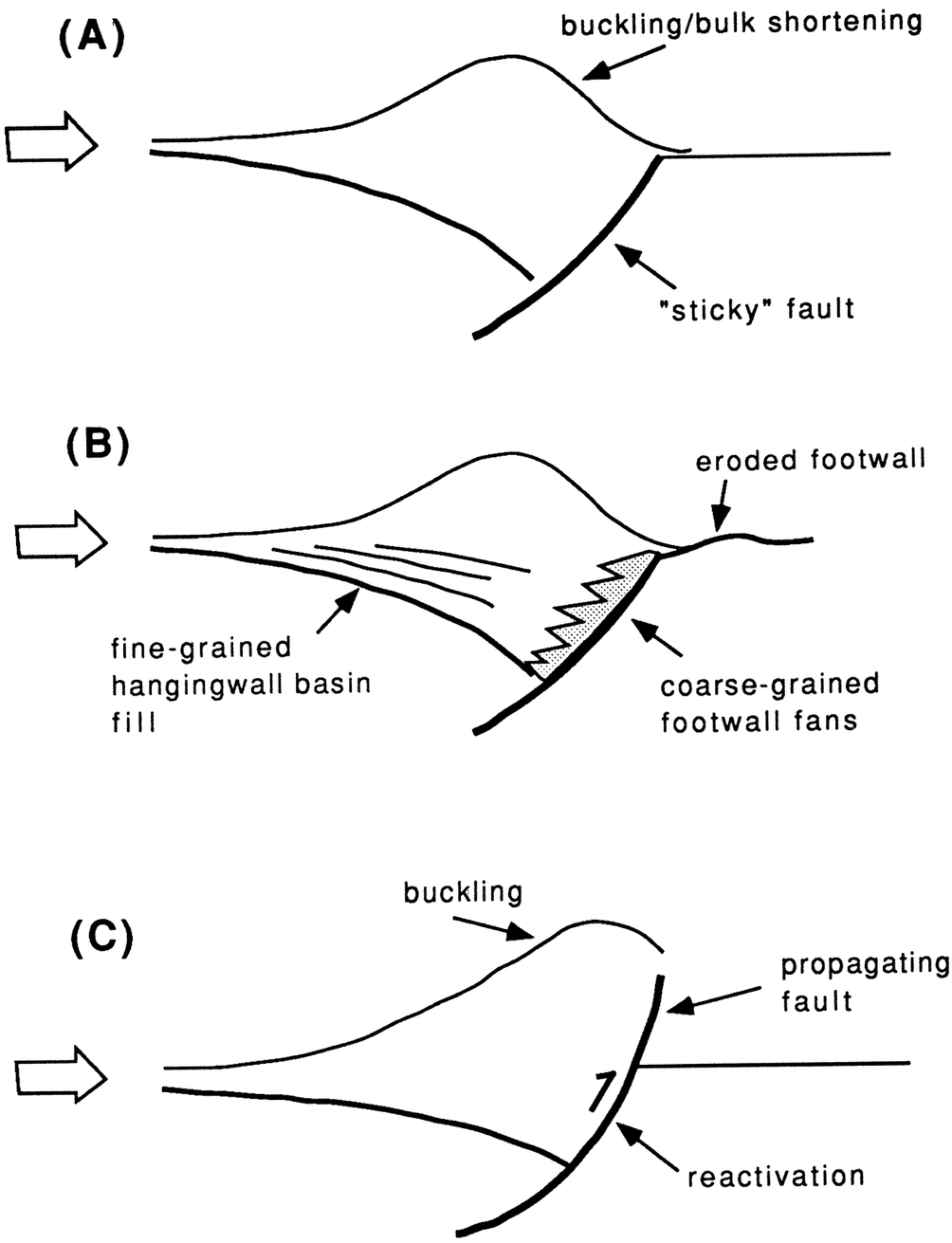

Figure 3.37. Modes of half-graben inversion in the Penyu Basin. (A) Symmetrical anticline formed by bulk shortening and buckling of basin fill. (B) Similar as in (A) but with inclusion of coarse-grained sediments adjacent to the footwall. Finer-grained sediments in the hangingwall basin deform more easily. (C) Asymmetrical anticline formed by reactivation of a relatively young "immature" half-graben border fault.

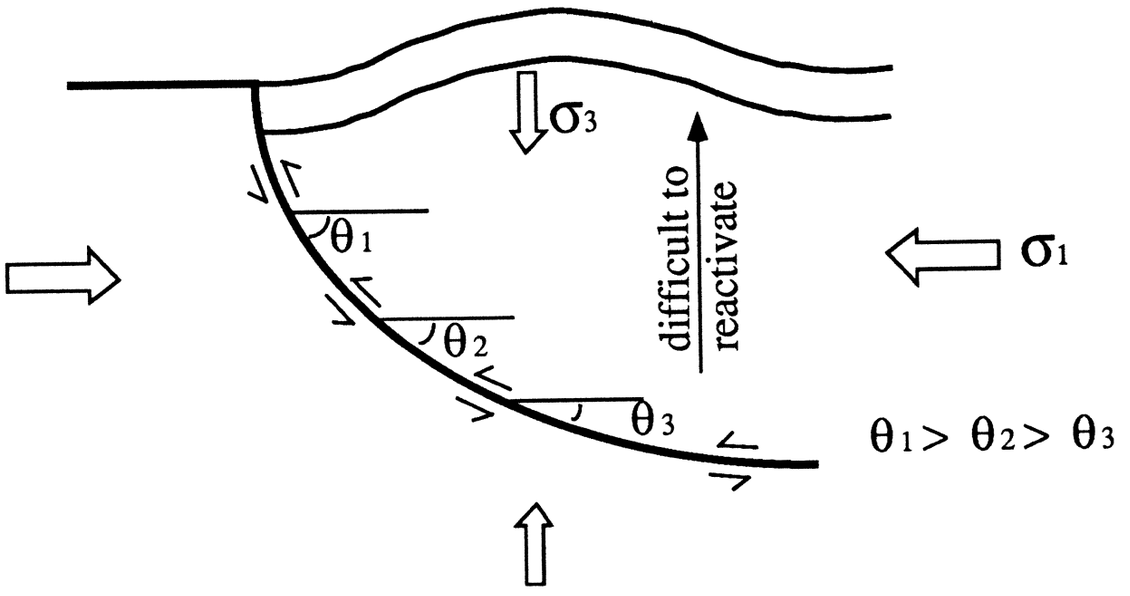

Figure 3.38. Reactivation of listric fault during basin inversion. Frictional resistance to reactivation depends on fault dip and, hence, depth. Reactivation of fault at depth results in buckling of hangingwall sediment. Modified from Sibson (1995).

Figure 3.18 is a dip section (line 90-105) across the Kuantan Fault, showing the footwall cutoff at Horizon 7 (Top Synrift Unconformity) at some distance downdip of the footwall scarp, suggesting that significant erosion of the footwall had taken place before it was buried by the overlying strata. Coarse-grained footwall fans, likely to be present, may have prevented reactivation of the fault during contractional deformation (Fig. 3.37B).

Another major inversion structure occurs in the southeastern part of the Rumbia Graben (Fig. 3.39). The underlying synrift half-grabens were produced by rotational (domino) fault blocks with NE-dipping border faults. Subsequent shortening across the closely-spaced half-grabens has produced two major south-verging, asymmetrical anticlines, each underlain by a half-graben. The steeper southern limbs of the folds were formed by fault-propagation folding and partial reactivation of the border faults. The crests of the folds, therefore, occur directly above the propagating faults. This is in contrast with the Kuantan Graben inversion structure whose crest is basinwards relative to the bounding fault (compare Fig. 3.37B and Fig. 3.37C). The amount of sediment eroded off the crest was

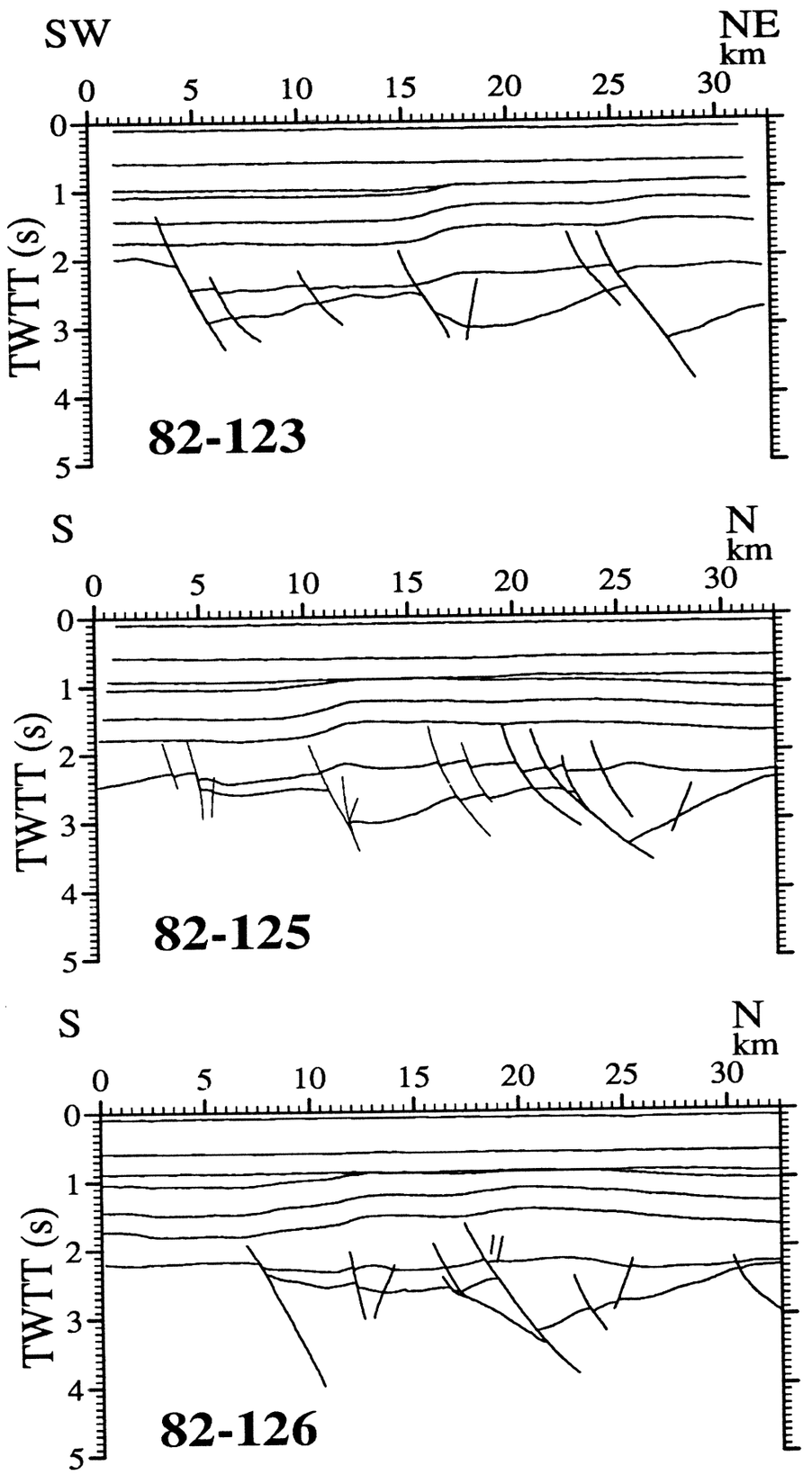

Figure 3.39. Profiles showing the fault style and geometry of inversion structures in southeastern Rumbia Graben. *Close-up of Line 82-126 shown in the foldout overleaf.*

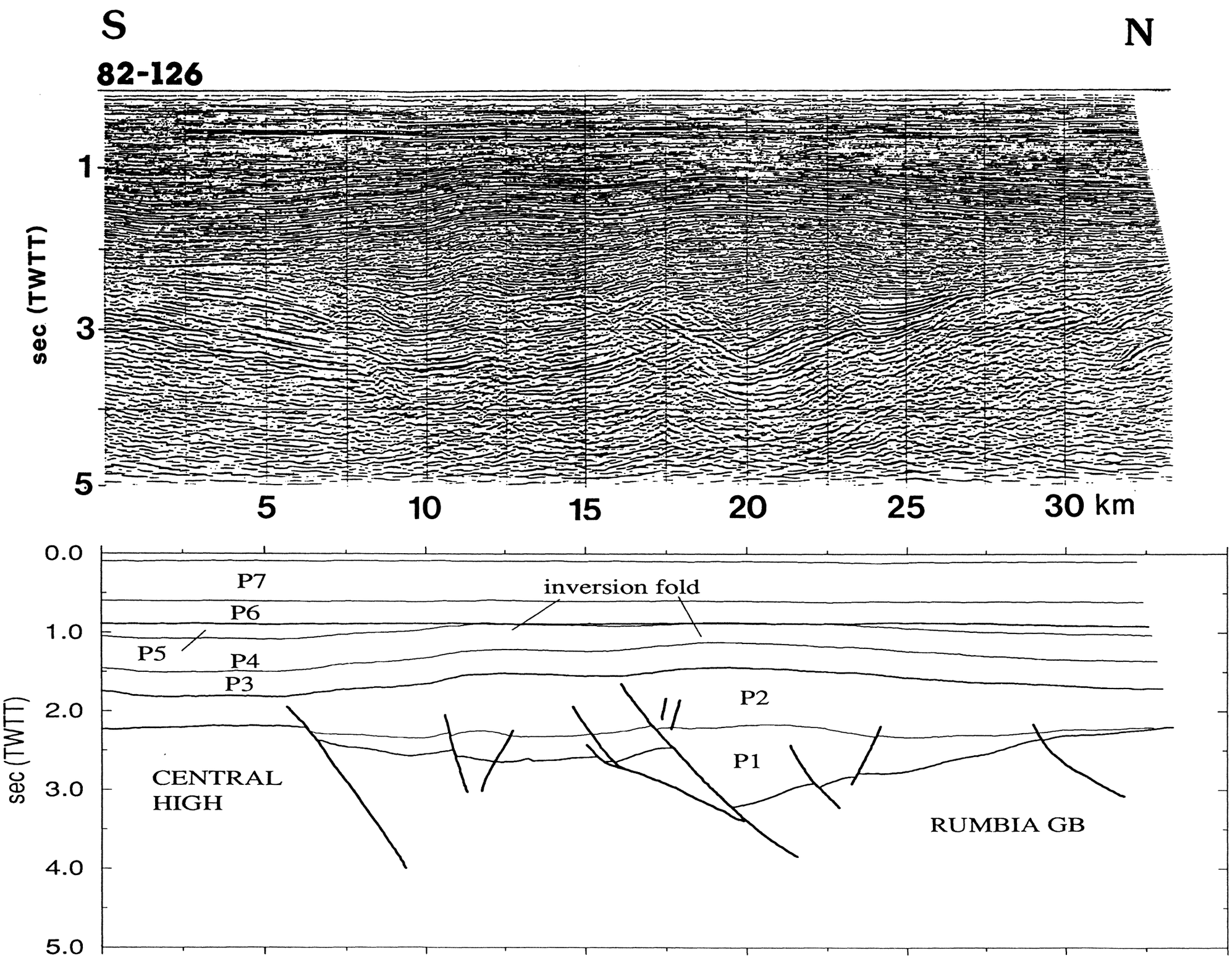

Figure 3.39 (cont.) Top: Seismic line 82-126 from the southeastern part of the Rumbia Graben. Bottom: Interpretation of the line showing the major inversion structures formed by reactivation of half-graben border faults.

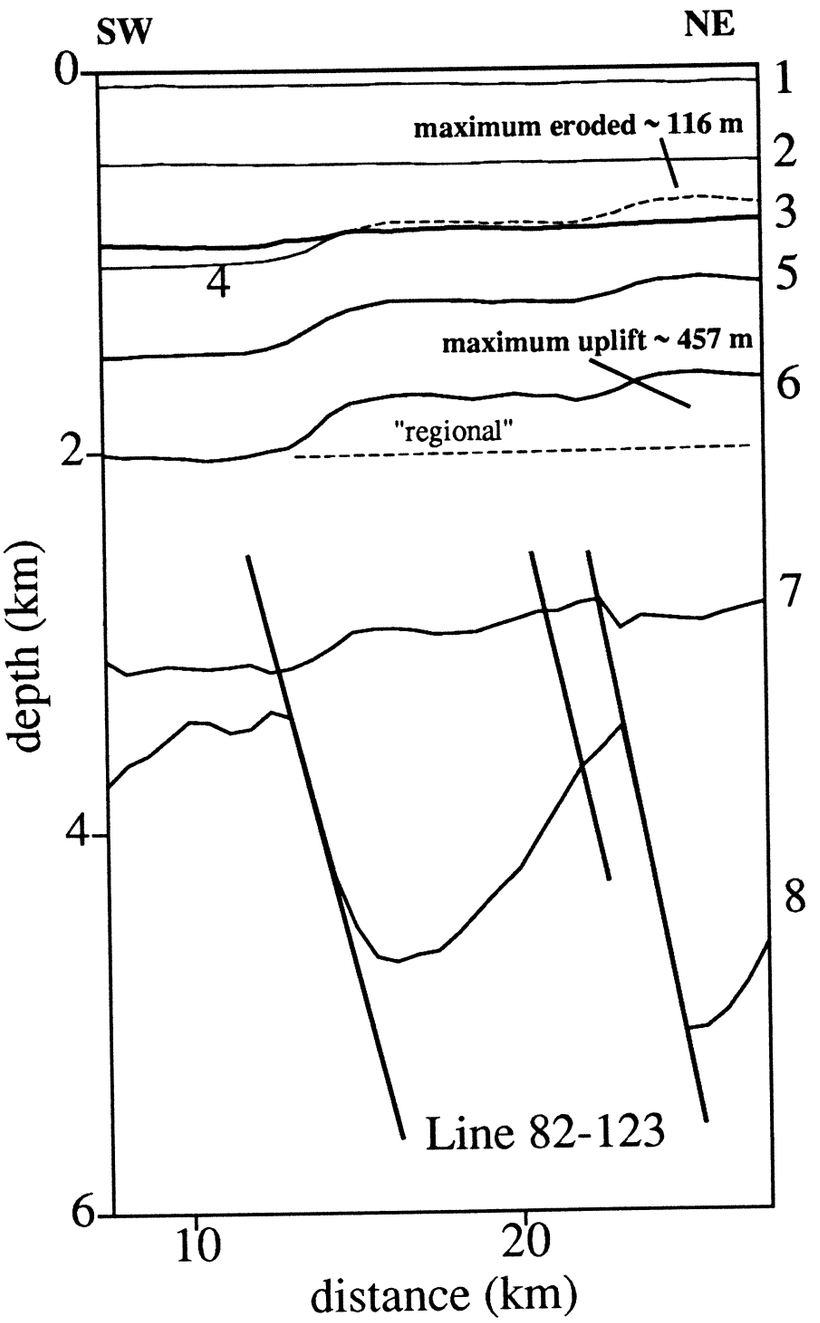

Figure 3.40. Exaggerated view of inversion structure in Line 82-123, showing truncation of the crest of the structure. Estimated amount of eroded material is ~116m, which may be higher than the actual amount because of the syndepositional nature of the structure.

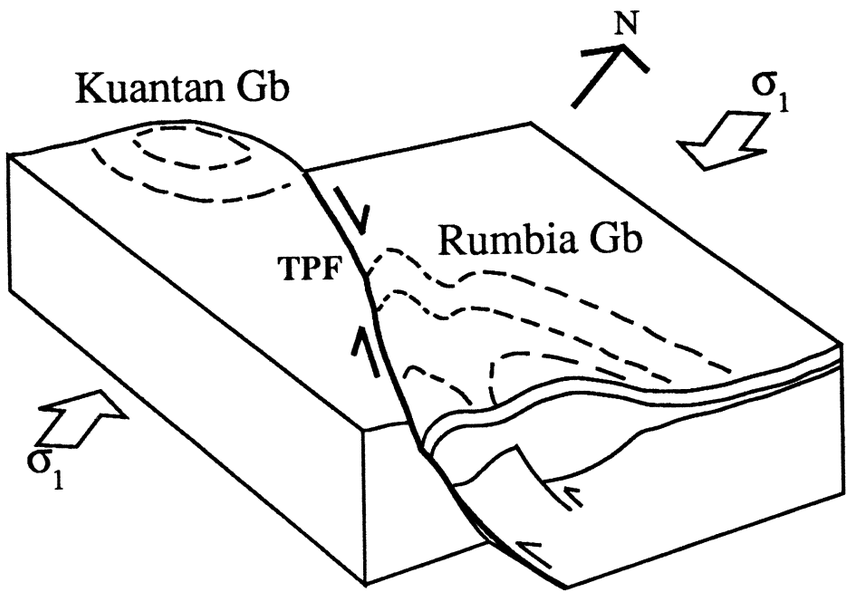

Figure 3.41. Geometry of inversion structures in the Kuantan and Rumbia Graben formed as a result of dextral reactivation of the Trans-Penyu Fault. Not to scale.

estimated by projecting Horizon 4 above the unconformity, and was found to be ~115 m (Fig. 3.40). This value is probably too high, considering that the structure is a growth feature. Figure 3.41 shows schematically the geometry of inversion structures in the Kuantan and Rumbia Grabens, resulting from transpressional reactivation of the Trans-Penyu Fault. E–W-trending anticlines developed on either side of the Fault, which have been reactivated as a dextral strike-slip fault during the inversion phase.

3.6 Conclusions

The Penyu Basin evolved from a nonmarine basin during Oligocene times, brackish in early–middle Miocene, to coastal–shallow marine during late Miocene–Recent. The Basin's structure is dominated by normal faults bounding major half-grabens or grabens. Two sets of faults are recognised: ENE and NW-trending faults. The orientation of the faults and geometry of half-grabens suggests that a regional N–S extension direction was responsible for the formation of the Basin. The rectilinear basement-fault pattern, which is similar to the regional fracture pattern

seen onshore in the west and in the adjacent basins, suggest a strong control by pre-existing basement weaknesses on the development of the Basin. Notably, the presence of a NW–SE fabric, parallel to known strike-slip faults on land, may have resulted in partitioning of the extension and reactivation of older faults. Evidence for strike-slip tectonics have been observed in areas where the border faults are oblique to the regional extension direction. The extensional geometry of bounding faults, such as the Trans-Penyu Fault which is a linear fault parallel to major strike-slip faults on land, and the internal architecture of the grabens and faults, particularly the shallow-dipping listric faults in the Rumbia Graben, suggest the possible role of upper-crustal detachment faulting in the Basin development. The style of faulting observed in the Penyu Basin is, in general, similar to that in the East African Rifts as described by Rosendahl (1987) and Morley (1995). Some of the key similarities are: half-graben geometries dominated by a main bounding fault and numerous synthetic faults in the hangingwall, alternating half-graben polarity along strike, lateral growth of border faults by segment linkage, and the co-existence of planar and listric faults.

Tectono-stratigraphic Evolution

The tectono-stratigraphic evolution of the Penyu Basin is summarised as follows:

1. Synrift I

   ?Latest Eocene to Oligocene (~40–30 Ma) extensional half-graben formation and deposition of Unit P1. Much of the subsidence in the major subbasins occurred during this phase and was controlled by the bounding faults, as indicated by the maps in Fig. 3.4 and Fig. 3.3.

2. Synrift II

   Late synrift phase, which continued probably until earliest Miocene (~25 Ma). Rifting had ended in the Rumbia Graben but fault-controlled subsidence continued in the Kuantan and Merchong Grabens with the deposition

of Unit P2. A map of Top-Synrift II (Horizon 7) in Fig. 3.42A shows the remanent fault-controlled subsidence in the two subbasins.

3. Postrift I

   Early postrift phase (early–middle Miocene) (~25–10 Ma), during which subsidence occurred over a wider area and was no longer controlled by the border faults. The resulting basin (Fig. 3.42B) bears no relationship with the basin-bounding faults. This phase of sedimentation was accompanied by basin inversion, which probably began in middle Miocene times, but peaked in the late Miocene during deposition of Units P3–P5. Figure 3.42C is an isopach map of Unit P3 showing the effect of basin inversion on its thickness. The inversion structures directly overlie the main half-grabens and are partly truncated by the Mid-Miocene Unconformity.

4. Postrift II

   Late postrift (late Miocene–present-day) Subsidence continued during this time without significant tectonic activity. Figure 3.42D shows the broad basinal subsidence associated with this phase of development. A gentle tilt of the Basin to the east suggests slightly greater subsidence rate away from the Peninsular Malaysian coastline, towards the deeper West Natuna Basin.

Kinematic Evolution

The kinematic evolution of the Penyu Basin is illustrated in Fig. 3.43. Basin evolution involved roughly N–S extension during the ?late Eocene–early Oligocene, followed by syndepositional inversion due to N–S shortening during early to late Miocene. Extension was achieved by reactivation of older basement faults. Two main fracture sets controlled the geometry of extension in the Basin: ?Late Cretaceous strike-slip faults and E-trending extensional fractures (Fig. 3.43A). Regional north-south extension in an overall dextral shear regime (Dewey *et al.*, 1989) resulted in the opening of half-grabens, whose geometry depends on the ori-

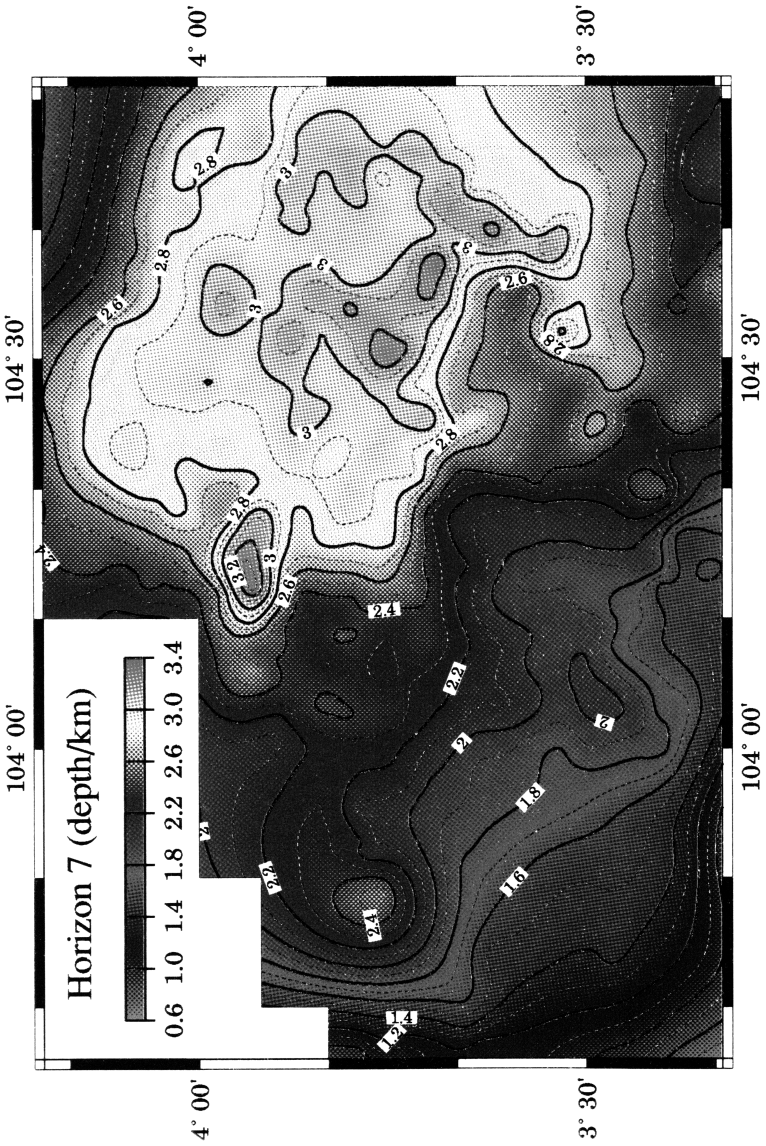

Figure 3.42. Structural maps of the Penyu Basin, showing the tectono-stratigraphic development. (A) Structure map of Horizon 7 — Mid-Oligocene Unconformity showing a broad "sag" basin centered over the Rumbia Graben. Fault controlled subsidence (see Fig. 3.4) is no longer controlled by the border faults except in the Kuantan Graben, where some subsidence still occurring close to the Kuantan Fault. Continued next page....